Digital Protection of Extra High Voltage Power Transmission Lines(Dissertation_全文)

AUTHOR(S):

Sakaguchi, Toshiaki

DIGITAL PROTECTION OF EXTRA HIGH VOLTAGE POWER TRANSMISSION LINES

by

TOSHIAKI SAKAGUCHI

Central Research Laboratory
Mitsubishi Electric Corporation

DIGITAL PROTECTION OF EXTRA HIGH VOLTAGE POWER TRANSMISSION LINES

by

TOSHIAKI SAKAGUCHI

Central Research Laboratory
Mitsubishi Electric Corporation

August 1981

ABSTRACT

Recent trends in electric power systems are analyzed to identify the impacts on extra high voltage (=EHV) transmission line protection. They call for high speed relaying under complex fault transients for reliable system operation. To achieve a solution meeting this requirement, this thesis undertakes systems approach as a scientific basis and computers approach as a technological basis.

A concept of the travelling wave difference is introduced for the first time as a protection principle for EHV transmission lines. Through the theoretical and simulation study, this thesis demonstrates that the concept is very effective to the design of an EHV computer relay meeting the basic requirement. One of the new trends in EHV network protection is to use the system transient for fast speed relaying. This thesis presents an effective computational technique to analyze the network transient for digital directional protection. Although lack of validation was felt on the working principle of such relays depending on system transients, a theoretical basis is established to the very fast directional protection. It appeared that the accurate eastimation of the distance to a fault would be impossible because of the phaseshifting effect of a fault impedance. This limit is overcome by two computational techniques. The algorithms depending on Fourier and Laplace transform technique are shown to be able to estimate the accurate fault distance in spite of the presence of a fault impedance. The final contribution is a provision of a method to deal with the uncertainty which seems innevitable in decision making in protection. A hypothesis testing approach is undertaken to make decision and extended to determine the sampling rate in computer relays.

Two areas are described as a future research: extension to total system protection and integration of protection and control system. Each arises from a system and technological need. The research in these areas is very vital to the reliable and efficient future power system operation.

ACKNOWLEDGEMENT

I would like to thank Prof. Chikasa Uenosono of Kyoto University for his constructive advice on my thesis. His advice has been essential in my preparing the thesis. Many thanks are due to the members of my reading committee: Prof. Akira Kijima and Prof. Takao Okada of Kyoto University for their critical reading my thesis.

I would like to thank Dr. Junichi Baba of Mitsubishi Electric Corporation for his leading me to the work in the systems engineering for electric power. His encouragement has been great enough to conduct my work. I also would like to thank Dr. Katsuhiko Uemura for numerous enlightening comments, suggestions and discussions. His continual concern has been invaluable for me to find concepts, to combine them and to create my work.

I would like to thank Mr. Toshio Takagi of the Tokyo Electric Power Co., Inc. for his helpful comments which reflect his long career in EHV network design, construction and operation. Many thanks are due to Mr. Yukinari Yamakoshi of the Tokyo Electric Power Co., Inc. for his helpful discussions on many reports which support each chapter of the thesis.

Finally, I would like to thank my friends in Japan and overseas countries. All of them have contributed to the completion of this thesis through written or oral discussions on my work.

This work was supported in part by the Tokyo Electric Power Co., Inc., Tokyo, Japan.

TABLE OF CONTENTS

LIST OF FIGURES

LIST OF TABLES

INTRODUCTION

This thesis deals with a systems approach to the extra high voltage power transmission line protection with digital computer. The scientific basis is placed on the systems methodology, and the technological basis is on the digital computer. The systems approach here is applied to the design problem of a protection algorithm for computer relaying. The design of a protection algorithm is involved with three subproblems: definition, verification and optimization of the algorithm. The systems approach plays an essential role in solving each subproblem of computer relaying. The following is a brief overview of the current problems in substation protection. An effort is concentrated on identifying the transmission line protection problems.

The efficient and reliable electric power supply is the final objective of electric utilities. At this time (1981), the largest unit capacity reaches well above 1,000 MW. Although the future unit capacity may not exceed the present record, the total capacity of a generation plant continues to increase. One can see an example in the power plant project. The electric power system has developed to a huge and complex network, because of a continuing effort made to operate the system more efficiently through a stronger interconnection. These result in an increase of current density. At the same time, great efforts have been made to incorporate new transmission technologies into present networks: UHV, HVDC, multi-terminal, and underground transmission [1, 2, 3]. Each novel scheme has its own opportunity for incorporation. These trends in systems and technologies have strong impacts on the transmission line protection. The increase of current density results in the reduction of transient stability margin. To keep the stability margin at the same or higher level, one must reduce the critical clearing time. In other words, the system needs high speed relaying. The new technologies, on the other hand, accompany complex fault transients largely due to an increase of the capacitive element. Accordingly, EHV relays must meet the severe requirements [4].

The new technology in electronics, particularly digital computer, has advanced and will keep advancing for the future. There are tremendous penetrations of computer systems into electric power system. Looking over carefully, one finds that the penetration is surprisingly slow in transmission [5]. Why have the computer systems moved so slow? Although one can see several reasons, the primary one for this is an attitude to replace the existing systems. However, the cost-effectiveness of computer systems has a great potential for transmission applications. Main objective of this thesis is to find more effective way of solving the substation protection problems with the digital computer systems.

To find the best solution, one must characterize the design problem of transmission line protection. This is done at each subproblem level as follows.

Definition level: the algorithm must work correctly over a wide band in frequency spectrum.

Verification level: the algorithm must be verified in more realistic environment.

Optimization level: the algorithm must be optimized on various factors that might affect the working principle.

The approach of this thesis is a systems analysis methodology and digital computer systems. In other words, scientific basis is placed on systems analysis and technological basis is on digital computer in the problem solving. Although the economical aspect is not dealt in this thesis, the cost-effectiveness of computer relaying seems to be maximized by an attempt to integrate the protection and control system in the transmission substation [6, 7, 8].

The following are the organization of this thesis. CHAPTER I describes the problem solving methodology of this thesis. It also contains a brief overview of the state of the art of computer relaying [9, 10]. A travelling wave concept regarding the transmission line protection is defined in CHAPTER II. As the concept is applied to the differential protection for the first time, substantial efforts are made to establish the theoretical basis of the concept in line protection. CHAPTER III is devoted to the verification and optimization of the protection algorithm through digital simulation and mathematical analysis techniques. CHAPTER IV defines a high speed directional protection algorithm, whose theoretical basis is upon the Laplace transform theory. Verification and optimization are also made here. The next two chapters deal with the fault location problem. The Laplace transform theory is applied to the fault location problem in CHAPTER V, where the algorithm is verified and optimized. CHAPTER VI defines a simplified version of the location algorithm studied in the previous chapter. The key here is an application of the Fourier transform theory. CHAPTER VII spots the decision making process of computer relay, which was not analyzed much before. A statistical approach is defined in the decision making process, and the sampling rate of computer relays is optimized with both the degree of uncertainty and operating time requirement. CHAPTER VIII summarizes main results of experiments which are performed using a prototype computer relay tested at an artificial transmission line. In CONCLUSION, several results obtained in each chapter are summarized. Also described are some future problems in computer protection of a transmission substation.

CHAPTER I SCOPE AND METHODOLOGY OF THE THESIS

1.1 INTRODUCTION

The main problem is the design of a high speed digital protection algorithm of a transmission line under complex fault transients. As the technological basis is placed on digital computer, a brief overview of the computer relaying is given with a particular reference to high speed protection. Three subproblems comprise the whole design problem.

--- Definition of the algorithm

--- Verification of the algorithm

--- Optimization of the algorithm

Systems approach is undertaken to each of these as a problem solving methodology.

1.2 BRIEF OVERVIEW OF COMPUTER RELAYING

Three logical processes comprise a relaying function, whatever technology is adopted. These are sensing, evaluating, and discriminating process as is shown in Fig. I-1 [1]. In the sensing process electrical system quantities such as voltage and current are measured with sensors, transmitted through cables or fibres, and conditioned appropriately. The evaluating process makes some computations to put out a fault criterion. The discriminating process makes a final decision whether a fault exists or not in the protected zone. When at least the last two processes are implemented with a digital computer, the whole process is referred to a computer relaying. This is a concept of computer relaying that is most widely accepted now [2]. An overview is made, emphasizing the key concept of each process.

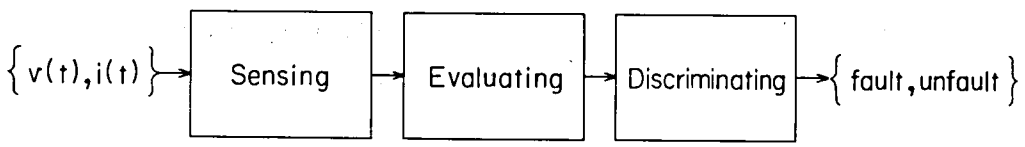

Fig. I-1 Functional decomposition of relaying process

Signal conditioning characterizes the first process. There are two problems here: determination of sampling rate and filter characteristics. Hope and Malik [3] tried to determine the sampling rate by minimizing the Fourier transform error. Another approach was to determine it by facilitating the computation at the middle process. Twelve samples per one cycle at the nominal frequency, for instance, are convenient to calculate the magnitude of voltage and current. Once the sampling rate is determined, the problem to determine filter characteristics simplifies because of the Nyquist sampling theorem [4]. Accordingly, the solution of major problems here highly depends upon the algorithm at the middle process.

Fault measuring is the key concept of the evaluating process. Each fault measuring algorithm is defined on its own transmission line model. Ordinary differential equation was used in many literatures.

$$v(t) = R\, i(t) + L\, di(t)/dt \tag{I-1}$$

There are two variations here. One is to measure the impedance $Z(j\omega)$:

$$Z(j\omega) = R + j\omega L \tag{I-2}$$

Mann and Morrison's method [5] was the first approach to measure $Z(j\omega)$ supposing that voltage and current are completely in their steady state sinusoidal forms. Obviously, their algorithm had a drawback in measuring $Z(j\omega)$ unless their assumption is true. Ramamoorty applied the Fourier transform algorithm to voltage and current [6]. The impedance $Z(j\omega)$, then was measured by $V(j\omega)/I(j\omega)$. His original algorithm required one cycle data at the nominal frequency. Phadke and et al. speeded up by proposing the half cycle transform algorithm [7]. Recently, John and Martin extended these approach to finite spectral analysis [8]. Their idea will be discussed in CHAPTER IV.

The other way is to measure R and L directly. This idea originated at McInne and Morrison's paper [9], where R and L are solved from a linear equation that is derived by integrating the eqn. (I-1) for two time periods. That is;

$$\int_{t_1}^{t_2} v(t)dt = R \int_{t_1}^{t_2} i(t)dt + L \int_{t_1}^{t_2} di(t) \tag{I-3}$$

$$\int_{t_3}^{t_4} v(t)dt = R \int_{t_3}^{t_4} i(t)dt + L \int_{t_3}^{t_4} di(t) \tag{I-4}$$

There may be large possibility that higher harmonics are included in the faulted voltage and current waveforms. To guarantee high accuracy in such a case, Ranjbar and Cory proposed an unique algorithm of integration [10] to filter out any higher harmonic components. Although their idea is very interesting, it has a disadvantage such that the long window data is needed to implement.

Partial differential equation is the other way of modelling a transmission line.

$$-\frac{\partial v(x,t)}{\partial x} = r\, i(x,t) + \ell \frac{\partial i(x,t)}{\partial t} \tag{I-5}$$

$$-\frac{\partial i(x,t)}{\partial x} = g\, v(x,t) + c \frac{\partial v(x,t)}{\partial t} \tag{I-6}$$

This telegram equation had not been used for relaying application for long time. Kohlas was the first to apply these to fault location problem [11], but not for relaying. Since the late seventies, many attempts have been made to develop a new type of relay. That is the travelling wave relay, whose theoretical basis lies in the above equations. This branch of relay engineering has grown rapidly in connection with a (very) high speed relaying. It appears that the operating time of the travelling wave relays is set at a quarter cycle at the nominal frequency or shorter. As CHAPTER II and III are devoted to the travelling wave relay, Table I-1 summarizes all of the travelling wave relay that are known at this time (1981). The relay of the first column was developed and demonstrated by Chamia, Esztergalyos, and et al. [12, 13]. Suppose that the notation $(\cdot)''$ be referred to a transient quantity. Their principle was:

If $v''(t)$ and $i''(t)$ have opposite signs, then a fault is before the relay.
If $v''(t)$ and $i''(t)$ have same signs, then a fault is behind the relay.

CHAPTER IV will discuss their idea in detail. Dommel and Michels proposed another directional protection scheme [14]. Their directional discriminant is consistent during the short time period after a fault inception. To the author's knowledge, the demonstration has not yet been made. Vitins published two papers [15, 16] on travelling wave relay. One paper dealt with a distance protection, and the other with a directional. His distance protection was defined as comparison between forward and backward wave vectors. His directional scheme was almost identical to the approach by Chamia and Esztergalyos [13].

Developer	ASEA BPA	University of British Columbia	BBC	TEPCO MELCO
Classification	directional	directional	distance	differential
Date of disclosure	1977 September CIGRE SC-34 (Austria)	1978 January IEEE Winter Meeting (New York)	1977 July IEEE Summer Meeting (Mexico City)	1977 July IEEE Summer Meeting (Mexico City)
Principle	For fault in forward direction, $v \cdot i < 0$ For fault behind, $v \cdot i > 0$	For fault in forward direction, $(v-Zi)^2 + \frac{1}{\omega^2}(\frac{dv}{dt} - Z\frac{di}{dt})^2 \geqslant 0$ For fault behind, $\cdots\cdots = 0$	For fault within the distance, $B(\omega)e^{-j2\omega a x_R}$ and $B(\omega)$ will come opposite side with $A(\omega)$.	For internal fault $\xi = 0$. For external fault $\xi \neq 0$.
Field Experience	Since 1976 April at 500 kV s/s of BPA	Not known, but may not be tested yet.	Not known.	Since 1977 June at 275 kV s/s of TEPCO
Feature & problems	Directional discriminant is good at earlier time after fault, but it is not so afterwards.	Directional discriminant is good at earliest time after fault. Exact detection of discriminant is questionable.	Data of remote end is not necessary. Original assertion $b(t+2\alpha x) = r \cdot a(t)$ is questionable with non-metallic fault.	Discriminant is good at any time. It requires high capacity of data link.

Table I-1 Comparative overview of travelling wave relay

Decision making is the last, but not the least concept in computer relaying. However, there have been no papers which deals with this concept explicitly. Heuristic method such as the majority decision rule was used. Most approaches were based on the fault measuring algorithm. For instance, consider an algorithm using successive three samples. If three successive decisions were idential to either trip or non-trip, then these were considered to be the final.

One can note a clear trend in the development of computer relays from the technological point of view. A prospect of digital protection with minicomputer was first cited by Rockefeller [17] in the sixties. Several joint development activities were started in the early seventies between the utility and manufacturing companies [18, 19, 20, 21, 22, 23]. These initial prototypes were designed to replace the existing protection system, and implemented with minicomputer. Although the field test results gained confidence in the computer relaying, the cost-effectiveness of minicomputer based systems was felt at that time not enough for fast penetration into protection. While these systems were being tested, there were two major technical breakthroughs in the seventies: microcomputer and fiber optic technology. The microprocessor is particularly suitable to improve the cost-effectiveness of computer systems. Accordingly, major projects were started to develop a microprocessor based prototype in the mid seventies. Japan has been most active in this field. The Tokyo Electric and the Kansai Electric Utility Companies have developed and tested the prototype systems with Mitsubishi [24], Toshiba [25] and Hitachi [26] Manufacturing Companies. The microprocessor based system is now accepted to be vital to the best architecture for computer relay design. The most recent trend is a concept of the integrated protection and control system [27]. There seems to be a concensus among the protection and control engineers such that the cost-effectiveness of computer systems will be maximized by the integration, and that computer systems will start penetrating fast into transmission.

1.3 SYSTEMS APPROACH TO DEFINITION OF PROTECTION ALGORITHM

There are three basic requirements in the fault protection of a transmission line. They are fault detection, fault selection, and fault location. As an algorithm for each is defined on the mathematical model of the transmission line, modelling is very vital to meet each requirement. On the other hand, modelling is the fundamental concept in systems analysis. In other words, one starts his systems analysis with building a model of the object. Accordingly, systems analysis has a great opportunity for definition of a protection algorithm.

Fig. I-2 illustrates the most general idea to make a fault detection. Suppose that one knows a mathematical equation of an unfaulted object:

$$F(x, y, a) = 0 \tag{I-7}$$

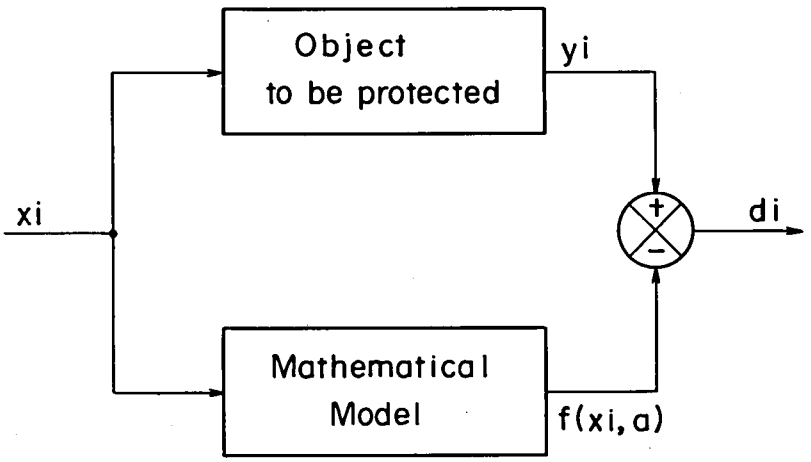

xi, yi = actual measurement
a = parameter
di = model difference

Fig. I-2 General idea of fault detection

where x and y are measured quantities, and a is a parameter. Let f(x, a), be a function relating x and a with y:

$$y = f(x, a) \tag{I-8}$$

Now suppose that x_i and y_i are measured at the time t_i. From the eqn. (I-8), one can define a quantity d_i which measures a correctness of the model.

$$d_i = y_i - f(x_i, a) \tag{I-9}$$

Ideally d_i is zero unless a fault takes place inside the object. However, if a fault happens inside, d_i is no longer zero. In this way one derives a general definition of the fault detection algorithm.

If $d_i = 0$, then no fault exists inside.
If $d_i \neq 0$, then a fault exists inside.

The fault selection is an essential requirement in the protection of a multi-phase system. One has a set of fault measure $[d_i]$ in the N-phase system.

$$[d_i] = \begin{bmatrix} d_{i0} \\ \vdots \\ d_{i,N-1} \end{bmatrix} \tag{I-10}$$

The k-th component of $[d_i]$ is defined on the k-th decoupled modal system. A proposition p_{ik} is defined here as follows:

$$p_{ik} \triangleq (d_{ik} \text{ is zero}) \tag{I-11}$$

Then one has a vector of propositions, $[p_i]$.

$$[p_i] = \begin{bmatrix} p_{i0} \\ \vdots \\ p_{i,N-1} \end{bmatrix} \tag{I-12}$$

As p_{ik} takes the value of true (= T) or false (= F), there are 2^n combinations in $[p_i]$. The fault selection algorithm is thought as a function from $\{[p_i]\}$ to {fault type}. The fault type means a phase-a-to-ground fault, · · ·, phase-a-to-b short circuit, · · ·, three-phase short circuit.

The fault location is considered to estimate the parameter value a using x and y. From the eqn. (I-7), one must define a function g such that:

$$a = g(x, y) \tag{I-13}$$

This is a general definition of the fault location algorithm. The problem gets solved when one can find an algorithm g to calculate a.

As one can see in the discussions above, the definition of each algorithm depends highly upon the modelling of a transmission line. Fig. I-3 illustrates a set of transmission line models in the increasing order of complexity. The simplest is a lumped-constant R-L series circuit representation, while the most complex is a distributed-constant circuit. There are many between two models. To determine an appropriate model, one needs to find the best compromise between model adequacy and algorithm simplicity. The model adequacy gets increasingly important when one wants to define an algorithm which works correctly under transient conditions. The first model of Fig. I-3 may be adequate for a phenomenon at the nominal frequency, but it will not at high frequency regions. On the other hand, the simpler model may be better from the algorithmical point of view. Accordingly, the ultimate objective is to define a simple algorithm based on an adequate transmission line model. The distributed-constant circuit representation is undertaken in CHAPTER II to meet the objective.

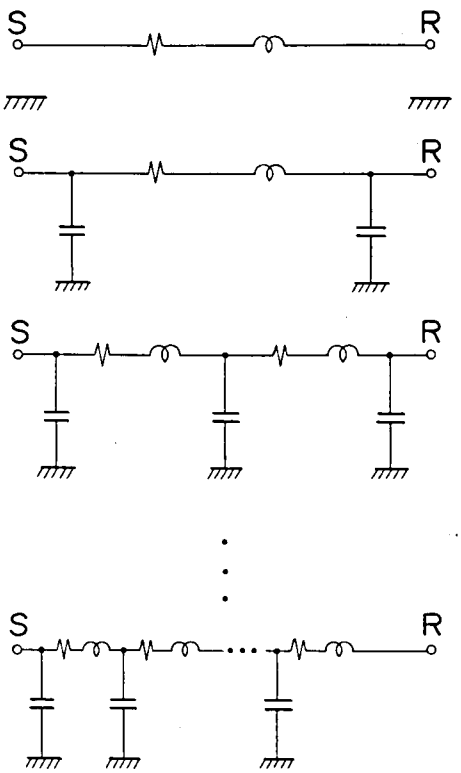

Fig. I-3 A set of transmission line model

1.4 SYSTEMS APPROACH TO VERIFICATION OF PROTECTION ALGORITHM

Once one defines a protection algorithm, what must be done next is the verification. An analytical and analogue method is well justified to be used for an algorithm that has a theoretical basis on modelling at the nominal frequency. One can see a good example in the distance protection. As the network reduction is made easily at the nominal frequency, the simple analytical method can be applied to verify the algorithm. However, this is no longer true for high speed computer relays that have their working principles on the transmission network transient phenomena. One cannot make the network reduction in a straight forward way. The analytical method here is not enough to be used for verification of the algorithm.

There is at least one way to do this. That is a digital simulation method. Systems methodology has advanced the computation techniques for power system dynamic behavior. Dommel and Scott recently overviewed its state of the art [28]. In connection with computer relays, the computation of electrical and magnetic transient in transmission system [29, 30] is the most important technique. Two simulation techniques are well known: frequency transform method, and travelling wave method. The former was developed mainly in Europe. A frequency response to an input time function is calculated at many points in the complex frequency plane. An output time function is obtained through the inverse frequency transform [31, 32, 34, 37]. The latter method was developed mainly in the North America. This is based on the solution of the telegram equation. A nodal equation at time t_i is established using the previous solution until time t_{i-1}, referred to the past history term, and it gives the solution at time t_i [33, 38]. Table I-2 compares the advantages and disadvantages of the two methods

The travelling wave method is used for the verification purpose throughout this thesis with the following reasons. This method is easily applied to a large scale transmission network. System changes like faults and switchings are easily manipulated. The frequency dependent nature of line constants is treated with an enough accuracy [39, 40] by Semlyen's [35] or Ametani's [36] convolution. The nonlinear characteristics of power transformer are also taken into account very well. Fault transients in transmission network are calculated with the digital simulation technique [41], and they are used as primary circuit quantities put into computer relays. It is very easy to verify the protection algorithms defined at the previous step by using the theoretical fault data. This methodology is undertaken in CHAPTER III, IV, V, and VI.

Item \ Method	Travelling Wave Method	Fourier Transform Method
Distributed Constant Elements	Solved directly	Solved directly
Lumped Constant Elements	Solved directly	Solved directly
Non-linear Elements	Both non-linear resistor and reactor have been built in.	Non-linear resistor has been built in, while reactor has not.
Multi-phase and Untransposed Line	Both multi-phase and untransposed lines have been modelled.	Both are taken into account upon operational solution.
Large Scale Network	Very easy to extend to large scale network.	Very difficult to extend to large scale network.
Computation Time	Relatively small. Approximate convolution method has been coded.	Relatively large. Speed up is possible with Fast Fourier Transform technique.
Accuracy	Good	Good
Comment	Both method are accurate when compared with analytical solution. Actual field data are too small to judge their accuracy.	

Table I-2 Digital technique for electromagnetic transient computation

1.5 SYSTEMS APPROACH TO OPTIMIZATION OF PROTECTION ALGORITHM

The opportunity for optimization exists at each process of Fig. I-1. Optimization is made on the sampling rate and signal filtering in the sensing process. One must keep in mind that these depend upon the fault measuring algorithm. In the evaluating process, optimization is made over the fault measuring algorithm. Two types of optimization are possible: functional optimization, and parametric optimization. Finally, the optimal decision making is searched in the discriminating process. The optimization at the second process is primary and vital to an effective design of a protection algorithm. Accordingly, the methodology at the evaluating process is dealt first.

There are two ways of optimizing an algorithm: direct method and simulation method. In terms of control theory, a transmission line protection can be considered as a decentralized state estimation problem. However, no attemps were made to define the objective function explicitly nor to write the system equation so as to facilitate the application of the control theory. It seems impractical to make the direct optimization at this time. Nevertheless, there is again a great opportunity for the simulation method. The digital simulation technique is so advanced as to be used for many engineering problems. Through a medium size computer one can access a simulation program which used to be run on a large digital computer. The Electro-Magnetic Transient Program (= EMTP) on VAX 11 system is a good example. Several alternative measuring algorithms are compared for their computational burden to accuracy analysis. In CHAPTER III, IV, V, and VI attempts are made to find the optimal measuring algorithm through the digital simulation method.

Once the measuring algorithm is defined, the decision making is then optimized. The objective function that is used in this thesis is a probability of relay misoperation. The concept of probability density function is introduced into the fault criterion, and the discriminating process is formulated with a statistical decision making. A sequential algorithm is optimized, taking into account the real time computation of the decision value. One of the outcomes of this approach is that it is possible to optimize the sampling rate. CHAPTER VII is devoted to study the optimization at the sensing and discriminating process.

CHAPTER II ALGORITHM DEFINITION OF TRAVELLING WAVE DIFFERENTIAL PROTECTION FOR TRANSMISSION LINES [13, 14]

2.1 INTRODUCTION

The emergence of UHV transmission lines and EHV cables produces some new and difficult problems to the conventional electromechanical or static protective devices. The problems include (1) the leakage current caused by the increasing stray capacitances, (2) the transient current of a few kHz caused by surge travelling after fault inception, (3) the transient current of a few hundreds Hz caused by the oscillation between the total inductance and capacitance of the system, and (4) the transient dc current weakly damped by the increasing L/R ratio. As is easily noted, these problems are featured by the "transient" behavior of the power system after fault inception. The conventional relays assume that the electromagnetic transients in a power system would be small and disappear very soon. This assumption, however, might not be true in recent systems and the protection system must be designed to take much account of the transient behaviors [1].

Another problem is the transient stability in modern power system [2]. The protection system must meet the requirement that the fault detection is made as fast as possible to maintain the transient stability. As one of the solutions to the problems above, a new protection method which is realized efficiently with digital techniques is proposed here.

In an earlier application of a digital computer to protection [3], the relaying principles of the conventional devices were shifted in use. The distance relaying of [4] and [5] used current, voltage, and their derivatives for impedance calculation. The relaying of [6] integrated a differential equation numerically for R and L calculation, and that of [7] improved this numerical integration by eliminating arbitrary harmonic components. The digital relayings proposed so far are all directed to calculate an impedance, assuming that a transmission line is represented by an L-R lumped circuit.

This chapter starts with modelling a transmission line as a distributed circuit rather than a lumped one. Then one can apply the travelling wave theory and introduce Bergeron's equation as a basis of the protection method. Fundamental properties of this equation are studied in a single phase line, and it is shown that the equation has several features desirable

to fault detection. High speed detection of internal fault, highly reliable discrimination of intermal and external faults, and low sensitivity to transient phenomena on a transmission line are some of them. It is well known that a three phase line can be decomposed into three single phase ones, namely modal lines. Therefore one can extend the protection method to three phase line applying modal transform. Also is studied its extension to multi-terminal line. Here another equation, Kirchhoff's 1st law, is required besides Bergeron's one. The new protection method is applied to fault selection. Bergeron's equation in each modal line defines a predicate on fault detection. One can build a truth table of each predicate to all types of internal faults, where fault selection is made by this table look up. Finally, two schemes of fault location are discussed.

The travelling wave differential protection scheme can detect an internal fault very rapidly. It hardly operates for an external fault, since Bergeron's equation is not violated by any external disturbances. These considerations conclude that the proposed method is quite promising for fault protection of the modern high voltage transmission lines and cables.

2.2 THEORY OF FAULT DETECTION

A theoretical basis of fault detection is presented with the assumption of no loss transmission lines.

2.2.1 Single Phase Two-Terminal Transmission Line

A single phase line in Fig. II-1 is represented by a distributed circuit with per unit length inductance ℓ and capacitance c. The current and voltage at two terminals satisfy the eqn. (II-1), which is known as Bergeron's equation [8].

$$-i_S(t) + \frac{1}{z}v_S(t) = i_R(t - \tau) + \frac{1}{z}v_R(t - \tau) \qquad \text{(II-1)}$$

where $\tau = \sqrt{\ell c}\,d$: surge travel time

$z = \sqrt{\frac{\ell}{c}}$: surge impedance

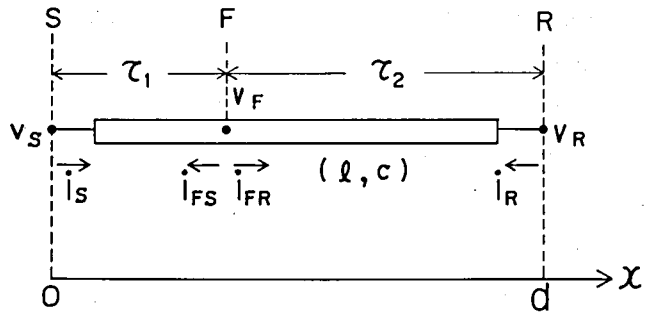

Fig. II-1 Single phase distributed constant transmission line

See APPENDIX I for its derivation. The equation implies that a travelling wave leaving R will arrive at S with the time delay τ. Let us consider the wave propagation in three states of the network. First, no fault has occurred anywhere in the network. The wave is not disturbed and the eqn. (II-1) is satisfied. Second, a fault external to the line S-R has occurred. The wave is not disturbed either and hence eqn. (II-1) is satisfied. Third, a fault has occurred in S-R. The wave is deformed in its propagation with reflecting and refracting at the fault point, and the eqn. (II-1) is not satisfied anymore. Here a time function $\xi(t)$ is defined as

$$\xi(t) \triangleq i_S(t) + i_R(t-\tau) - \frac{1}{z}\{v_S(t) - v_R(t-\tau)\} \qquad \text{(II-2)}$$

It has the property that

$\xi(t) = 0$ implies no internal fault.

$\xi(t) \neq 0$ implies internal fault.

Thus one can detect an internal fault by $\xi(t)$.

The principle of fault detection proposed has some desirable properties for fault protection in modern transmission network. One can use the instantaneous values of i(t) and v(t), which are suitable for implementation with digital techniques. It is also noted that the detection is not disturbed by any transient phenomena due to a fault. One can detect a fault very rapidly. Theoretically, the detection is made within the total of surge travelling

time and data communication time. The former is less than a few hundred microsecond, and the latter is about a few milliseconds. Therefore it can be said that the detection speed mainly depends on the time for data communication, which will be expected to become faster in future. Reliability is one of the important factors in relaying. In this respect, the travelling wave differential method cannot be affected by any external disturbances, like faults and switching operations. Thus it hardly operates for an external fault.

In the above, $\xi(t)$ is defined by the wave proceeding from R to S. The other wave from S to R defines a time function $\zeta(t)$ as

$$\zeta(t) \triangleq i_R(t) + i_S(t-\tau) - \frac{1}{z}\left\{v_R(t) - v_S(t-\tau)\right\} \tag{II-3}$$

which can be used for detection in the same way as $\xi(t)$. It is noted that the functions $\xi(t)$ and $\zeta(t)$ are independent of each other.

Let F in Fig. II-1 be an internal fault point, τ_1 the surge travelling time from F to S, τ_2 the surge travelling time from F to R, and $i_F(t)$ the fault current. It is shown in APPENDIX II that

$$\xi(t) = i_F(t - \tau_1) \tag{II-4}$$

$$\zeta(t) = i_F(t - \tau_2) \tag{II-5}$$

This is a physical meaning of $\xi(t)$ and $\zeta(t)$, which is used in later sections.

2.2.2 Three Phase Two-Terminal Transmission Line

Fig. II-2 shows a three phase line with series per unit length inductance matrix [L] and shunt capacitance matrix [C]. It is a well known fact that a three phase line can be separated into three single phase lines by a modal transform [9],

$$[v(t)] = [S]\,[v^{(mode)}(t)] \tag{II-6}$$

$$[i(t)] = [Q]\,[i^{(mode)}(t)] \tag{II-7}$$

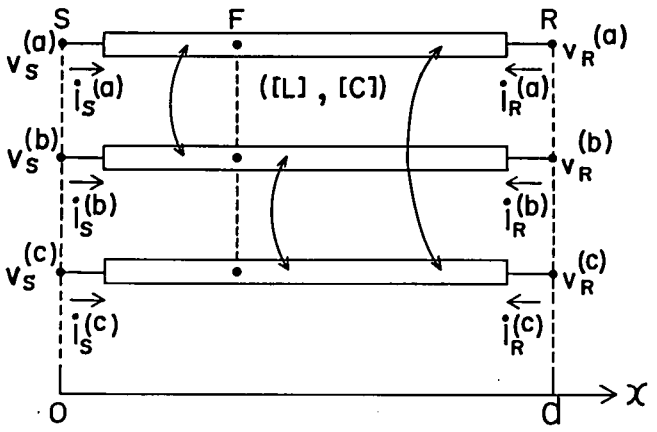

Fig. II-2 Three phase distributed constant transmission line

The discussion in a single phase line is applicable to each modal line. Thus the fault criteria in a three phase line are written as

$$\xi^{(k)}(t) = i_S^{(k)}(t) + i_R^{(k)}(t - \tau^{(k)}) - \frac{1}{z^{(k)}}\{v_S^{(k)}(t) - v_R^{(k)}(t - \tau^{(k)})\} \qquad \text{(II-8)}$$

$$\zeta^{(k)}(t) = i_R^{(k)}(t) + i_S^{(k)}(t - \tau^{(k)}) - \frac{1}{z^{(k)}}\{v_R^{(k)}(t) - v_S^{(k)}(t - \tau^{(k)})\} \qquad \text{(II-9)}$$

where $z^{(k)}$ is the mode-k surge impedance, $\tau^{(k)}$ the mode-k surge travelling time, and $k = 0, 1, 2$. Let Π and Σ be the logical operations AND and OR. Fault detection in a three phase line can be done as the following logic.

If $\prod_{k=0}^{2} \xi^{(k)}(t) = 0$ is true, it implies no internal fault.

If $\sum_{k=0}^{2} \xi^{(k)}(t) \neq 0$ is true, it implies internal fault.

As in single phase line, each of $\{\xi^{(k)}(t)|k = 0,1,2\}$ is defined by the differential value of each modal travelling wave from R to S, and each of $\{\zeta^{(k)}(t)|k = 0,1,2\}$ by each modal wave from S to R. One can calculate modal current and voltage by the eqn. (II-6) and (II-7), where [S] and [Q] are determined from a solution of eigen value problem on matrix [L] · [C] or [C] · [L]. In a transposed line, the eigen value problem has a solution independent of [L] and [C] matrix [10, 11]. Some well known are:

(i) Fortesque transform

$$[S] = [Q] = \begin{bmatrix} 1 & 1 & 1 \\ 1 & a^2 & a \\ 1 & a & a^2 \end{bmatrix} \quad a = \exp(j\frac{2}{3}) \tag{II-10}$$

(ii) Clarke transform

$$[S] = [Q] = \begin{bmatrix} 1 & 1 & 0 \\ 1 & -\frac{1}{2} & \frac{\sqrt{3}}{2} \\ 1 & -\frac{1}{2} & -\frac{\sqrt{3}}{2} \end{bmatrix} \tag{II-11}$$

(iii) Karrenbauer transform

$$[S] = [Q] = \begin{bmatrix} 1 & 1 & 1 \\ 1 & -2 & 1 \\ 1 & 1 & -2 \end{bmatrix} \tag{II-12}$$

The physical meanings of $\xi^{(k)}(t)$ and $\zeta^{(k)}(t)$ are given by the equations:

$$\xi^{(k)}(t) = i_F{}^{(k)}(t - \tau_1{}^{(k)}) \tag{II-13}$$

$$k = 0,1,2$$

$$\zeta^{(k)}(t) = i_F{}^{(k)}(t - \tau_2{}^{(k)}) \tag{II-14}$$

where $i_F{}^{(k)}(t)$ is a fault current, $\tau_1{}^{(k)}$ surge travelling time from F to S, and $\tau_2{}^{(k)}$ that from F to R in the mode-k line.

2.2.3 Single Phase Multi-Terminal Transmission Line

An attempt is made to extend the theory to a multi-terminal line, using three-terminal single phase line in Fig. II-3. The Bergeron's equation is satisfied in two-terminal zones.

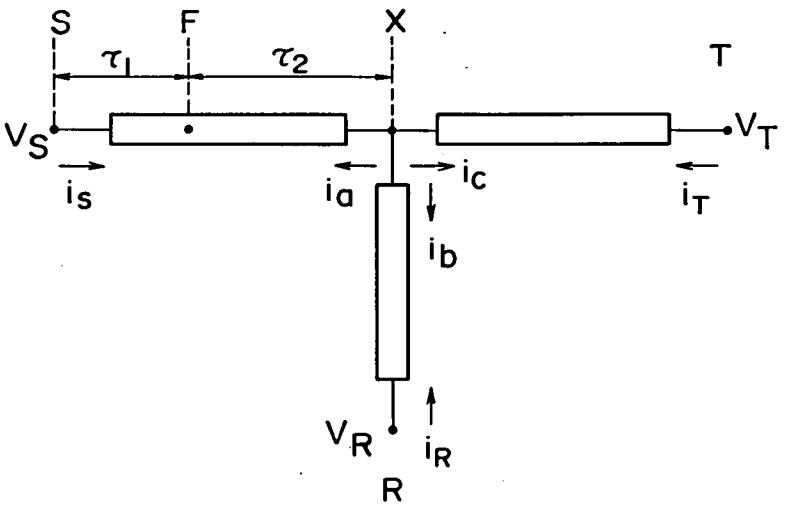

Fig. II-3 Single phase three-terminal transmission line

(zone S-X)

$$i_a(t) + \frac{1}{z}v_x(t) = -i_S(t+\tau_S) + \frac{1}{z}v_S(t+\tau_S) \qquad \text{(II-15)}$$

$$-i_a(t) + \frac{1}{z}v_x(t) = i_S(t-\tau_S) + \frac{1}{z}v_S(t-\tau_S) \qquad \text{(II-16)}$$

(zone R-X)

$$i_b(t) + \frac{1}{z}v_x(t) = -i_R(t+\tau_R) + \frac{1}{z}v_R(t+\tau_R) \qquad \text{(II-17)}$$

$$-i_b(t) + \frac{1}{z}v_x(t) = i_R(t-\tau_R) + \frac{1}{z}v_R(t-\tau_R) \qquad \text{(II-18)}$$

(zone T-X)

$$i_c(t) + \frac{1}{z}v_x(t) = -i_T(t+\tau_T) + \frac{1}{z}v_T(t+\tau_T) \qquad \text{(II-19)}$$

$$-i_c(t) + \frac{1}{z}v_x(t) = i_T(t-\tau_T) + \frac{1}{z}v_T(t-\tau_T) \qquad \text{(II-20)}$$

where τ_S, τ_R, and τ_T are surge travelling times in each zone. Another equation is the Kirchhoff's current law at X:

$$i_a(t) + i_b(t) + i_c(t) = 0 \tag{II-21}$$

Elimination of $v_x(t)$, $i_a(t)$, $i_b(t)$ and $i_c(t)$ leads to a new equation:

$$i_S(t+\tau_S) + i_S(t-\tau_S) + i_R(t+\tau_R) + i_R(t-\tau_R) + i_T(t+\tau_T) + i_T(t-\tau_T) - \frac{1}{z}\{v_S(t+\tau_S) - v_S(t-\tau_S) + v_R(t+\tau_R) - v_R(t-\tau_R) + v_T(t+\tau_T) - v_T(t-\tau_T)\} = 0 \tag{II-22}$$

A fault criterion $\xi(t)$ is defined by

$$\xi(t) = \text{the left hand side of eqn. (II-22)} \tag{II-23}$$

Then it has a property that

$\xi(t) = 0$ implies no internal fault
$\xi(t) \neq 0$ implies internal fault

Thus one can detect an internal fault in a 3-terminal line S-R-T by $\xi(t)$. Assume that F in Fig. II-3 is a fault point. The physical interpretation of $\xi(t)$ is the sum of two fault currents,

$$\xi(t) = i_F(t + \tau_2) + i_F(t - \tau_2) \tag{II-24}$$

where τ_2 is the surge travelling time from F to X.

One can extend the eqn. (II-23) to a three phase three-terminal line, using modal quantities at each terminal.

$$\xi^{(k)}(t) = i_S^{(k)}(t+\tau_S^{(k)}) + i_S^{(k)}(t-\tau_S^{(k)}) + i_R^{(k)}(t+\tau_R^{(k)}) + i_R^{(k)}(t-\tau_R^{(k)}) + i_T^{(k)}(t+\tau_T^{(k)}) + i_T^{(k)}(t-\tau_T^{(k)}) - \frac{1}{z^{(k)}}\{v_S^{(k)}(t+\tau_S^{(k)}) - v_S^{(k)}(t-\tau_S^{(k)}) + v_R^{(k)}(t+\tau_R^{(k)}) - v_R^{(k)}(t-\tau_R^{(k)}) + v_T^{(k)}(t+\tau_T^{(k)}) - v_T^{(k)}(t-\tau_T^{(k)})\} \quad (k = 0,1,2) \tag{II-25}$$

Fault detection logic is that

$$\prod_{k=0}^{2} \xi^{(k)}(t) = 0 \text{ implies no internal fault}$$

$$\sum_{k=0}^{2} \xi^{(k)}(t) \neq 0 \text{ implies internal fault}$$

From the result in a single phase line, one can deduce that

$$\xi^{(k)}(t) = i_F{}^{(k)}(t+\tau_2{}^{(k)}) + i_F{}^{(k)}(t-\tau_2{}^{(k)}) \tag{II-26}$$

which is the physical meaning of $\xi^{(k)}(t)$.

The extension of the theory to an arbitrary multi-terminal line is possible, but only basic principle for extension is described here. In Fig. II-4 let (n−1) and (n) be internal points, and assume that the electrical values up to (n−1) are known, but those after (n) are unknown. From the equations of

$$i_n(t) + \frac{1}{z_n} v_n(t) = -i_{n-1}(t+\tau_n) + \frac{1}{z_n} v_{n-1}(t+\tau_n) \tag{II-27}$$

and

$$-i_n(t) + \frac{1}{z_n} v_n(t) = i_{n-1}(t-\tau_n) + \frac{1}{z_n} v_{n-1}(t-\tau_n) \tag{II-28}$$

$i_n(t)$ and $v_n(t)$ can be solved as

$$i_n(t) = -\frac{1}{2}\left[i_{n-1}(t+\tau_n) + i_{n-1}(t-\tau_n) - \frac{1}{z_n}\{v_{n-1}(t+\tau_n) - v_{n-1}(t-\tau_n)\}\right] \tag{II-29}$$

$$v_n(t) = \frac{1}{2}\left[z_n\{i_{n-1}(t-\tau_n) - i_{n-1}(t+\tau_n)\} + v_{n-1}(t-\tau_n) + v_{n-1}(t+\tau_n)\right] \tag{II-30}$$

Therefore, the unknown voltage and current are calculated inductively, and their combination with Kirchhoff's current law will give a fault criterion $\xi(t)$ for the multi-terminal line.

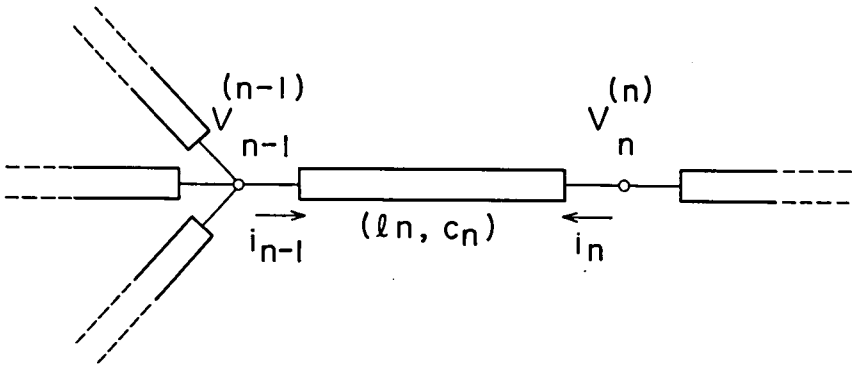

Fig. II-4 General multi-terminal transmission line

2.3 THEORY OF FAULT SELECTION

Selection of a faulted phase is important as well as fault detection. Consider an internal fault at F in a transposed line (Fig. II-5). Let a fault current vector in phase domain be $[i_F(t)]$. Then modal fault current vector is given by

$$[i_F^{(mode)}(t)] = [S]^{-1}[i_F(t)] \qquad \text{(II-31)}$$

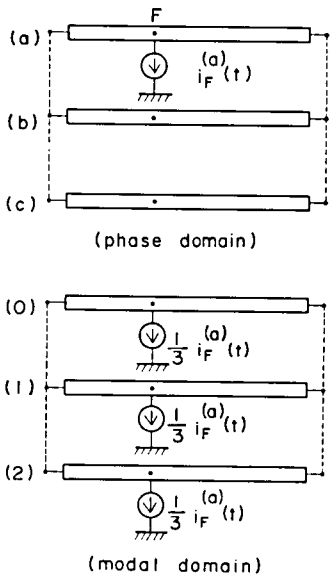

Fig. II-5 Representation of a single-phase fault in phase and modal domain

The fault criterion function of mode-k, $\xi^{(k)}(t)$, corresponds to the fault current of mode-k.

$$\xi^{(k)}(t) = i_F{}^{(k)}(t-\tau_1{}^{(k)}) \qquad k = 0,1,2 \tag{II-32}$$

To a phase-a-to-ground fault, the Karrenbauer transform gives the modal fault current vector as follows.

$$\begin{bmatrix} i_F{}^{(0)}(t) \\ i_F{}^{(1)}(t) \\ i_F{}^{(2)}(t) \end{bmatrix} = [S]^{-1} \begin{bmatrix} i_F{}^{(a)}(t) \\ 0 \\ 0 \end{bmatrix} = \begin{bmatrix} \frac{1}{3} i_F{}^{(a)}(t) \\ \frac{1}{3} i_F{}^{(a)}(t) \\ \frac{1}{3} i_F{}^{(a)}(t) \end{bmatrix} \tag{II-33}$$

Thus $\xi^{(0)}(t) \neq 0$, $\xi^{(1)}(t) \neq 0$, and $\xi^{(2)}(t) \neq 0$. It is noted here that phase-a is the basis of modal transform in the eqn. (II-33). If one changes the basis of transform from phase-a to -b, the modal current vector also changes to

$$\begin{bmatrix} i_F{}^{(0)}(t) \\ i_F{}^{(1)}(t) \\ i_F{}^{(2)}(t) \end{bmatrix} = \begin{bmatrix} \frac{1}{3} i_F{}^{(a)}(t) \\ 0 \\ \frac{1}{3} i_F{}^{(a)}(t) \end{bmatrix} \tag{II-34}$$

In this transform $\xi^{(0)}(t) \neq 0$, $\xi^{(1)}(t) = 0$, and $\xi^{(2)}(t) \neq 0$. Another basis change from phase-b to -c is possible, giving modal fault current vector as

$$\begin{bmatrix} i_F{}^{(0)}(t) \\ i_F{}^{(1)}(t) \\ i_F{}^{(2)}(t) \end{bmatrix} = \begin{bmatrix} \frac{1}{3} i_F{}^{(a)}(t) \\ \frac{1}{3} i_F{}^{(a)}(t) \\ 0 \end{bmatrix} \tag{II-35}$$

where $\xi^{(0)}(t) \neq 0$, $\xi^{(1)}(t) \neq 0$, and $\xi^{(2)}(t) = 0$. It is shown that the modal fault current vector is not invariant with the transform basis change. The calculations of $\xi^{(0)}(t)$, $\xi^{(1)}(t)$, and $\xi^{(2)}(t)$ to all types of fault are listed in Table II-1. It is noted that one can select correctly only 1LG fault when using the Karrenbauer transform. The same calculations as the above using the Clarke transform, are also listed in Table II-2. In this case the Clarke transform can select faulted phase not only in 1LG fault but also in 2LS and 3LS fault. It is interesting to note that the ability of fault selection is dependent on the transform method. This dependence seems due to the symmetry of transform matrix. Karrenbauer's transform matrix is symmetric, while Clarke's is not symmetric. As a matter of fact, asymmetry of [S] is desirable to fault selection. The inspection of two tables shows that two transforms can select the faulted phase in 1LG. This is promising in application, because the percentage of 1LG fault is very high in fault statistics.

fault / predicate		1LG			2LG			2LS			3LG	3LS
		a	b	c	a-b	b-c	c-a	a-b	b-c	c-a		
transform (a)	$\xi^{(0)}$	○	○	○	○	○	○	×	×	×	○	×
	$\xi^{(1)}$	○	○	×	○	○	○	○	○	○	○	○
	$\xi^{(2)}$	○	×	○	○	○	○	○	○	○	○	○
transform (b)	$\xi^{(0)}$	○	○	○	○	○	○	×	×	×	○	×
	$\xi^{(1)}$	×	○	○	○	○	○	○	○	○	○	○
	$\xi^{(2)}$	○	○	×	○	○	○	○	○	○	○	○
transform (c)	$\xi^{(0)}$	○	○	○	○	○	○	×	×	×	○	×
	$\xi^{(1)}$	○	×	○	○	○	○	○	○	○	○	○
	$\xi^{(2)}$	×	○	○	○	○	○	○	○	○	○	○

Table II-1 Truth value table of fault criterion $\xi^{(k)}(t)$ defined by Karrenbauer transform
'○' means $\xi^{(k)}(t) \neq 0$, and '×' means $\xi^{(k)}(t) = 0$.

predicate \ fault		1LG			2LG			2LS			3LG	3LS
		a	b	c	a-b	b-c	c-a	a-b	b-c	c-a		
transform (a)	$\xi^{(0)}$	○	○	○	○	○	○	×	×	×	○	×
	$\xi^{(1)}$	○	○	○	○	○	○	○	×	○	○	○
	$\xi^{(2)}$	×	○	○	○	○	○	○	○	○	○	○
transform (b)	$\xi^{(0)}$	○	○	○	○	○	○	×	×	×	○	×
	$\xi^{(1)}$	○	○	○	○	○	○	○	○	×	○	○
	$\xi^{(2)}$	○	×	○	○	○	○	○	○	○	○	○
transform (c)	$\xi^{(0)}$	○	○	○	○	○	○	×	×	×	○	×
	$\xi^{(1)}$	○	○	○	○	○	○	×	○	○	○	○
	$\xi^{(2)}$	○	○	×	○	○	○	○	○	○	○	○

Table II-2 Truth value table of fault criterion $\xi^{(k)}(t)$ defined by Clarke transform

2.4 THEORY OF FAULT LOCATION

Two schemes of fault location based on the travelling wave theory are proposed in a single phase line. Its extension to a three phase line is made simply.

2.4.1 Fault Location Scheme-1

An internal fault can be located by using v(t) and i(t) of single terminal [12]. Consider a fault at F in Fig. II-1, and assume that only $v_S(t)$ and $i_S(t)$ are available. According to eqn. (II-30), $v_F(t)$ is estimated by

$$\hat{v}_F(t,\tau_x) = \frac{1}{2}\left[v_S(t+\tau_x) + v_S(t-\tau_x) - z\{i_S(t+\tau_x) - i_S(t-\tau_x)\}\right] \qquad \text{(II-36)}$$

where τ_x is the unknown surge travelling time from F to S. It is possible to calculate $\hat{v}_F(t,\tau_x)$ with τ_x as a parameter. Suppose that the voltage at F be as

$$\hat{v}_F(t) \begin{cases} \neq 0 & \text{before fault inception} \\ = 0 & \text{after fault inception} \end{cases} \qquad \text{(II-37)}$$

Then one can locate a fault by finding τ_x^* which satisfies

$$\hat{v}_F(t,\tau_x^*) = 0 \qquad \text{(II-38)}$$

for any time t after fault inception. Fig. II-6 illustrates the location scheme-1. It would become less reliable when a fault impedance Z_F is not zero. In a case of $Z_F \neq 0$, $v_F(t)$ is not identically zero even after fault inception.

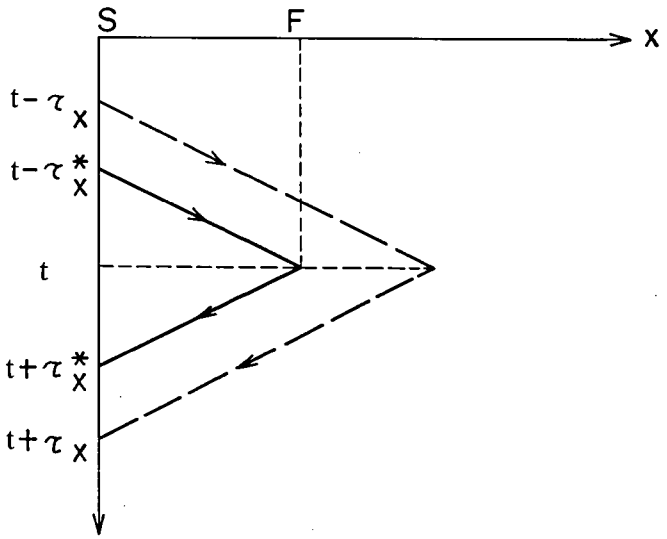

Fig. II-6 Fault location scheme-1

2.4.2 Fault Location Scheme-2

Two travelling waves propagating backward and forward are utilized in this method. The fault detection functions, $\xi(t)$ and $\zeta(t)$, measure the fault current at the point F:

$$\xi(t) = i_F(t - \tau_1) \tag{II-39}$$

$$\zeta(t) = i_F(t - \tau_2) \tag{II-40}$$

Before fault inception both $\xi(t)$ and $\zeta(t)$ are identically zero. But once fault happens they are neither identically zero nor equal each other. Fig. II-7 illustrates the idea of location scheme-2. The criterion $\zeta(t+\Delta t)$ is not equal to $\xi(t)$, for two waves pass through F at different time. The criterion $\zeta(t+\Delta t^*)$ is equal to $\xi(t)$, because two waves meet at the point F. In the latter case, the estimate given by the equation:

$$\tau_x = \frac{\tau - \Delta t^*}{2} \tag{II-41}$$

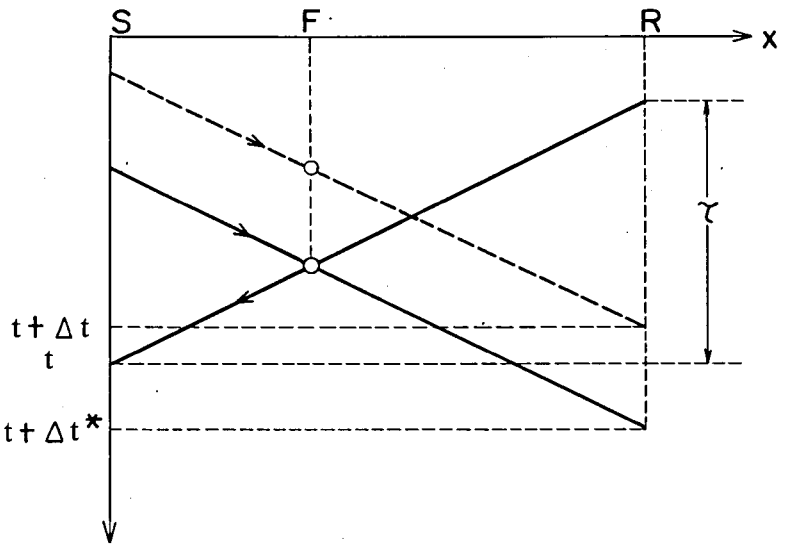

Fig. II-7 Fault location scheme-2

coincides correctly with the surge travelling time from F to S. Thus one can locate a fault by finding Δt^*. It is noted that the fault location by this method is possible regardless of the fault impedance, because it depends upon not the estimated values of fault current but the comparison of these.

When applied to a three phase line, two schemes are implemented in the modal lines. The ability of fault location is discussed here. When the Karrenbauer transform is applied to modal analysis, the fault current source is injected in the modal line where the symbol O is entered in Table II-1. For instance, the current source appears in every modal line at the 2LG of phase-a and b. The inspection of Table II-1 shows that at least one symbol X is entered in every row. This symbol is entered when a modal line does not contain the current source to a fault. In this case both $\xi(t)$ and $\zeta(t)$ are always zero in spite of a fault. Therefore one cannot locate all types of fault with single modal line. Of course, when using more than two modal lines, one can locate all types of faults.

The above discussions are also valid in applying Clarke transform. Single modal line is not enough to locate all types of fault, since every row of Table II-2 contains at least one X entry. The use of more than two modal lines, however, are sufficient to locate them.

2.5 CONCLUSION

This chapter has presented a new fault protection method based on the travelling wave theory. Its applications to fault detection, selection and location have been studied. The fundamental properties of the new protection method have been clarified, some of which are high speed in detection, high reliability in external fault, and low sensitivity with transient phenomena in a transmission line. It has been also shown that the method can be applied not only to three phase lines but also to multi-terminal lines. In a three phase case fault detection is performed in each modal line. One can build a truth table in which the decisions in modal lines are listed for all types of fault, and fault selection is made by this table. This chapter have also proposed two methods for fault location, and studied their ability.

The theoretical basis of the new protection method has been developed on a no-loss transmission line. An actual line, however, has series resistance, frequency dependent parameters and tends to be untransposed recently. Furthermore it is problematic whether one can know the precise line parameters. The effects of these factors in practical implementation will be discussed in CHAPTER III.

CHAPTER III ALGORITHM VERIFICATION AND OPTIMIZATION OF TRAVELLING WAVE DIFFERENTIAL PROTECTION FOR TRANSMISSION LINES [10, 11]

3.1 INTRODUCTION

In the previous chapter, the use of distributed parameter transmission line model was proposed. A fault transient analysis in this model leads one to note the behavior of the "travelling wave". Thus a new type of differential relay, referred to the d'Alembert relay was developed [1, 2]. The relay computes the travelling waves at local and remote ends, and takes their difference for the fault criterion. In a three-phase line,

$$\xi^{(k)}(t) = i_S{}^{(k)}(t) + i_R{}^{(k)}(t - \tau^{(k)}) - \frac{1}{z^{(k)}}\{v_S{}^{(k)}(t) - v_R{}^{(k)}(t - \tau^{(k)})\} \qquad \text{(III-1)}$$

defines the modal fault detecting function (k = 0,1,2). The direct implementation of the eqn. (III-1), however, makes the hardware system and the detection algorithm complex. So, a simplified version of the eqn. (III-1) is proposed here.

$$\xi(t) = i_S(t) + i_R(t-\tau) - \frac{1}{z}\{v_S(t) - v_R(t-\tau)\} \qquad \text{(III-2)}$$

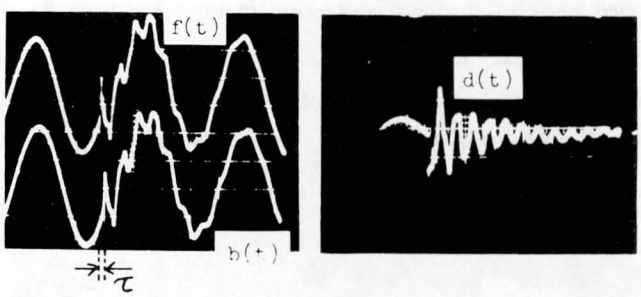

Fig. III-1 Comparison between travelling wave differential criterion and current differential one

which is a phasor implementation. Parameter τ (surge travel time) and z (surge impedance) are set to, for instance, the positive sequence values. To illustrate the unique protection scheme, a typical simulation result for an external fault by Transient Network Analyzer (=T.N.A.) is shown in Fig. III-1. f(t) and b(t) (see 3.4.1 for their definitions) are travelling waveforms at two terminals. Since $f(t-\tau)$ is nearly congruent to b(t), $\xi(t) \cong 0$. On the other hand, the differential current d(t) has an undesired output before and after fault inception. Thus d(t) may cause a misoperation to the external fault, but $\xi(t)$ does not.

The simplified d'Alembert relay (simply d'Alembert relay) is based on the eqn. (III-2). Since this is an approximation of the exact relation, studies on various factors affecting its performance are necessary. First of all, the d'Alembert relay neglects the mutual coupling. It approximates $\tau^{(0)}$ and $z^{(0)}$ with $\tau^{(1)}$ and $z^{(1)}$. Thus one has to evaluate this effect in the zero sequence circuit. Secondly, the line parameters more or less contain some amount of uncertainty. So the exact values of $\tau^{(1)}$ and $z^{(1)}$ could not be known. This necessitates the parameter sensitivity analysis in the positive sequence circuit. Thirdly, $\xi(t)$ of the eqn. (III-2) is calculated from the sampled values at time t and $t-\tau$. The sampling signals may deviate slightly from their preset times. This might be equivalent to the uncertainty of τ. Fourthly, the eqn. (III-2) neglects the series resistance of a line. It is necessary to evaluate its effect on the d'Alembert relay. Last, the actual line parameters are frequency dependent, especially the zero sequence resistance [3]. The eqn. (III-2) is correct for frequency independent model, so this assumption must be evaluated. These considerations call for studying the performance of eqn. (III-2) when some amount of uncertainty exists in τ and z, and when series resistance and frequency dependency are modelled exactly.

This chapter presents the verification and optimization studies of $\xi(t)$ with respect to τ and z, based on the transient analysis in a model power system. From these studies, the performance is optimized at the positive sequence parameter values. Let $\Delta\tau$ and Δz be the deviations from optimal values. It is shown that $\Delta\tau$ affects $\xi(t)$ much, but Δz does little. The former must be carefully suppressed, but the latter may be ignored in practical implementation. It is also shown that the series resistance adds only a negligibly small error to $\xi(t)$. On frequency dependency, the independent nature proves more sensitive to $\xi(t)$. Thus, the dependent nature is preferable to the d'Alembert relay. The above conclusions are derived from a lot of case studies. Their theoretical validations are followed.

3.2 VERIFICATION OF TRAVELLING WAVE DIFFERENTIAL PROTECTION FOR TRANSMISSION LINES

3.2.1 Digital Computation of Fault Transient

To verify the performance of the d'Alembert relay, one needs to prepare the relay input data whose frequency spectrum spreads well above the nominal frequency. In other words, one needs the data reflecting well the transient behavior of a transmission network. Digital computation of fault transients was performed to meet the requirement. Fig. III-2 shows a one-line diagram, and Table III-1 gives the line constants of the model transmission system. The model network consists of 500 kV and 275 kV overhead transmission lines, and 275 kV underground cables. One should be aware of the low surge impedance at the underground cables, which likely causes a waveform distortion, particularly a current waveform distortion. This has already been shown in Fig. III-1. The primary reason for the low surge impedance is the magnitude of a per unit length capacitance at the underground cable that is far greater than at the overhead line.

As is written in CHAPTER I, there are two alternatives in digital computation of fault transients: travelling wave method, and frequency transform method. The former method is used throughout this thesis, because of the simplicity in modelling system changes and the flexibility in applying to a large scale transmission network [4].

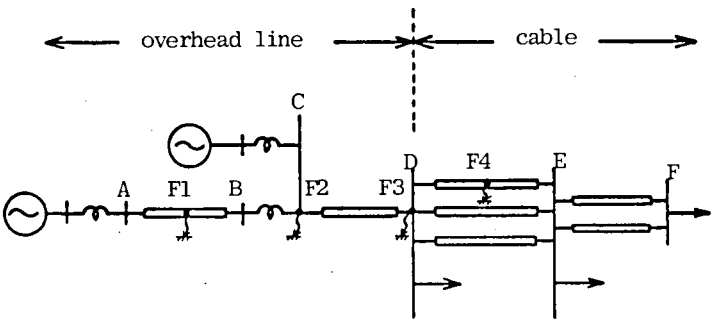

Fig. III-2 One line diagram of a model transmission system

A phase-a-to-ground fault and a phase-a-to-b short circuit fault were chosen to simulate. The choice is partly because of their high probabilities in actual systems and partly because of a motivation to examine an effect of the zero sequence circuit. Fig. III-3 illustrates some of the fault voltage and current waveforms for a phase-a-to-b short circuit fault at the point F4. The severe waveform distortion, particularly at the current waveform, is observed there. If one applies the conventional current differential protection scheme to the zone EF, the relay would be likely to misoperate for this fault.

Const / Zone	$r^{(0)}$	$\ell^{(0)}$	$C^{(0)}$	$\tau^{(0)}$	$Z^{(0)}$
A - B	0.00047	0.00252	0.00066	0.2321	1.954
C - D	0.00152	0.00955	0.00013	0.0301	8.571
D - E	0.00246	0.00228	0.00834	0.0972	0.529
E - F	0.00246	0.00234	0.00834	0.0985	0.530

Const / Zone	$r^{(1)}$	$\ell^{(1)}$	$C^{(1)}$	$\tau^{(1)}$	$Z^{(1)}$
A - B	0.00008	0.00114	0.00099	0.1912	1.073
C - D	0.00026	0.00331	0.00034	0.0286	3.120
D - E	0.00027	0.00156	0.00844	0.0819	0.432
E - F	0.00027	0.00153	0.00844	0.0797	0.428

Table III-1 Line constants of the model transmission system

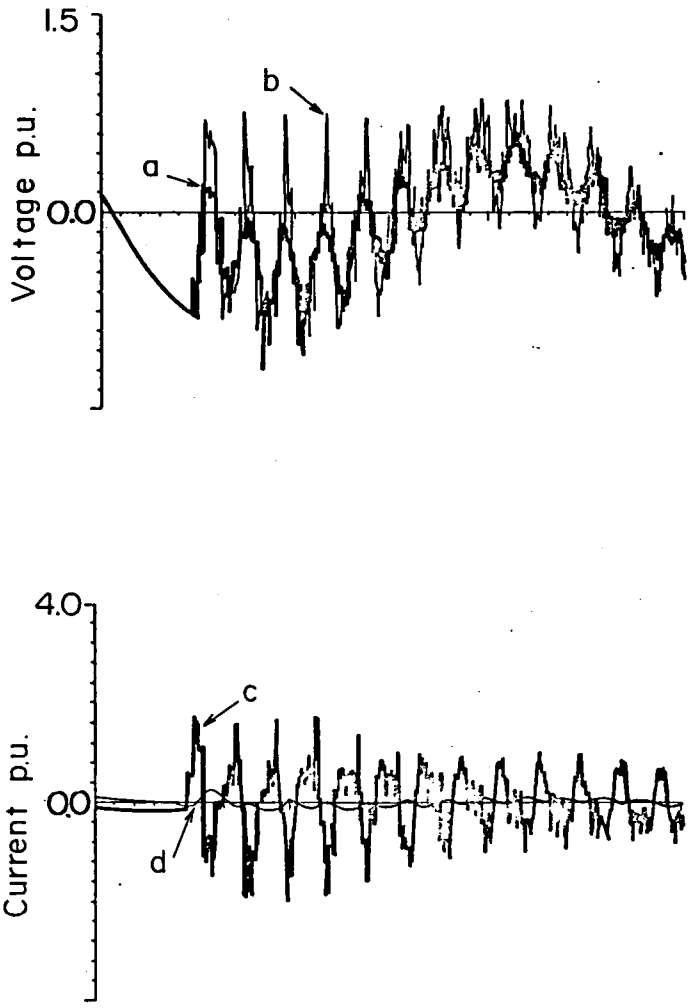

Fig. III-3 Fault voltage and current waveform in a phase-a-to-b short circuit at the point F4

(a) phase-a voltage at E
(b) phase-a voltage at F
(c) phase-a current at E flowing toward F
(d) phase-a current at F flowing toward E

3.2.2 Travelling Wave Differential Relay Simulation with Theoretical Fault Data

As digital computation of fault transients was made every 40.0 μsec, the travelling wave differential relay simulation, that is the computation of $\xi(t)$ of the eqn. (III-2), is also made at the same interval. Fig. III-4 shows typical results of the fault criterion function $\xi(t)$ calculated at the zone DE and EF. The top three are $\xi(t)$'s of the faulted and unfaulted zones at a single phase-to-ground fault, and the bottom three are those at a double phase short circuit fault. The criterion $\xi(t)$ of the faulted zone indicates the capability of detecting the fault in a short time period. On the other hand, the criterion of the unfaulted zone stays either at zero or around zero. One can see a difference in $\xi(t)$ between a ground fault and a short circuit fault. This is because of the simplification of the eqn. (III-1) with the eqn. (III-2). In other words, the zero sequence wave propagation is approximated by the positive sequence parameters. As there are no quantities of mode zero at the short circuit fault, the fault criterion indicates the zero value at the unfaulted zone even after the fault. But the criterion of the unfaulted zone is not identical to zero at the ground fault.

One can find a great advantage of the d'Alembert relay over the conventional current differential relay when comparing Fig. III-3 and Fig. III-4. Although a fault happens in the external zone, the magnitude of fault criterion of Fig. III-3 is so large as likely to make a misoperation. On the other hand, there is no possibility of misoperation in the bottom of Fig. III-4.

3.3 NUMERICAL APPROACH TO THE OPTIMIZATION OF TRAVELLING WAVE DIFFERENTIAL PROTECTION

3.3.1 Determination of Optimal Value of τ

Positive sequence line parameters were used for τ and z of the eqn. (III-2) to verify the protection performance of the d'Alembert relay. Here, an attempt is made to search the optimal setting in the (τ, z) plane. The reference point is taken at ($\tau^{(1)}$, $z^{(1)}$). This is the positive sequence surge propagation time and surge impedance. The optimization is made first on τ. Let $\Delta\tau$ be a deviation of τ from the reference $\tau^{(1)}$:

$$\Delta\tau = \tau - \tau^{(1)} \qquad \text{(III-3)}$$

and $\xi_{\Delta\tau}(t)$ be the fault criterion using $\tau = \tau^{(1)} + \Delta\tau$ and $z = z^{(1)}$:

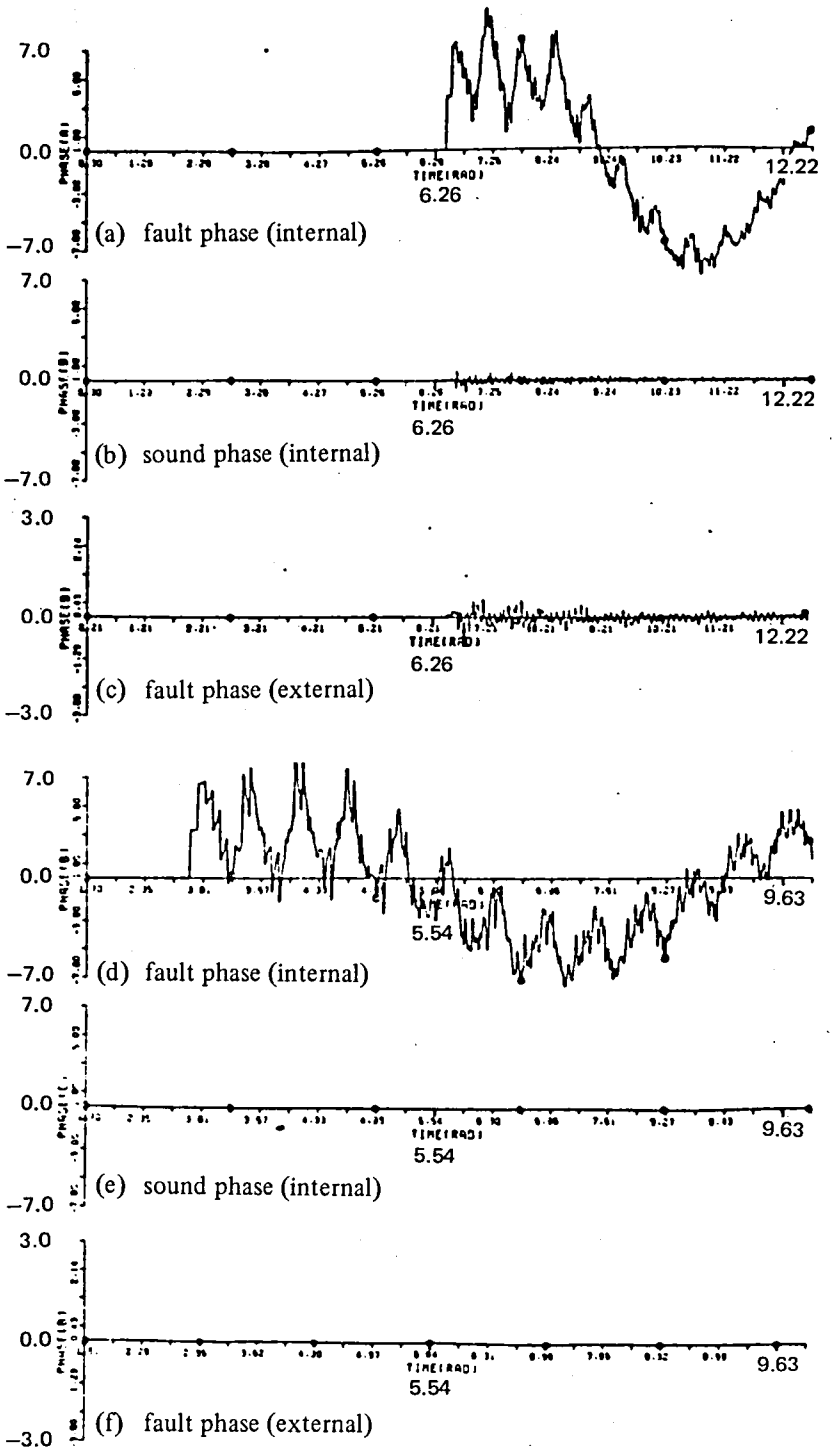

Fig. III-4 Some results of fault criterion $\xi(t)$ calculated at the zone DE and EF

$$\xi_{\Delta\tau}(t) = i_S(t) + i_R(t - (\tau^{(1)} + \Delta\tau)) - \frac{1}{z}\{v_S(t) - v_R(t - (\tau^{(1)} + \Delta\tau)\} \qquad \text{(III-4)}$$

The fault criterion $\xi_{\Delta\tau}(t)$ of the phase-a relay protecting the zone EF is simulated changing the fault point from F1 through F4. Fig. III-5 illustrates the criterion with $\Delta\tau = \pm 0.15\tau^{(1)}$ for a short circuit fault at the point F4. One needs a measure to compare the relaying performance. The measure, referred to a performance index, is defined as the maximum value of $|\xi_{\Delta\tau}(t)|$ for the external fault. That is

$$\xi_{\Delta\tau}^{max} \triangleq \max_t \{|\xi_{\Delta\tau}(t)|\} \qquad \text{(III-5)}$$

Fig. III-6 plots the index $\xi_{\Delta\tau}^{max}$, indicating the optimal value at $\tau = \tau^{(1)}$.

This analysis has shown that the surge propagation time be set at the positive sequence parameter $\tau^{(1)}$. One must deal with uncertainty in the parameter $\tau^{(1)}$ of a transmission line at the design of an actual relay. There are several reasons for uncertainty. An ideal transposition assumed in CHAPTER II may not be made at recent EHV and UHV transmission lines. An actual line may not be modelled by an uniform distributed-constant circuit. A computer relay calculates the fault criterion $\xi(t)$ using voltages and currents sampled at time t and $t-\tau^{(1)}$. However, one will see a slight deviation of the sampling time at both ends. Finally, the d'Alembert relay approximates the zero sequence parameters with the positive sequence ones. These factors create the uncertainty of $\tau^{(1)}$. Fig. III-6 shows clearly an impact of the uncertainty on the performance index. A small error in setting the surge propagation time constant results in degrading the relaying performance. Accordingly, one needs some countermeasures. The use of a low pass filter is discussed in the section 3.5.5.

3.3.2 Determination of Optimal Value of z

An attempt is made to search the optimal value of z, keeping the surge propagation time constant τ at $\tau^{(1)}$ and changing the surge impedance setting around $z^{(1)}$. Let Δz be a deviation of z from the reference $z^{(1)}$:

$$\Delta z = z - z^{(1)} \qquad \text{(III-6)}$$

and $\xi_{\Delta z}(t)$ be the fault criterion using $\tau = \tau^{(1)}$ and $z = z^{(1)} + \Delta z$:

$$\xi_{\Delta z}(t) = i_S(t) + i_R(t - \tau^{(1)}) - \frac{1}{z^{(1)}+\Delta z}\{v_S(t) - v_R(t - \tau^{(1)})\} \qquad \text{(III-7)}$$

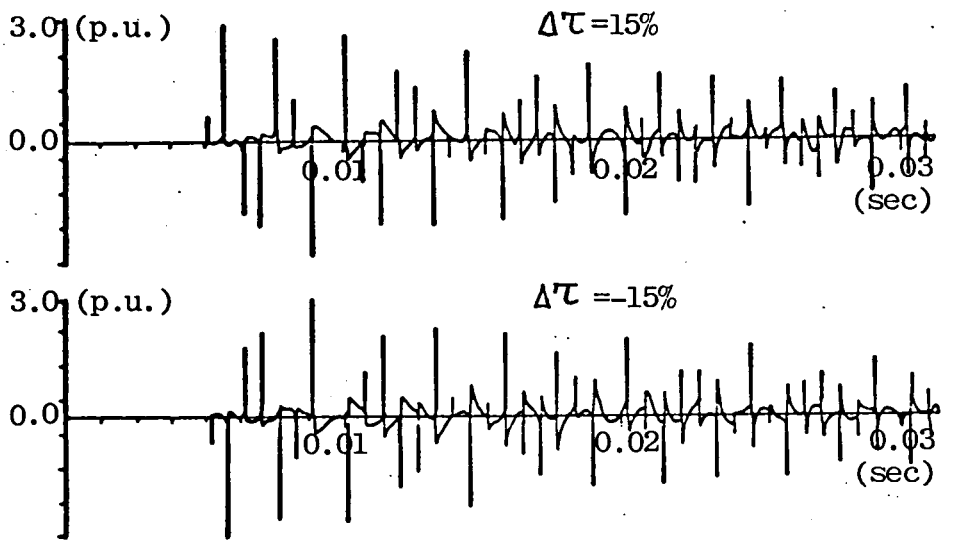

Fig. III-5 Fault criterion $\xi_{\Delta\tau}(t)$ with $\Delta\tau = \pm 0.15\tau^{(1)}$

The criterion $\xi_{\Delta z}(t)$ is computed for the faults at F1, F2, F3 and F4. Fig. III-7 shows the fault criterion with $z = \pm 0.15z^{(1)}$ for a short circuit fault at the point F4. The performance index here is defined as

$$\xi_{\Delta z}^{max} \triangleq \max_t \{ |\xi_{\Delta z}(t)| \} \tag{III-8}$$

That is the maximum value of $|\xi_{\Delta z}(t)|$ for the external faults. Fig. III-8 plots the index $\xi_{\Delta z}^{max}$ and indicates that the optimal value of z be $z^{(1)}$.

Like setting the surge propagation constant, one must deal with uncertainty in the parameter $z^{(1)}$ of a transmission line at the design of a relay. As is shown in Fig. III-8, the performance is not much degraded even if one sets a wrong value to the surge impedance constant. Therefore, a small error may be ignored at the implementation of the d'Alembert relay. One should compare the impact of the uncertainty in z with that in τ.

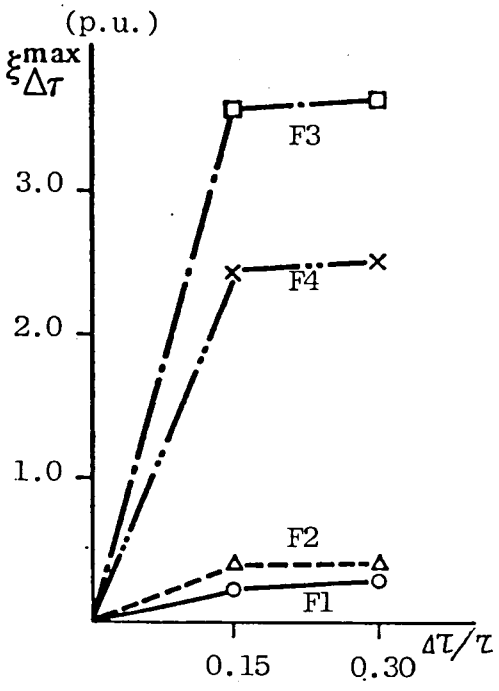

Fig. III-6 Performance index $\xi^{max}_{\Delta\tau}$

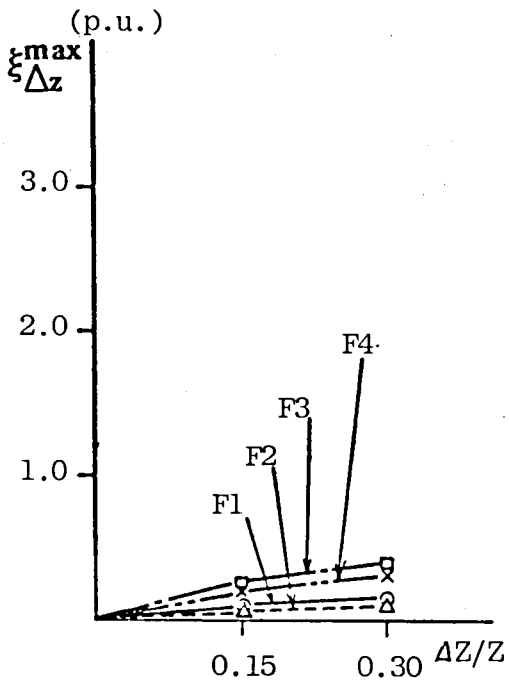

Fig. III-8 Performance index $\xi^{max}_{\Delta z}$

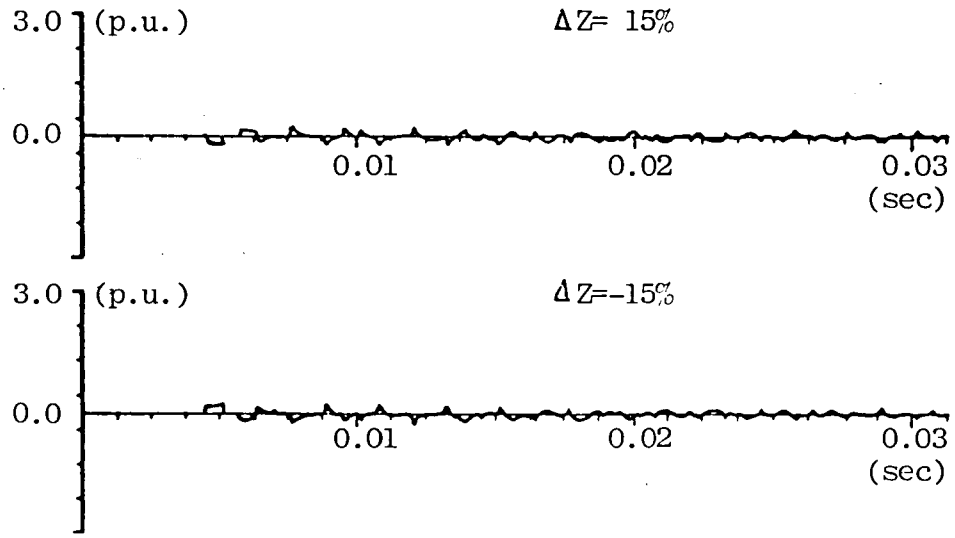

Fig. III-7 Fault criterion $\xi_{\Delta z}(t)$ with $\Delta z = \pm 0.15z$[1]

3.3.3 Numerical Evaluation of Transmission Line Loss Effect

A lossy transmission line can be treated putting a series resistance of (R/2) at the midpoint of no-loss line and that of (R/4) at both ends [5], as in Fig. III-9. In this model, a backward wave is expressed by the sum of two forward waves leaving both ends simultaneously. So the exact form of the wave difference should be written by the equation,

$$\xi_R(t) = i_S(t) + (\frac{1+h}{2})hi_R(t-\tau) + (\frac{1-h}{2})hi_S(t-\tau)$$
$$-\frac{1}{z'}\{v_S(t) - (\frac{1+h}{2})v_R(t-\tau) - (\frac{1-h}{2})v_S(t-\tau)\} \quad \text{(III-9)}$$

where,

$$h = \frac{z - \frac{R}{4}}{z + \frac{R}{4}} \quad \text{(III-10)}$$

$$z' = z + \frac{R}{4} \quad \text{(III-11)}$$

The eqn. (III-9) can be rewritten as

$$\xi_R(t) = \text{(backward wave at s)} + \alpha\cdot\text{(forward wave at R)} + (1-\alpha)\cdot\text{(forward wave at s)} \quad \text{(III-12)}$$

$$\alpha = \frac{1+h}{2}$$

In most cases, the actual value of α is very close to unity. For instance, α = 0.995 in the section EF in Fig. III-2. Therefore one can conclude $\xi_R(t) \cong \xi(t)$. The simulation results also show that $\xi_R(t)$ is almost congruent to $\xi(t)$. Thus the existence of the series resistance does not cause $\xi(t)$ to produce a critical error even if neglected.

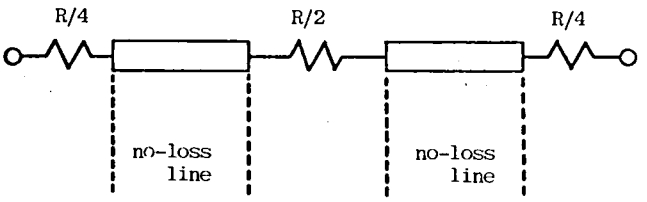

Fig. III-9 An approximate modelling of transmission line loss

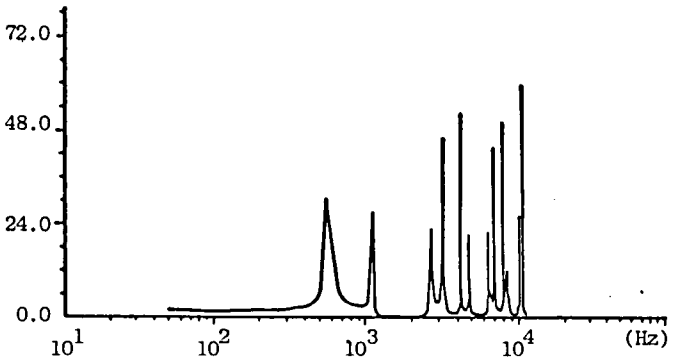

Fig. III-10 Frequency spectrum of $\xi_{\Delta T}(t)$ calculated from one cycle during fault data

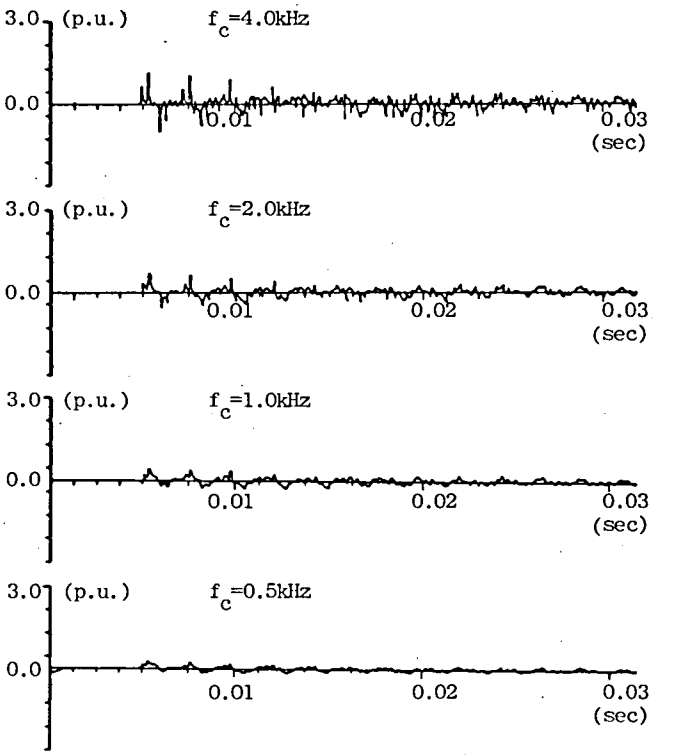

Fig. III-11 Effect of low pass filter on fault criterion $\xi_{\Delta T}(t)$
f_c=cut off frequency

3.3.4 Numerical Evaluation of Frequency Dependent Line Parameter Effect

As one of the clues to evaluate the frequency dependency, a frequency spectrum of $\xi(t)$ is calculated for post-fault one cycle data. Fig. III-10 plots the spectrum, which is obtained from the $\xi_{\Delta\tau}(t)$ in Fig. III-5. It should be noted that the high frequency components contribute much to the peaky output of $\xi_{\Delta\tau}(t)$. Roughly speaking, these components will be damped to small values when frequency dependency is assumed in the line parameters. This will result in smoothing the peaky output of $\xi_{\Delta\tau}(t)$. This is mainly due to the resistance highly dependent on frequency. Thus, the frequency dependency has a desired property to the d'Alembert relay.

Mathematical validations of the conclusions so far, are described in the section 3.4.

3.3.5 Discussion on Practical Protection Algorithm

Now a method is discussed to suppress the undesired output in $\xi(t)$, like in Fig. III-5, by means of a filter. Since the suppression of high frequency components has proved effective for the purpose, the use of a low pass filter with comparably high cutoff frequency is introduced. It should be noted here that most of the conventional relays utilize the band pass filter to extract the system frequency. Here is used the K/(1+sT) type of filters. First, the original v(t) and i(t) are fed into the filter, and then into the relay. A typical example is illustrated in Fig. III-11, where the filter damps the peaks of $\xi_{\Delta\tau}(t)$ to small values. Fig. III-12 summarizes the improvement of $\xi_{\Delta\tau}(t)$ by using filters. The low cutoff frequency is more preferable from the viewpoint of the relaying sensitivity. It, however, causes a long delay time in relay operation. So there would be a trade-off between sensitivity and speed.

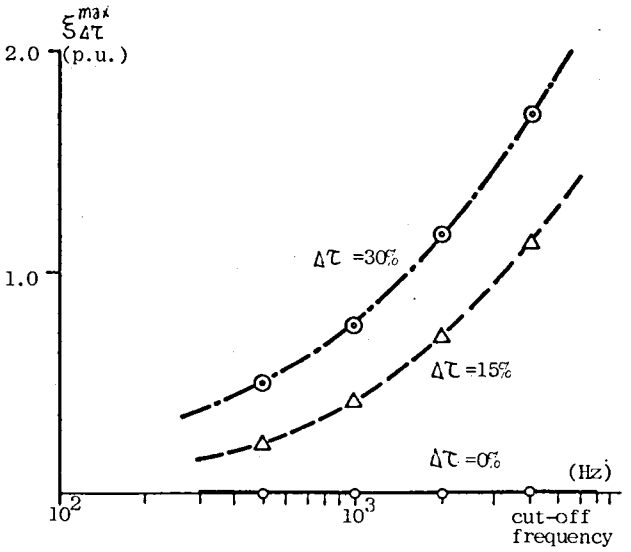

Fig. III-12 Improvement of performance index $\xi_{\Delta\tau}^{max}$ by the use of low pass filter

3.4 ANALYTICAL APPROACH TO THE OPTIMIZATION OF TRAVELLING WAVE DIFFERENTIAL PROTECTION

3.4.1 Travelling Wave Propagation Characteristics

In a transposed line shown in Fig. III-13, new variables f(t) and b(t) are defined:

$$f(t) = i(t) + \frac{1}{z}v(t) \tag{III-13}$$

$$b(t) = -i(t) + \frac{1}{z}v(t) \tag{III-14}$$

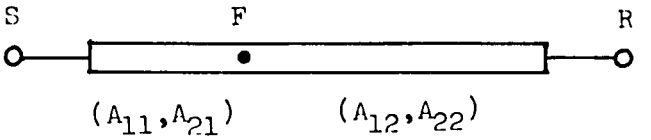

Fig. III-13 Definition of forward and backward response

As Snelson showed in his paper [6], the Fourier transforms of f(t) and b(t) satisfy the following relation:

$$\begin{bmatrix} B_S^{(k)}(j\omega) \\ B_R^{(k)}(j\omega) \end{bmatrix} = \begin{bmatrix} A_1^{(k)}(j\omega) & A_2^{(k)}(j\omega) \\ A_2^{(k)}(j\omega) & A_1^{(k)}(j\omega) \end{bmatrix} \cdot \begin{bmatrix} F_S^{(k)}(j\omega) \\ F_R^{(k)}(j\omega) \end{bmatrix}$$

$$k = 0,1,2 \tag{III-15}$$

where

$$A_1^{(k)}(j\omega) = \frac{(Z_0^{(k)}/z^{(k)} - z^{(k)}/Z_0^{(k)})\sinh\lambda^{(k)}d}{2\cosh\lambda^{(k)}d + (Z_0^{(k)}/z^{(k)} + z^{(k)}/Z_0^{(k)})\sinh\lambda^{(k)}d} \tag{III-16}$$

$$A_2^{(k)}(j\omega) = \frac{2}{2\cosh\lambda^{(k)}d + (Z_0^{(k)}/z^{(k)} + z^{(k)}/Z_0^{(k)})\sinh\lambda^{(k)}d} \tag{III-17}$$

$$Z_0^{(k)} = \sqrt{\frac{r^{(k)} + j\omega\ell^{(k)}}{g^{(k)} + j\omega c^{(k)}}} \qquad \text{(III-18)}$$

(characteristic impedance)

$$\lambda^{(k)} = \sqrt{(r^{(k)} + j\omega\ell^{(k)})\,(g^{(k)} + j\omega c^{(k)})} \qquad \text{(III-19)}$$

(propagation constant)

$z^{(k)}$ = real constant

The real constant $z^{(k)}$ is usually selected as in [7] to be

$$z^{(k)} = \lim_{\omega\to\infty} Z_0^{(k)} \qquad \text{(III-20)}$$

in the transient analysis for handling the transmission line loss and the frequency dependent nature [8, 9]. Unlike the transient analysis, one needs to use a real constant $z^{(k)}$ common to all modes in the d'Alembert relay. The positive sequence surge impedance at the nominal frequency

$$z^{(k)} = z = \sqrt{\frac{\ell^{(1)}(\omega_0)}{c^{(1)}(\omega_0)}} \qquad \text{(III-21)}$$

has been used. Although the use of $z^{(k)}$ of the eqn. (III-21) may modify $A_1{}^{(k)}(j\omega)$ and $A_2{}^{(k)}(j\omega)$, the eqn. (III-15) is still satisfied. Suppose that f(t) be a forward wave and b(t) a backward wave. As $A_1{}^{(k)}(j\omega)$ is defined to be (a backward wave at the local end)/(a forward wave at the local end), it is referred to a backward response of the transmission line. On the other hand, as $A_2{}^{(k)}(j\omega)$ is defined to be (a backward wave at the locan end)/(a forward wave at the remote end), it is referred to a forward response of the transmission line.

3.4.2 Analytical Evaluation of Practical Protection Algorithm

The Fourier transform of the Bergeron's equation is given by

$$B_S(j\omega) = e^{-j\omega\tau}F_R(j\omega) \tag{III-22}$$

Thus, the d'Alembert relay assumes that the wave propagation characteristics are

$$A_1^{(k)}(j\omega) = 0 \tag{III-23}$$

$$A_2^{(k)}(j\omega) = e^{-j\omega\tau} \tag{III-24}$$

This approximations will produce an undesired relay output.

< For external fault >

The eqn. (III-15) represents the exact relation between $B^{(k)}(j\omega)$ and $F^{(k)}(j\omega)$. Define $\Delta_1(j\omega)$, $\Delta_2(j\omega)$, $\Delta_3(j\omega)$ and $\Delta_4(j\omega)$ as follows:

$$\Delta_1(j\omega) = A_2^{(1)}(j\omega) - e^{-j\omega\tau} \tag{III-25}$$

$$\Delta_2(j\omega) = A_2^{(0)}(j\omega) - A_2^{(1)}(j\omega) \tag{III-26}$$

$$\Delta_3(j\omega) = A_1^{(0)}(j\omega) \tag{III-27}$$

$$\Delta_4(j\omega) = A_1^{(0)}(j\omega) - A_1^{(1)}(j\omega) \tag{III-28}$$

Transforming the model relations of the eqn. (III-15) into the phasor relations by using $\Delta_i(j\omega)$, one obtains a new relation

$$B_S(j\omega) = e^{-j\omega\tau}F_R(j\omega) + \Delta_1(j\omega)F_R(j\omega) + \Delta_2(j\omega)F_R^{(0)}(j\omega) + \Delta_3(j\omega)F_S(j\omega) + \Delta_4(j\omega)F_S^{(0)}(j\omega) \tag{III-29}$$

where $B_S(j\omega)$ and $F_R(j\omega)$ define the phasor quantities. Thus the error component $\epsilon(j\omega)$ of the simplified d'Alembert relay becomes

$$\epsilon(j\omega) = \Delta_1(j\omega)F_R(j\omega) + \Delta_2(j\omega)F_R^{(0)}(j\omega) + \Delta_3(j\omega)F_S(j\omega) + \Delta_4(j\omega)F_S^{(0)}(j\omega) \tag{III-30}$$

The physical interpretation of $\Delta_1(j\omega)$ is the difference between the forward response of mode-1 and $e^{-j\omega\tau}$. That of $\Delta_2(j\omega)$ is the model difference of two forward responses. $\Delta_3(j\omega)$ is the backward response of mode-1. And $\Delta_4(j\omega)$ is the model difference of two backward responses. It should be noted that $\Delta_2(j\omega)$ and $\Delta_4(j\omega)$ will not contribute to $\epsilon(j\omega)$ for a short circuit fault.

<For internal fault>

When an internal fault occurs, $B^{(k)}(j\omega)$ and $F^{(k)}(j\omega)$ are related as follows:

$$B_S^{(k)}(j\omega) = A_2^{(k)}(j\omega)F_R^{(k)}(j\omega) + A_1^{(k)}(j\omega)F_S^{(k)}(j\omega) - \Lambda^{(k)}(j\omega)I_F^{(k)}(j\omega) \quad \text{(III-31)}$$

where

$$\Lambda^{(k)}(j\omega) = A_{21}^{(k)}(j\omega)\{1 - A_{12}^{(k)}(j\omega)A_{11}^{(k)}(j\omega)^{-1}\}\{1 + A_{12}^{(k)}(j\omega)\} \quad \text{(III-32)}$$

$I_F^{(k)}(j\omega)$ = fault current in mode-k circuit

$A_{11}^{(k)}(j\omega)$ and $A_{21}^{(k)}(j\omega)$ are the wave propagation characteristics in subsection SF. $A_{12}^{(k)}(j\omega)$ and $A_{22}^{(k)}(j\omega)$ are those in subsection FR. Define $\Delta_5(j\omega)$ as

$$\Delta_5(j\omega) = \Lambda^{(0)}(j\omega) - \Lambda^{(1)}(j\omega) \quad \text{(III-33)}$$

Like the eqn. (III-29), the phasor form of the eqn. (III-31) becomes

$$B_S(j\omega) = e^{-j\omega\tau}F_R(j\omega) + \Delta_1(j\omega)F_R(j\omega) + \Delta_2(j\omega)F_R^{(0)}(j\omega) + \Delta_3(j\omega)F_S(j\omega) + \Delta_4(j\omega)F_S^{(0)}(j\omega) - \Delta_5(j\omega)I_F^{(0)}(j\omega) - \Lambda^{(1)}(j\omega)I_F(j\omega) \quad \text{(III-34)}$$

Thus one has an additional error component $\Delta_5(j\omega)I_F^{(0)}(j\omega)$ for the internal fault case. It should be noted that $\Lambda^{(1)}(j\omega)\ I_F(j\omega)$ does not contribute to the error. The physical

meaning of $\Delta_5(j\omega)$ is clear from the eqn. (III-33). $\Lambda(j\omega)$ defines the total effect of the wave travelling which is due to the existence of a fault current source. $\Lambda(j\omega)$ can be expanded in power series form,

$$\begin{aligned}\Lambda &= A_{21}(1 - A_{12}A_{11})^{-1}(1 + A_{12}) \\ &= A_{21}\{1 + A_{12} + A_{12}A_{11} + A_{12}A_{11}A_{12} + (A_{12}A_{11})^2 + \cdots\cdots\cdots\}\end{aligned} \qquad \text{(III-35)}$$

which defines all forms of propagation from F to S. All the error components of the d'Alembert relay are identified in terms of the transfer responses $\Delta_1(j\omega) \sim \Delta_5(j\omega)$. The followings are analytical considerations on the optimization of the d'Alembert relay.

The study is done using a typical 500 kV long transmission line of $r^{(0)} = 0.00114$, $c^{(0)} = 0.00066$, and $c^{(1)} = 0.00099$ (all values are p.u./km). This model line has the mode-1 surge impedance of 268Ω and surge travel time of 338 μsec. One can plot $\Delta_1(j\omega)$ in Fig. III-14 when the uncertainties of τ are 15% and 30%. If τ is correctly set to the mode-1 parameter, $\Delta_1(j\omega)$ is almost equal to zero. Fig. III-14 shows that the sensitivity of $\Delta_1(j\omega)$ to τ is fairly big. On the other hand the uncertainty of z affects the vector diagram of $A_2^{(1)}(j\omega)$ very little. So it can be concluded that the sensitivity to Δz is negligibly small. Fig. III-15 shows $\Delta_2(j\omega)$ when line parameters are frequency dependent. For comparison purpose $\Delta_2(j\omega)$ is also drawn when frequency independent. It should be noted that the frequency dependency has retained $\Delta_2(j\omega)$ in the vicinity of the origin more than the frequency independent case. This is explained as follows. In general the surge travel velocity of mode-1 is faster than that of mode-0, and this difference causes $\Delta_2(j\omega)$. When line parameters are dependent on frequency, the higher the frequency is the smaller the difference is. And it has been proved that $\ell^{(0)}$ contributes to this phenomena best of all parameters. It is ideal for $\Delta_2(j\omega)$ to be zero, since this causes no error output to the d'Alembert relay. In general it can be said that the smaller $\Delta_2(j\omega)$ the smaller the error is. As is noted above, the frequency dependent nature has the effect of shrinking the vector diagram of $\Delta_2(j\omega)$. This implies that the nature works for decreasing the error output caused by $\Delta_2(j\omega)$. It can be shown that other vectors, $\Delta_1(j\omega)$, $\Delta_3(j\omega)$, $\Delta_4(j\omega)$ and $\Delta_5(j\omega)$ have the same property as $\Delta_2(j\omega)$. Thus, the frequency dependent nature does have the desired property to the d'Alembert relay.

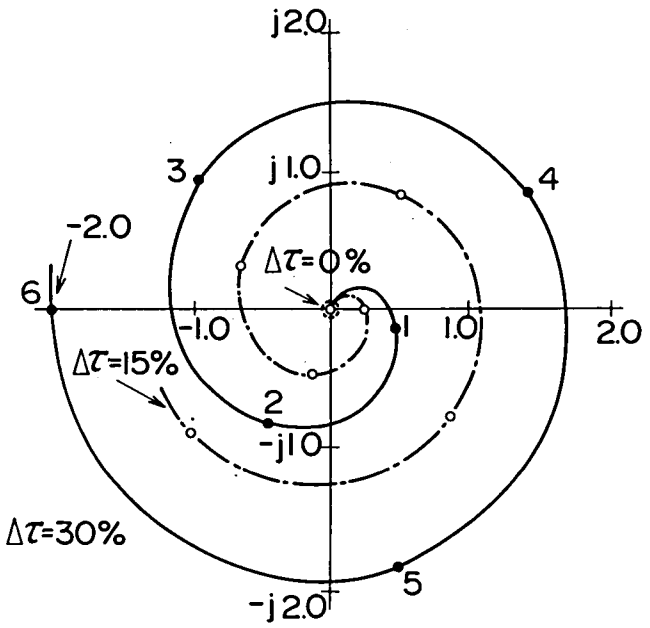

Fig. III-14 Vector diagram of $\Delta_1(j\omega)$ with $\Delta\tau$ being $0.15\tau^{(1)}$ and $0.30\tau^{(1)}$

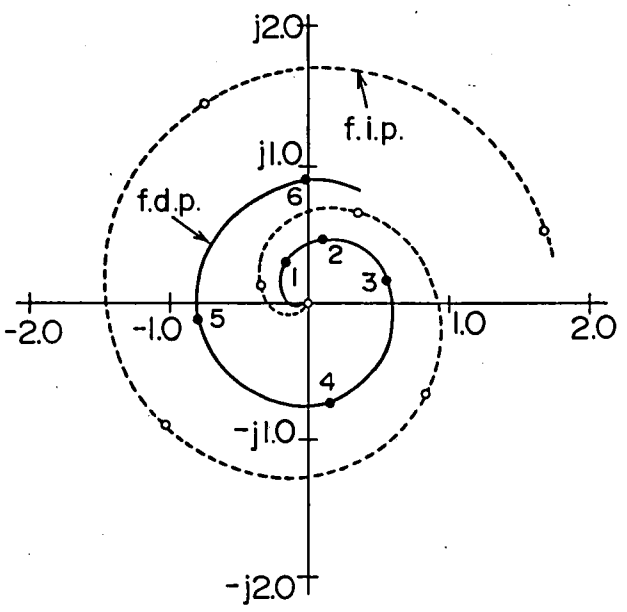

Fig. III-15 Vector diagram of $\Delta_2(j\omega)$ with and without frequency dependent line parameter

3.5 CONCLUSION

Following the theoretical development [2], this chapter has presented some sensitivity studies on the d'Alembert relay for its practical implementation. The study has covered the analysis on the effect of parameter uncertainty, series resistance and frequency dependent nature. The uncertainty of τ has proved more critical to the relay, but that of z less critical. Some countermeasures will be needed for suppression of $\xi_{\Delta\tau}(t)$. In this chapter a low pass filter has been proposed to suppress it and the filter method has worked effectively for this purpose. It has also been shown that the series resistance can be ignored without affecting $\xi(t)$. On the frequency dependency of line parameters, it has proved to be preferable to the d'Alembert relay. These results have been validated by a mathematical analysis.

CHAPTER IV HIGH SPEED DIRECTIONAL PROTECTION FOR TRANSMISSION LINES BASED ON LAPLACE TRANSFORM THEORY [9]

4.1 INTRODUCTION

One of the ideas identifying the functional requirements of a computer relay is to divide the process into 3 blocks: signal sensing, fault measuring, and decision making. The first block deals with signal acquisition and conditioning for later processing. The second block generally provides a fault criterion as an output. As there are many fault measures, there have been many computer algorithms to measure the criterion to identify a fault. The most common is an impedance observed at a relaying point. The final block is to decide whether to issue or not to issue a trip signal, and it begins to interest relay engineers with particular reference to computer relaying [1].

The following equation is widely used for distance protection of a transmission line.

$$v(t) = Ri(t) + L\frac{di(t)}{dt} \tag{IV-1}$$

Two approaches are possible to measure the fault distance. One is to make the Fourier transform of the eqn. (IV-1), that is

$$V(j\omega) = RI(j\omega) + j\omega LI(j\omega) \tag{IV-2}$$

and to measure the impedance $Z(j\omega)$ by the equation [2],

$$Z(j\omega) \triangleq \frac{V(j\omega)}{I(j\omega)} = R + j\omega L \tag{IV-3}$$

The major concern of this approach is how to get $V(j\omega)$ and $I(j\omega)$. The other is to solve R and L from a set of algebraic equation, for instance

$$\int_{t_1}^{t_2} v(t)dt = R \int_{t_1}^{t_2} i(t)dt + L[i(t_2) - i(t_1)] \qquad \text{(IV-4)}$$

$$\int_{t_3}^{t_4} v(t)dt = R \int_{t_3}^{t_4} i(t)dt + L[i(t_4) - i(t_3)] \qquad \text{(IV-5)}$$

which are obtained by integrating the eqn. (IV-1). The major concern here is how to do an effective integration [3]. The distance concept has provided relay engineers with an effective measure to identify a fault and its direction.

The prime purpose of this chapter is to present a new concept of directional detection and to provide more effective measure for high speed computer relaying. On the condition that $i(t) = 0$ for $t < 0$, the Laplace transform of the eqn. (IV-1) is written as

$$I(s) = \frac{1}{R + sL} V(s) \qquad \text{(IV-6)}$$

which leads to an equivalent equation in the time domain,

$$i(t) = \int_0^t v(t - u)y(u)du \qquad \text{(IV-7)}$$

where $y(t)$ is the inverse Laplace transform of $1/(R + sL)$, and called a weighting function (or an impulse response). The eqn. (IV-7) is a Volterra's integral equation of the first kind, and $y(t)$ can be solved when $i(t)$ and $v(t)$ are known. This chapter explores the ability of $y(t)$ to identify a fault and its direction through theoretical studies, comparing with the Finite Spectral Approach by John and Martin [4]. This chapter also discusses the effect of a filter used for signal conditioning on the accuracy of the directional detection. Finally, the new scheme is discussed with relation to a recent development of the directional protection based on the travelling wave concept [5]. A numerical solution method of the Volterra's integral equation of the first kind is provided in APPENDIX III.

4.2 THEORETICAL BASIS OF HIGH SPEED DIRECTIONAL PROTECTION FOR TRANSMISSION LINES

4.2.1 Signal Requirement for Laplace Transform

In applying the Laplace transform to the eqn. (IV-1), the voltage v(t) is chosen such that $v(t) = 0$ for $t < 0$ and $v(t) \neq 0$ for $t \geq 0$. On the other hand, the current i(t) must be carefully chosen such that i(t) be the response of a network to the input of v(t). Although the object was different, John and Martin's idea [6] was felt adequate to meet the requirement. They proposed to pick up the voltage and current such that

$$v_{ro}(t) = \begin{cases} 0 & t < 0 \\ v(t) & t \geq 0 \end{cases} \qquad \text{(IV-8)}$$

$$i_{ro}(t) = \begin{cases} 0 & t < 0 \\ i(t) - i(0)\exp(-t/T_c) & t \geq 0 \end{cases} \qquad \text{(IV-9)}$$

where T_c is the time constant of a line. Then, the fault direction was identified from the solution of the eqn. (IV-7) in a way that if $y(t) > 0$, the fault is ahead and if $y(t) < 0$, the fault is behind. This scheme proved effective to detect a fault direction, but it turned out to be susceptible to failure in a limited case. One major drawback of their scheme is the possibility to measure a wrong direction of the fault when the current has a dc offset component. APPENDIX IV explains why. As one of the solutions to circumvent the difficulty, the following approach is presented.

4.2.2 Protection Algorithm Definition for Single Phase Transmission Line

According to the superposition principle of the linear network theory, a faulted network is decomposed into a pre-fault and pure-fault network. Fig. IV-1 shows the decomposition. The voltage v"(t) and current i"(t) of the pure-fault network are represented by

$$v''(t) = v(t) - v'(t) \qquad \text{(IV10)}$$

$$i''(t) = i(t) - i'(t) \qquad \text{(IV-11)}$$

where v'(t) and i'(t) are defined in the pre-fault network. Let $v_{r1}(t)$ and $i_{r1}(t)$ be defined as

$$v_{r1}(t) \triangleq v''(t) \tag{IV-12}$$

$$i_{r1}(t) \triangleq -i''(t) \tag{IV-13}$$

Then, $v_{r1}(t)$ and $i_{r1}(t)$ satisfy the following equation.

$$i_{r1}(t) = \int_0^t v_{r1}(t - u)y(u)du \tag{IV-14}$$

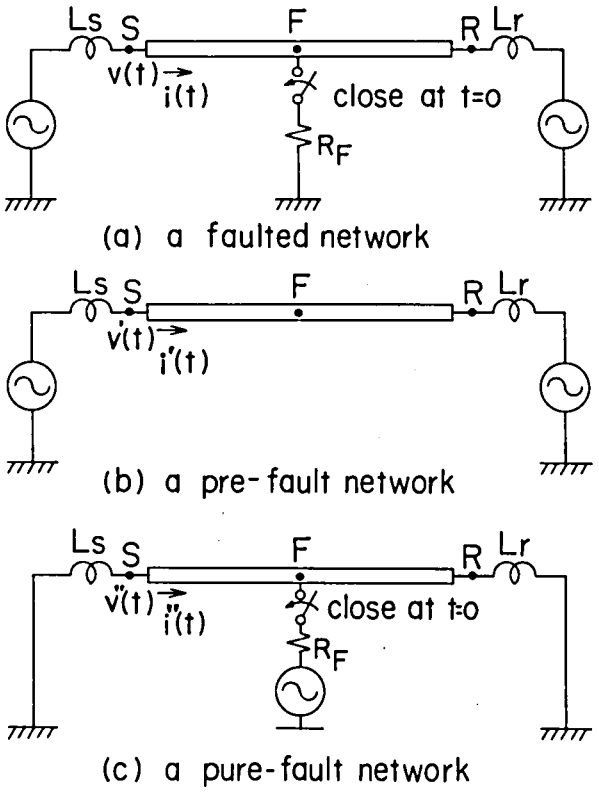

Fig. IV-1 A faulted network and its equivalent decomposition.

where the time zero is chosen at the instance of a fault occurrence. It should be noted that from their definitions $v_{r1}(t)$ and $i_{r1}(t)$ are theoretically zero for $t < 0$, and both satisfy the signal requirement for Laplace transform.

Assume that both the behind loop and ahead loop impedance of the pure-fault network be inductive, that is $j\omega L_b$ and $j\omega L_f$ respectively. As the transfer function Y(s) corresponding to y(t) is $1/sL_b$ for an ahead fault, the weighting function becomes

$$y(t) = \frac{1}{L_b} > 0 \qquad \text{(IV-15)}$$

As Y(s) at a behind fault is $-1/sL_f$, the weighting function becomes

$$y(t) = -\frac{1}{L_f} < 0 \qquad \text{(IV-16)}$$

Therefore, the fault direction is decided from the rule such that if $y(t) > \delta$, the fault is in the forward direction otherwise the fault is in the backward direction, where $\delta > 0$ is a pick up constant value.

4.2.3 Protection Algorithm Definition for Three Phase Transmission Lines

A mutual coupling exists in a 3-phase line. Taking into account the main object that is to detect a fault and its direction, a simplified scheme represented by the equation:

$$i_{r1}^{(p)}(t) = \int_0^t v_{r1}^{(p)}(t - u)y^{(p)}(u)du$$

$$p = \{a, b, c\} \qquad \text{(IV-17)}$$

is studied throughout this chapter, ignoring the mutual coupling effect. The directional detection is carried out independently at each phase in a way that if $y^{(p)}(t) > \delta$ then the fault is ahead at phase-p, otherwise it is behind.

4.3 VERIFICATION OF HIGH SPEED DIRECTIONAL PROTECTION FOR TRANSMISSION LINES

4.3.1 Outline of Digital Computer Simulation

The theoretical data of fault transients in a model power system shown in Fig. IV-2 is calculated by the electromagnetic transient program [7], and stored in a disk file for later simulation. The relaying program consists of 3 subprograms: signal sensing, fault measuring, and decision making subprograms. The signal sensing subprogram reads the theoretical data and simulates a filter for signal conditioning. The filter whose transfer function is given by

$$F_1(s) = \frac{K_1\left(1 + \frac{s^2}{\omega_p{}^2}\right)}{\left(1 + \frac{s}{\omega_1}\right)\left(1 + \alpha\frac{s}{\omega_2} + \frac{s^2}{\omega_2{}^2}\right)} \qquad \text{(IV-18)}$$

where $K_1 = 1.03386$, $f_1 = \omega_1/2\pi = 188.46$ Hz, $f_2 = \omega_2/2\pi = 243.69$ Hz, $f_p = \omega_p/2\pi = 600.00$ Hz, $\alpha = 1.2633$, is simulated by an equivalent digital filter. The fault measuring subprogram solves the eqn. (IV-17) by the MacLaurin's method of the first order [8]. According to the method, a numerical solution of the eqn. (IV-17) is obtained as follows. Let T be a sampling interval and let $\{x_1, x_2, \cdots\}$ be a set of sampled value $\{x(T), x(2T), \cdots\}$ of a time function x(t).

$$\text{at } t = T,\ i_1 \cong v_1 \cdot y_1 \cdot T \qquad \text{(IV-19)}$$

$$\text{at } t = 2T,\ i_2 \cong v_2 \cdot y_1 \cdot T + v_1 \cdot y_2 \cdot T \qquad \text{(IV-20)}$$

$$\text{at } t = 3T,\ i_3 \cong v_3 \cdot y_1 \cdot T + v_2 \cdot y_2 \cdot T + v_1 \cdot y_3 \cdot T \qquad \text{(IV-21)}$$

$$\vdots$$

First, y_1 is obtained from the eqn. (IV-19), then y_2 is obtained from the eqn. (IV-20), and then y_3 is obtained from the eqn. (IV-21), and then $\cdots$. Thus, the solution $y(t) = \{y_1, y_2, \cdots\}$ is reached.

The decision making subprogram accumulates $\{y_1, y_2, \cdots\}$ to get a scalar function $\eta(t) = \{\eta_1, \eta_2, \cdots\}$ defined by

$$\eta_K \triangleq \sum_{j=1}^{K} y_j \qquad \text{(IV-22)}$$

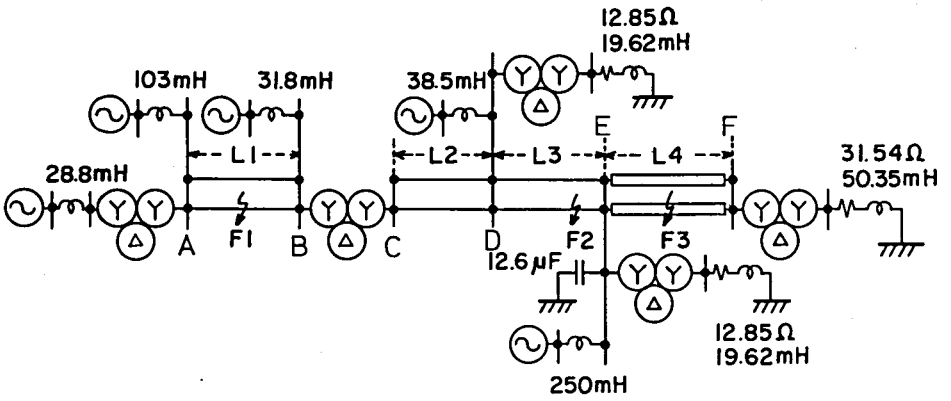

Constant / line	$r^{(0)}$ Ω/Km	$\ell^{(0)}$ mH/Km	$C^{(0)}$ μF/Km	$\lambda^{(0)}$ $\times 10^{-3}$ rad/Km	$Z^{(0)}$ Ω
	$r^{(1)}$ Ω/Km	$\ell^{(1)}$ mH/Km	$C^{(1)}$ μF/Km	$\lambda^{(1)}$ $\times 10^{-3}$ rad/Km	$Z^{(1)}$ Ω
L 1	0.11480	2.2886	0.00523	1.0869	662
	0.02083	0.8984	0.01291	1.0699	264
L 2	0.11570	2.2989	0.00526	1.0925	661
	0.01974	0.7968	0.01456	1.0701	234
L 3	0.11570	2.2989	0.00526	1.0925	661
	0.01974	0.7968	0.01456	1.0701	234
L 4	0.55400	0.9942	0.35567	5.9076	53
	0.02549	0.4020	0.35567	3.7565	34

Fig. IV-2 A model power system and its line constants.

and makes decision whether a fault has or has not taken place in the forward direction by the rule that for a threshold $\delta > 0$ and a positive integer $K > 0$, if $\eta_K > \delta$ then a fault is ahead, otherwise a fault is behind. In the later simulations, the sampling interval time T is chosen at 800 μsec.

4.3.2 Some Examples of Simulation Results

The results are discussed for a single phase fault and a double phase fault at the point F_3 in Fig. IV-2, in which the maximum dc offset current exists in the fault current. Fig. IV-3 (a) and (b) show y(t) of the faulted and unfaulted phase for the single phase fault. The decision function $\eta(t)$ goes up rapidly at the faulted phase, while $\eta(t)$ increases slowly at the unfaulted phase. The latter phenomena comes from the neglection of the mutual coupling. Thus, it seems reasonable to adopt an inverse-time characteristics for making final decision.

Fig. IV-3 (c) shows y(t) of the faulted phase of the phase-b to phase-c circuit fault. Like the case of Fig. IV-3 (a), the decision function $\eta(t)$ increases steeply enough to detect the fault direction. On the other hand, both $v_{r1}{}^{(a)}(t)$ and $i_{r1}{}^{(a)}(t)$ are zero throughout the simulation period. (Note that phase-a is unfaulted.) This is because the voltage and current of the unfaulted phase keep their steady state value even after the double phase short circuit has taken place. It is noted that the fault measuring subprogram starts solution of y(t) as soon as it detects nonzero $v_{r(t)}$.

For another fault condition, for instance the fault without dc offset current, the decision function $\eta(t)$ shows almost the same nature as the above one. The heart of the scheme lies in the idea applying the eqn. (IV-12) and (IV-14) to the solution of a weighting function. The idea shows some advantages over the previous one [4] which was based on the eqn. (IV-8) and (IV-9). First, it is easier to have a signal satisfying the requirement for the Laplace transform. The computational burden of the relay program is reduced. Second, as shown in Fig. IV-1 (c), a weighting function y(t) is invariant with a fault resistance R_F. This nature plays a central role in making the directional detection stable and accurate. Third, $v_{r1}(t)$ and $i_{r1}(t)$ satisfy the eqn. (IV-14) exactly, assuring that the scheme detects a fault direction correctly. Last, the time to reach the final decision is very short. As shown in Fig. IV-3, one quarter cycle is long enough to identify a fault and its direction. Therefore, the scheme will find its application in the high-speed line protection, that is primary protection use.

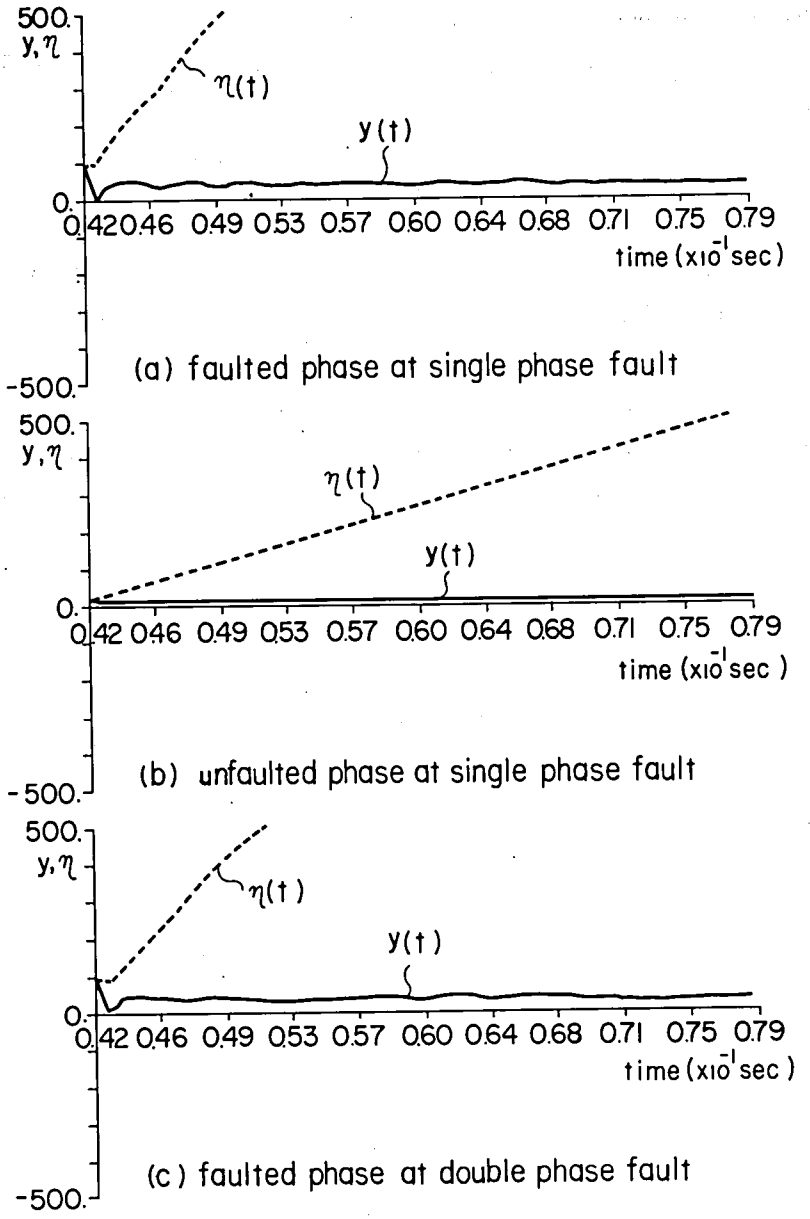

Fig. IV-3 Result of y(t) (= weighting function) and η(t) (= decision function) based on theoretical data.

4.4 OPTIMIZATION OF HIGH SPEED DIRECTIONAL PROTECTION FOR TRANSMISSION LINES

4.4.1 Optimization on Filter Characteristics

The filter expressed by the eqn. (IV-18) has been used for signal conditioning for both theoretical and experimental studies. As a filter transient is overlaid on a fault transient just after a fault inception and the proposed scheme has the working principle on the latter one, it is very important to design a filter so that it will not mask the actual fault transient. To discuss such an effect, two filters are studied. One is the filter of the eqn. (IV-18), and the other is a Butterworth low pass filter whose transfer function is

$$F_2(s) = \frac{K_2}{\prod_{k=1}^{7} (s - s_k)} \tag{IV-23}$$

where

$$s_k = \omega_c \exp j\pi[1/2 + 2(k - 1)/14]$$
$$k = 1,2, \cdots ,7 \tag{IV-24}$$

and $f_c = \omega_c/2\pi = 500.00$ Hz.

The theoretical data for $v_{r1}(t)$ and $i_{r1}(t)$ of the eqn. (IV-14) are shown in Fig. IV-4, where the solid curves are obtained by the filter $F_1(s)$, while the dashed curves are obtained by the filter $F_2(s)$. $F_1(s)$ reproduces the original fault transient faithfully, but $F_2(s)$ modulates the original transient, making the relay susceptible to failure in detecting a fault direction.

The scheme bases its operating principle on the fault transient which is observed in the pure-fault network of Fig. IV-1 (c). Much care must be taken for the filter selection, prior to applying the scheme.

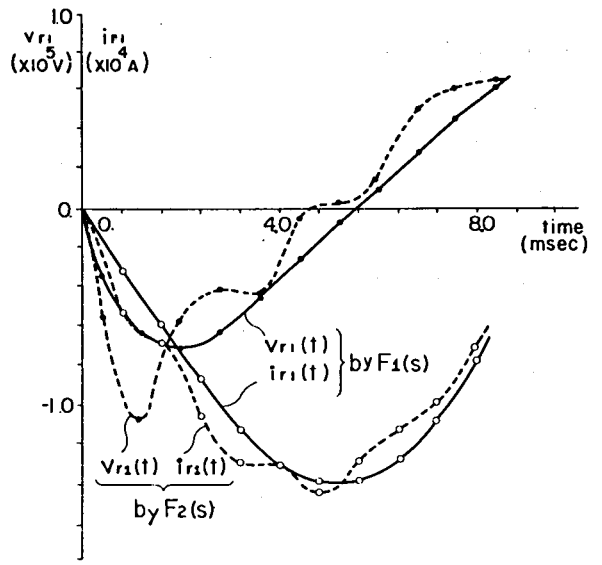

Fig. IV-4 Comparison of the theoretical signals provided by different filter.

4.4.2 Optimization on Solution Method of the Volterra's Integral Equation

As the fundamental idea is to identify the fault direction through the weighting function y(t) of the eqn. (IV-17), it is mandatory to solve the integral equation. For the type of the eqn. (IV-17), that is the Volterra's integral equation of the 1st kind, the MacLaurin's numerical solution method goes following way.

Consider a numerical integration of

$$I = \int_{-\frac{H}{2}}^{\frac{H}{2}} f(x)dx \qquad \text{(IV-25)}$$

by a weighted summation

$$A = (R_1^n f_1 + R_2^n f_2 + \cdots R_n^n f_n)H \qquad \text{(IV-26)}$$

where f_i is the value of f(x) at $x = x_i$, and R_i^n is the weight attached to the value f_i. The weighting values are determined so as to minimize the difference |I-A|. The MacLaurin's method partitions the interval $[-\frac{H}{2}, \frac{H}{2}]$ into n subintervals each having an equal length,

and selects x_i at the center of the i-th subinterval. Then $\{R_1^n, R_2^n, \cdots, R_n^n\}$ is determined as follows,

for n=1, $x_1 = 0$, $R_1^1 = 1$; 1st order formula

for n=2, $x_1 = -\frac{1}{4}H$, $R_1^2 = \frac{1}{2}$

$x_2 = \frac{1}{4}H$, $R_2^2 = \frac{1}{2}$; 2nd order formula

for n=3, $x_1 = -\frac{1}{3}H$, $R_1^3 = \frac{3}{3}$

$x_2 = 0$, $R_2^3 = \frac{2}{8}$

$x_3 = \frac{1}{3}H$, $R_3^3 = \frac{3}{8}$; 3rd order formula

for n=4, $x_1 = -\frac{3}{8}H$, $R_1^4 = \frac{13}{48}$

$x_2 = -\frac{1}{8}H$, $R_2^4 = \frac{11}{48}$

$x_3 = \frac{1}{8}H$, $R_3^4 = \frac{11}{48}$

$x_4 = \frac{3}{8}H$, $R_4^4 = \frac{13}{38}$; 4th order formula

$\vdots$

The n-th order formula is applied iteratively to the intervals [0, nT], [nT, 2nT], $\cdots$ [n(k−1)T, nkT], $\cdots$.

Table IV-1 shows a comparison of y(t) calculated by the 1st, 2nd, 3rd, and 4th order formula. As easily noted, there is no significant difference among these results. The MacLaurin's method of the 1st order, which has been used in the digital simulations, will be sufficiently accurate.

E3=x10^3

time (msec)	1st order	2nd order	3rd order	4th order
0.040	0.335 E3	0.335 E3	0.335 E3	0.335 E3
0.120	0.279 E3	0.279 E3	0.279 E3	0.279 E3
0.200	0.232 E3	0.232 E3	0.231 E3	0.231 E3
0.280	0.193 E3	0.193 E3	0.193 E3	0.193 E3
0.360	0.161 E3	0.161 E3	0.161 E3	0.161 E3
0.440	0.134 E3	0.134 E3	0.133 E3	0.134 E3
0.520	0.111 E3	0.111 E3	0.111 E3	0.111 E3
0.600	0923 E2	0.923 E2	0.923 E2	0.921 E2
0.680	0.766 E2	0.766 E2	0.763 E2	0.767 E2
⋮	⋮	⋮	⋮	⋮

Table IV-1 Comparison of the MacLaurin's numerical solution methods in solving the Volterra's integral equation of the 1st kind

4.5 THEORETICAL COMPARISON WITH TRAVELLING WAVE BASED HIGH SPEED DIRECTIONAL PROTECTION

A very high-speed directional relay has been recently developed based on the travelling wave concept [5]. The relay applies the signals of the eqn. (IV-12) and (IV-13), that is $v_{r1}(t)$ and $i_{r1}(t)$, to the analog relaying circuit. If a transmission line is modelled by a distributed-constant circuit, and if a back impedance is pure resistive R, then $i_{r1}(t)$ is represented by the equation

$$i_{r1}(t) = \int_0^t v_{r1}(t - u)y(u)du \tag{IV-27}$$

where y(t) is a weighting function satisfying

for $0 \leq t < 2\tau$,

$$y(t) = \frac{1}{Z}\delta(t) \tag{IV-28}$$

for $2\tau \leq t < 4\tau$,

$$y(t) = \frac{1}{Z}\left[\delta(t) + 2 \cdot \frac{Z - R}{Z + R}\delta(t - 2\tau) + \cdots\right] \tag{IV-29}$$

$$\vdots$$

where τ is the surge travel time of the behind line, and Z is the surge impedance of the line, and $\delta(t)$ is the Dirac's delta function. After a forward fault takes place, $i_{r1}(t)$ and $v_{r1}(t)$ are related as follows,

for $0 \leq t < 2\tau$,

$$i_{r1}(t) = \frac{1}{Z}v_{r1}(t) \tag{IV-30}$$

for $2\tau \leq t < 4\tau$,

$$i_{r1}(t) = \frac{1}{Z}\left[v_{r1}(t) + 2\frac{Z - R}{Z + R}v_{r1}(t - 2\tau)\right] \mp \frac{1}{Z}v_{r1}(t) \tag{IV-31}$$

Therefore, the basic principle that $i_{r1}(t)$ and $v_{r1}(t)$ take the same sign for all $t \geq 0$, is satisfied during the first short interval $0 \leq t < 2\tau$, and it is not satisfied any longer for $t \geq 2\tau$. An extensive analysis has been done for other type of the back impedance, leading to the result which supports the conclusion.

The above analysis seems to place a theoretical limit to the travelling wave based directional relay. It is interesting to note that this travelling wave relay extends the signal frequency to a wide range, but limits the time period to a narrow range for a correct operation. On the contrary, the scheme of this paper has limited the frequency to a relatively narrow range, and has extended the time period to a wide range, assuring sufficient time for the relay decision making.

4.6 CONCLUSION

The time domain analysis of a faulted network has provided relay engineers with a new concept in a directional protection of a transmission line. The concept is mathematically expressed by the Volterra's integral equation of the first kind, whose solution noted as a weighting function provides an ability to detect a fault direction.

The mathematical background and effectiveness of the integral equational approach have been studied throught the theoretical fault transient date. A particular reference has been made to the design consideration of a filter used for signal conditioning. Finally, the discussions have been extended to compare the proposed scheme with a travelling wave based directional relay, clarifying a theoretical relation of each other.

As it is mandatory to solve an integral equation, the scheme essentially needs a numerical calculation capability, and it will be suitable for a digital processor based relaying application.

CHAPTER V ACCURATE FAULT LOCATION ALGORITHM ON TRANSMISSION LINES BASED ON LAPLACE TRANSFORM THEORY [6]

5.1 INTRODUCTION

One of the important tasks of substation protection and control is the fault location, which means locating a faulted point on a transmission line. An accurate fault location is very critical to a rapid and reliable restoration of electric power transmission. The fault location scheme widely used now relies its operating principle on the travelling wave propagation on a transmission line. One approach is to observe the time at which a locator of each terminal detects the first incoming fault surge from a faulted point. Another one is to transmit an electrical pulse into the line, and to measure the time period from emission to return of the pulse, thus known as a pulse radar method. Both methods depend upon the travelling wave propagation, which is a complex phenomena difficult to analyze perfectly. Wave propagations are influenced by the system parameters and network configurations. Accordingly, those fault locators would have to solve problems concerned with wave propagations before getting higher accuracy than they have now.

Computer relays for distance protection [1, 2] can be applied to the fault location, because a reactance jx they measure is proportional to the distance to the faulted point. The measured reactance provides the exact distance particularly when a fault resistance is zero. In other words, this resistance is fully compensated for by the reactance measurement. On long lines carrying heavy load and infeed from both sides, the fault resistance acts as a phase shifter. The locator at the sending end measures a lower reactance while the locator at the receiving end does a higher reactance. Fig. V-1 shows clearly the measured reactance dependent on the fault resistance [3]. Accordingly, the computerized distance relays tend to failure in measuring the exact reactance to the fault.

Westlin and Bubenko recently presented a computation algorithm of the fault location [4]. They applied the Newton-Raphson method to the non-linear algebraic equations to solve the distance to the fault. Their scheme is superior to the others, because all variables they use are locally available except the source impedance at the remote end. Although their theory is correct, it seems impractical to update the source impedance of the remote end every time a system change occurs.

This chapter presents a computation algorithm for an accurate fault location. Applying the law of superposition to the transient state fault analysis, one can obtain an algebraic equation which includes an unknown variable corresponding to the fault distance, and Laplace transforms of current and voltage at the local end. It should be noted that the equation does not include a fault resistance. Therefore, the location algorithm can measure the distance based on the locally measurable data set without being influenced by the fault resistance.

The transient state fault analysis is made with the Laplace transform theory. In this chapter the theoretical basis of the Laplace transform-based fault location is first given. Then, the location scheme is simulated using the theoretical fault data to estimate the performance. Such factors as transmission line loss, fault resistance, dc offset current, and back impedance angle are studied to understand their effects on the locating accuracy. Finally, efforts are made to determine the optimal values of the complex variable s.

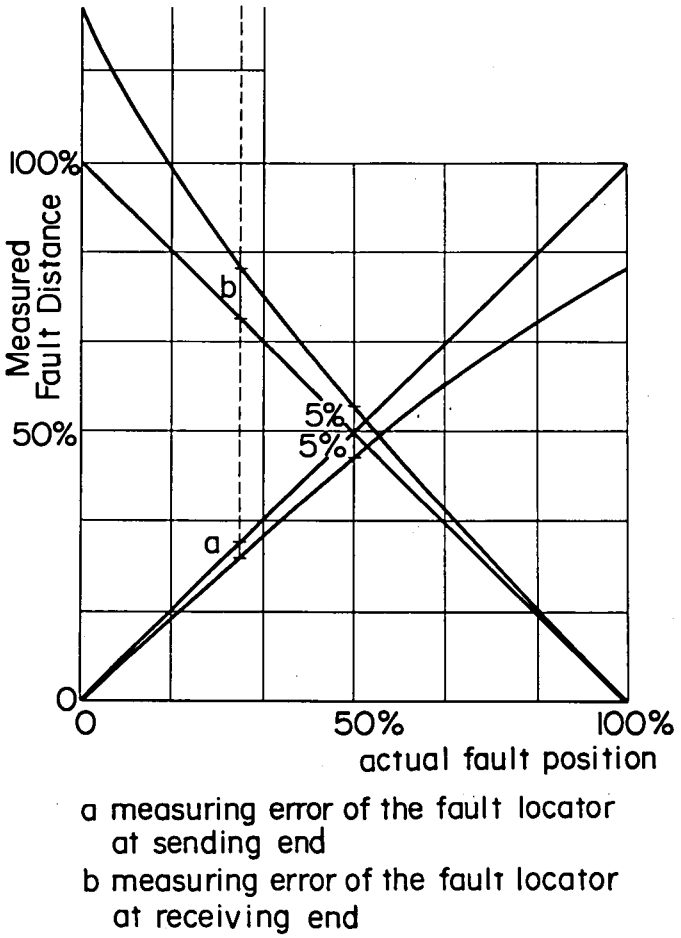

Fig. V-1 Measuring error due to fault resistance under load flow conditions

5.2 THEORETICAL BASIS OF ACCURATE FAULT LOCATION BASED ON LAPLACE TRANSFORM THEORY

5.2.1 Fault Location Theory for Single Phase Transmission Line

Suppose that a fault happens at time zero and at the point F on the transmission line shown in Fig. V-2 (a). With the superposition principle applied to the faulted network, fault voltages and currents are calculated by summing these in the pre- and pure-fault networks. Let $(\cdot)'$ be referred to the quantity in the pre-fault network, and $(\cdot)''$ be in the pure-fault one. The steady state voltage at the point F of Fig. V-2 (b) is calculated by the voltage and current at the terminal S.

$$\dot{V}_F' = \cosh(\dot{q}x)\dot{V}_S' - \dot{z}\sinh(\dot{q}x)\dot{I}_S' \tag{V-1}$$

where

$$\begin{aligned}\dot{q} &= j\omega_0\sqrt{\ell c} \\ &= j\omega_0\lambda \quad : \text{propagation constant}\end{aligned} \tag{V-2}$$

and

$$\begin{aligned}\dot{z} &= \sqrt{\ell/c} \\ &= z \qquad : \text{characteristic impedance}\end{aligned} \tag{V-3}$$

Then, the point F voltage at time t is given as:

$$v_F'(t) = V_S' \sin(\omega_0 t + \theta_v^*)\cos(\omega_0\lambda x) - z\, I_S' \cos(\omega_0 t + \theta_i^*)\sin(\omega_0\lambda x) \tag{V-4}$$

Applying the Laplace transform to the eqn. (V-4), one obtains

$$\begin{aligned}v_F'(s) = &\frac{V_S'}{s^2 + \omega_0^2}(s\sin\theta_v^* + \omega_0\cos\theta_v^*)\cos(\omega_0\lambda x) - \\ &\frac{zI_S'}{s^2 + \omega_0^2}(s\cos\theta_i^* - \omega_0\sin\theta_i^*)\sin(\omega_0\lambda x)\end{aligned} \tag{V-5}$$

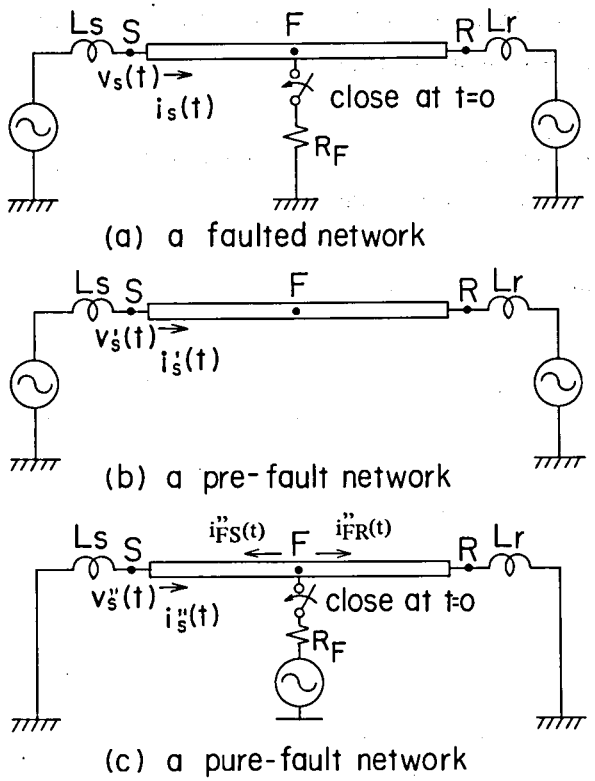

Fig. V-2 A faulted network and its equivalent decomposition.

V_S' and I_S' are the crest values, and θ_v^* and θ_i^* are the voltage and current phase angle at time zero the fault happens. $v_S^{*''}(s)$ be the Laplace transform of $v_S''(t)$, and $i_S^{*''}(s)$ be that of $i_S''(t)$ in Fig. V-2 (c). The operational voltage at F is calculated by $v_S^{*''}(s)$ and $i_S^{*''}(s)$:

$$v_F''(s) = \cosh(s\lambda x)v_S^{*''}(s) - z\sinh(s\lambda x)i_S^{*''}(s) \tag{V-6}$$

Define k(s, x) as the ratio of $i_{FR}''(s)$ to $i_{FS}''(s)$, that is the fault current distribution factor, then the eqn. (V-7) gives the fault current $i_F(s)$.

$$\begin{aligned} i_F(s) &= -\{i_{FS}''(s) + i_{FR}''(s)\} \\ &= -\{1 + k(s, x)\} i_{FS}''(s), \quad k(s, x) = \frac{i_{FR}''(s)}{i_{FS}''(s)} \end{aligned} \tag{V-7}$$

and

$$i''_{FS}(s) = \frac{1}{z} \sinh(s\lambda x)\ v^{*''}_{S}(s) - \cosh(s\lambda x)\ i^{*''}_{S}(s) \tag{V-8}$$

From the equation:

$$v_F(s) = R_F\ i_F(s) \tag{V-9}$$

the following is obtained.

$$v'_F(s) + v''_F(s) = -\{1 + k(s, x)\} R_F\ i''_{FS}(s) \tag{V-10}$$

If k(s, x) takes the same value at two distinct points s_1 and s_2, the fundamental equation for fault location is derived.

$$\frac{v'_F(s_1) + v''_F(s_1)}{i''_{FS}(s_1)} = \frac{v'_F(s_2) + v''_F(s_2)}{i''_{FS}(s_2)} \tag{V-11}$$

In the eqn. (V-11), the locator must start the Laplace transforms at the time the fault happens at the point F. As is shown in Fig. V-3, there is a time delay until the locator detects a sudden change of the voltage waveform. The time delay is identical to the time that an incoming fault surge propagates from F to S. It should be noted that the locator can only start the Laplace transform at time t_1, instead of time zero. This is simply because of the causality. So, the locator must compensate the time delay to perform the correct Laplace transforms for $v^{*''}_{S}(s)$, $i^{*''}_{S}(s)$, θ^{*}_{v}, and θ^{*}_{i}. This is done as follows:

$$\theta^{*}_{v} = \theta_v - \omega_0 \lambda x \tag{V-12}$$

$$\theta^{*}_{i} = \theta_i - \omega_0 \lambda x \tag{V-13}$$

$$v^{*''}_{S}(s) = \exp(-s\lambda x)\ v''_S(s) \tag{V-14}$$

$$i^{*''}_{S}(s) = \exp(-s\lambda x)\ i''_S(s) \tag{V-15}$$

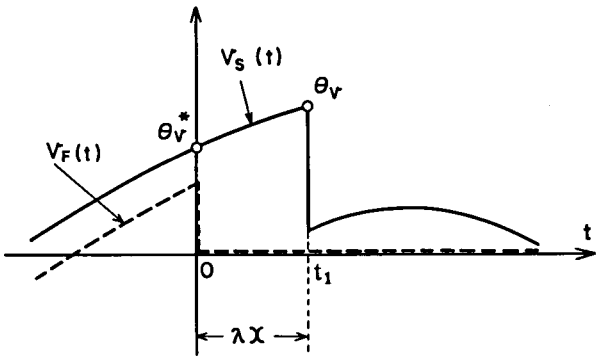

Fig. V-3 Time delay in detecting voltage sudden change at the relaying point

where θ_v and θ_i are the voltage and current phase angles at the time the voltage makes a sudden change at the point S, on the other hand $v_S''(s)$ and $i_S''(s)$ are the Laplace transforms obtained by starting at time t_1. Substituting the eqn. (V-12) to (V-15) to the eqn. (V-11), one derives the final equation to locate a fault on a single phase transmission line. Final equation for fault location is represented as follows.

$$F(x) = 0 \tag{V-16}$$

where

$$F(x) = \left[\begin{array}{l} V_S' \cos(\omega_0 \lambda x)\ (s_1 \sin\theta_v^* + \omega_0 \cos\theta_v^*) - z\, I_S' \sin(\omega_0 \lambda x) \\ (s_1 \cos\theta_i^* - \omega_0 \sin\theta_i^*) + (s_1^2 + \omega_0^2)\ \{\cosh(s_1 \lambda x) v_S^{*''}(s_1) - \\ z \sinh(s_1 \lambda x) i_S^{*''}(s_1)\} \end{array} \right]$$

$$\times\ (s_2^2 + \omega_0^2)\{\frac{1}{2}\sinh(s_2 \lambda x) v_S^{*''}(s_2) - \cosh(s_2 \lambda x) i_S^{*''}(s_2)\}$$

$$- \left[\begin{array}{l} V_S' \cos(\omega_0 \lambda x)\ (s_2 \sin\theta_v^* + \omega_0 \cos\theta_v^*) - z\, I_S' \sin(\omega_0 \lambda x) \\ (s_2 \cos\theta_i^* - \omega_0 \sin\theta_i^*) + (s_2^2 + \omega_0^2)\{\cosh(s_2 \lambda x) v_S^{*''}(s_2) - \\ z \sinh(s_2 \lambda x) i_S^{*''}(s_2)\} \end{array} \right]$$

$$\times \quad (s_1^2 + \omega_0^2)\{\frac{1}{2}\sinh(s_1\lambda x)v_S^{*''}(s_1) - \cosh(s_1\lambda x)i_S^{*''}(s_1)\} \qquad \text{(V-17)}$$

5.2.2 Fault Location Theory for Three Phase Transmission Line

(Phase-a-to-ground fault): Let $(\cdot)^{(j)}$ be referred to the mode-j quantity. The equation:

$$v_F^{(0)}(s) + v_F^{(1)}(s) + v_F^{(2)}(s) = 3\ R_F\ i_F^{(m)}(s) \qquad \text{(V-18)}$$
$$m = \{0,\ 1,\ 2\}$$

holds at the faulted point F. If the mode-m fault current distribution factor $k^{(m)}(s, x)$ is determined independently of s, that is $k^{(m)}(s_1, x) = k^{(m)}(s_2, x)$ for $s_1 \neq s_2$, then one obtains the following:

$$\frac{\sum_{j=0}^{2}\{v_F^{'(j)}(s_1) + v_F^{''(j)}(s_1)\}}{i_{FS}^{''(m)}(s_1)} = \frac{\sum_{j=0}^{2}\{v_F^{'(j)}(s_2) + v_F^{''(j)}(s_2)\}}{i_{FS}^{''(m)}(s_2)} \qquad \text{(V-19)}$$

Accordingly, the final equation to locate a single phase ground fault is reached.

$$F_{1LG}(x) = 0 \qquad \text{(V-20)}$$

where

$$F_{1LG}(x) = \left[\begin{array}{l} \sum_{j=0}^{2}\ [V_S^{'(j)}\cos(\omega_0\lambda^{(j)}x)\{s_1\sin\theta_v^{*(j)} + \omega_0\cos\theta_v^{*(j)}\} - \\ z^{(j)}I_S^{'(j)}\sin(\omega_0\lambda^{(j)}x)\{s_1\cos\theta_i^{*(j)} - \omega_0\sin\theta_i^{*(j)}\} + (s_1^2 + \omega_0^2) \\ \{\cosh(s_1\lambda^{(j)}x)v_S^{*''(j)}(s_1) - z^{(j)}\sinh(s_1\lambda^{(j)}x)i_S^{*''(j)}(s_1)\}] \end{array}\right]$$

$$\times\ (s_2^2 + \omega_0^2)\{\frac{1}{z^{(m)}}\sinh(s_2\lambda^{(m)}x)v_S^{*''}(s_2) - \cosh(s_2\lambda^{(m)}x)i_S^{*''}(s_2)\}$$

$$-\left[\begin{array}{l} \sum_{j=0}^{2}\ [V_S^{'(j)}\cos(\omega_0\lambda^{(j)}x)\{s_2\cos\theta_v^{*(j)} + \omega_0\cos\theta_v^{*(j)}\} - \\ z^{(j)}I_S^{'(j)}\sin(\omega_0\lambda^{(j)}x)\{s_2\cos\theta_i^{*(j)} - \omega_0\sin\theta_i^{*(j)}\} + (s_2^2 + \omega_0^2) \\ \{\cosh(s_2\lambda^{(j)}x)v_S^{*''(j)}(s_2) - z^{(j)}\sinh(s_2\lambda^{(j)}x)i_S^{*''(j)}(s_2)\}] \end{array}\right]$$

$$\times (s_1^2 + \omega_0^2)\left\{\frac{1}{z^{(m)}} \sinh(s_1\lambda^{(m)}x)v_S^{*''}(s_1)\right.$$

$$\left. - \cosh(s_1\lambda^{(m)}x)i_S^{*''}(s_1)\right\} \qquad \text{(V-21)}$$

(Phase-a-to-b fault): From the equation holding at the faulted point F

$$v_F^{(1)}(s) - v_F^{(2)}(s) = R_F\, i_F^{(m)}(s) \qquad \text{(V-22)}$$

$$m = \{1,2\}$$

the following is derived.

$$\frac{v_F^{'(1)}(s_1) + v_F^{''(1)}(s_1) - v_F^{'(2)}(s_1) - v_F^{''(2)}(s_1)}{i_{FS}^{''(m)}(s_1)}$$

$$= \frac{v_F^{'(1)}(s_2) + v_F^{''(1)}(s_2) - v_F^{'(2)}(s_2) - v_F^{''(2)}(s_2)}{i_{FS}^{''(m)}(s_2)} \qquad \text{(V-23)}$$

The final equation is in the form of

$$F_{2LS}(x) = 0 \qquad \text{(V-24)}$$

where

$$F_{2LS}(x) = \left[\sum_{j=1}^{2} [V_S^{'(j)}\cos(\omega_0\lambda^{(j)}x)\{s_1\sin\theta_v^{*(j)} + \omega_0\cos\theta_v^{*(j)}\} - z^{(j)}I_S^{'(j)}\sin(\omega_0\lambda^{(j)}x)\{s_1\cos\theta_i^{*(j)} - \omega_0\sin\theta_i^{*(j)}\} + (s_1^2 + \omega_0^2)\{\cosh(s_1\lambda^{(j)}x)v_S^{*''(j)}(s_1) - z^{(j)}\sinh(s_1\lambda^{(j)}x)i_S^{*''(j)}(s_1)\}]\right.$$

$$\times (s_2^2 + \omega_0^2)\left\{\frac{1}{z^{(m)}} \sinh(s_2\lambda^{(m)}x)v_S^{*''}(s_2)\right.$$

$$\left. - \cosh(s_2\lambda^{(m)}x)i_S^{*''}(s_2)\right\}$$

$$-\left[\sum_{j=1}^{2} [V_S^{'(j)}\cos(\omega_0\lambda^{(j)}x)\{s_2\sin\theta_v^{*(j)} + \omega_0\cos\theta_v^{*(j)}\} - z^{(j)}I_S^{'(j)}\sin(\omega_0\lambda^{(j)}x)\{s_2\cos\theta_i^{*(j)} - \omega_0\sin\theta_i^{*(j)}\} + (s_2^2 + \omega_0^2)\{\cosh(s_2\lambda^{(j)}x)v_S^{*''(j)}(s_2) - z^{(j)}\sinh(s_2\lambda^{(j)}x)i_S^{*''(j)}(s_2)\}]\right.$$

$$\times (s_1^2 + \omega_0^2)\left\{\frac{1}{z^{(m)}} \sinh(s_1\lambda^{(m)}x)v_S^{*''}(s_1)\right.$$

$$\left. - \cosh(s_1\lambda^{(m)}x)i_S^{*''}(s_1)\right\} \qquad \text{(V-25)}$$

As the fundamental equations are non-linear, the iterative solution technique like the Newton-Raphson method is essential to the scheme.

5.3 VERIFICATION OF LAPLACE TRANSFORM BASED FAULT LOCATION ALGORITHM

5.3.1 Digital Simulation of Fault Location Algorithm

The locating performance is estimated through the digital computer simulations using the theoretical fault data. The digital fault transient analysis [5], which is now well known among the relay engineers, is performed on a model power system shown in Fig. V-4. Voltages and currents are computed every 40 μsec for 100 msec time period, and faults are initiated at time t = 40 msec. The locator detects a fault with a voltage sudden change, and it is assumed that the locator picks up the crest values of the relaying voltage and current during the pre-fault period. In the base case study, no-loss lines are assumed.

Fig. V-5 illustrates a locating process at the locator disposed at the terminal E for a phase-a-to-ground fault. The estimated distance settles at 10.88 km, which is 0.12 km short to the fault. The locator uses $s_1 = 200.0$ and $s_2 = 300.0$ for the complex variable s. These two values are determined empirically at this time, and the optimal value setting problem will be discussed in the following section. The estimation error to the true distance ratio has been at most (±)1.5 percent for all the base case studies.

As is shown in Fig. V-1, one needs to bear in mind five percent location error when he depends on the impedance measuring type fault locator. On the other hand, the present scheme can reduce the estimation error below one percent and a half. Accordingly, the scheme is more than three times as accurate as the distance relay scheme. The key thing here is the following equation:

$$k(s_1, x) = k(s_2, x) \qquad \text{for } s_1 \neq s_2 \tag{V-26}$$

In what follows we will study the correctness of the eqn. (V-26) at an actual transmission system.

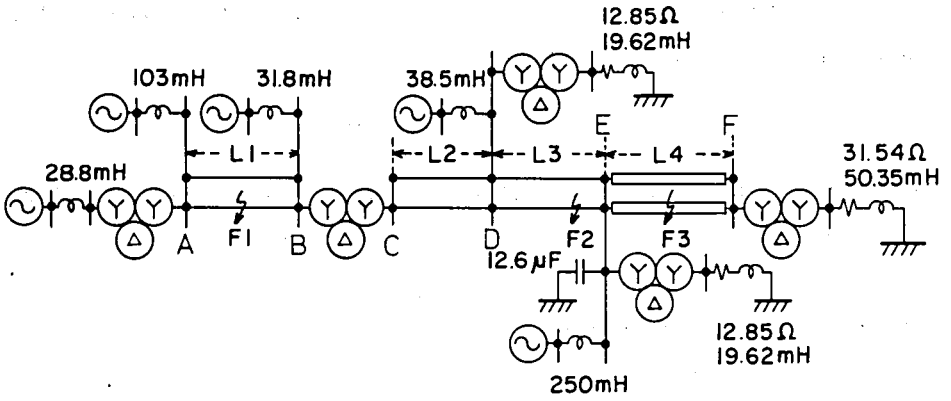

Constant / line	$r^{(0)}\ \Omega/Km$	$\ell^{(0)}$ mH/Km	$C^{(0)}\ \mu F/Km$	$\lambda^{(0)}\ rad/Km \times 10^{-3}$	$Z^{(0)}\ \Omega$
	$r^{(1)}\ \Omega/Km$	$\ell^{(1)}$ mH/Km	$C^{(1)}\ \mu F/Km$	$\lambda^{(1)}\ rad/Km \times 10^{-3}$	$Z^{(1)}\ \Omega$
L 1	0.11480	2.2886	0.00523	1.0869	662
	0.02083	0.8984	0.01291	1.0699	264
L 2	0.11570	2.2989	0.00526	1.0925	661
	0.01974	0.7968	0.01456	1.0701	234
L 3	0.11570	2.2989	0.00526	1.0925	661
	0.01974	0.7968	0.01456	1.0701	234
L 4	0.55400	0.9942	0.35567	5.9076	53
	0.02549	0.4020	0.35567	3.7565	34

Fig. V-4 A model power system and its line constants.

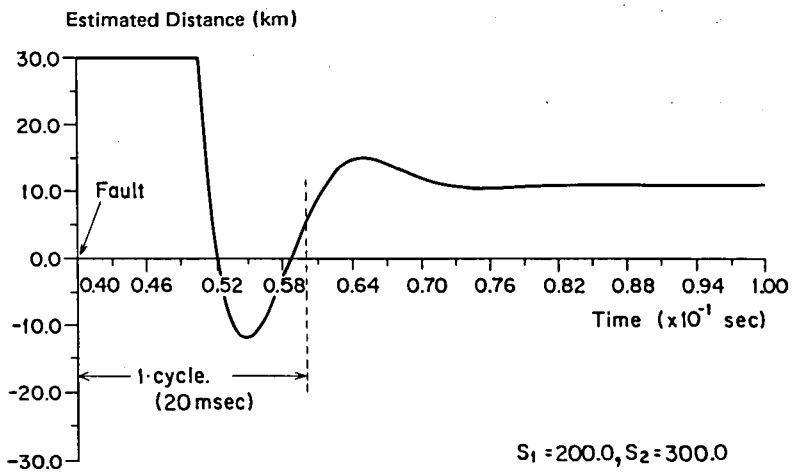

Fig. V-5 Fault location process until settling at 10.88 km

5.3.2 Numerical Evaluation of Transmission Line Loss Effect

The effect of line loss on the accuracy is studied using the fault data from transient analysis, where the line loss was modelled exactly. The curve (1) in Fig. V-6 shows the result of a fault at 11.0 km, indicating the estimated distance at 7.93 km. The locator estimated the fault at a significantly short distance. The reason for this is explained as follows. Let the line constants be r Ω/km, ℓ H/km, and c F/km. Then, the propagation constant λ(s) and the surge impedance z(s) are given by

$$\lambda(s) = s\sqrt{\ell c}\,\sqrt{1 + (r/s\ell)} \qquad \text{(V-27)}$$

$$z(s) = \sqrt{\ell/c}\,\sqrt{1 + (r/s\ell)} \qquad \text{(V-28)}$$

The term $\sqrt{1 + (r/s\ell)}$ of each line is calculated at $s_1 = 200.0$ and $s_2 = 300.0$ and shown in Table V-1. While the locator assumes the term to be 1.0, the mode-0 value at the line L4 is significantly larger than 1.0. This is the primary reason for the inaccurate result in Fig. V-6.

There are two countermeasures for this. One is to use a large value for the complex variable s, making the term $\sqrt{1 + (r/s\ell)}$ approach to 1.0. The other is to use the mode-1 quantity for $v_S''(s)$ and $i_S''(s)$ of the eqn. (V-11), taking advantage of the mode less sensitive to the line loss. The curve (2) settling at 10.66 km is obtained by applying the former measure, and the curve (3) settling at 11.43 km by the latter one. Both measures have been effective to improve the accuracy. Although these might have the similar effect on the

accuracy improvement, the latter will be preferred to the former because of the potential for the numerical calculation error by the use of large value for s. Accordingly, the use of mode-1 quantities will be recommended.

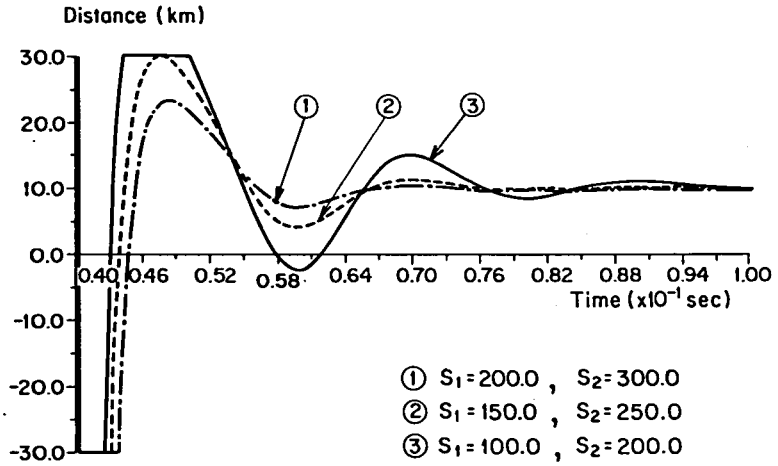

Fig. V-6 Effect of transmission line loss on the accuracy and two countermeasures for performance improvement

zone / s	L 1		L 2		L 3		L 4	
	mode 0	mode 1	mode 0	mode 1	mode 0	mode 1	mode 0	mode 1
200.0	1.118	1.056	1.119	1.060	1.119	1.060	1.946	1.148
300.0	1.080	1.038	1.081	1.040	1.081	1.040	1.690	1.101

Table V-1 The term $\sqrt{1 + (r/s\ell)}$ evaluated at each line section

5.3.3 Numerical Evaluation of Fault Resistance Effect

Although the eqn. (V-11) has guaranteed the high immunity to the fault resistance effect, some simulations are carried out to confirm the effect of the fault resistance on the working principle. Faults with the fault resistance of 10.0, 20.0, and 40.0 ohm are simulated at the point F3. Fig. V-7 summarizes the distances estimated by the locator at the terminal E. The locating errors are well below 0.5 km.

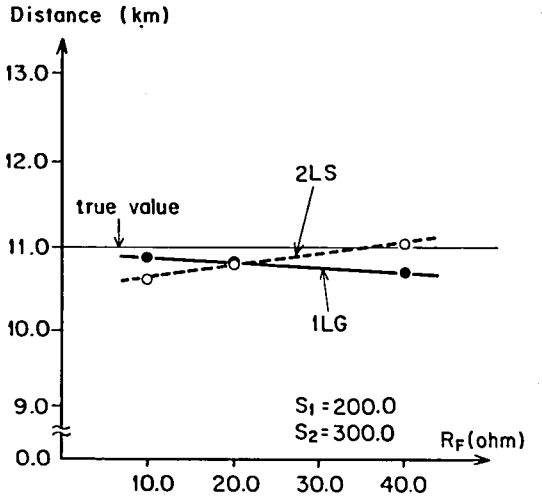

Fig. V-7 Summary of distances estimated by the locator at the terminal E

5.3.4 Numerical Evaluation of DC Offset Current Effect

It was assumed until now that the fault happened at the voltage maximum. Here, the fault at the voltage zero is examined. Using 200.0 and 300.0 for the complex variable s, the locator calculates the distance at 9.73 km, that is 1.27 km short to the fault of voltage zero. The accuracy is checked with the various settings for s. Table V-2 summarizes the relation of the accuracy versus the variable values used, and Fig. V-8 plots each locating process. Table V-2 implies that the small values of s have improved the locating accuracy. This is understood in terms of the numerical accuracy of Laplace transform. Roughly speaking, the use of small values is quite effective to do an accurate Laplace transform of the waveform which has the dc offset component. As a fault of voltage zero causes the dc offset current, the small values are desired for better locating performances.

S_1	S_2	Estimated distance (km)	Estimated error (%)
200.0	300.0	9.73	12.0
150.0	250.0	9.98	9.2
100.0	200.0	10.38	6.0

Table V-2 Estimated distance dependent on the values of s_1 and s_2

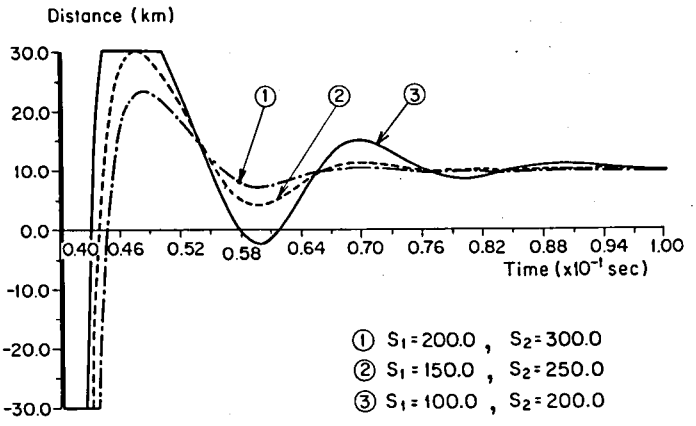

Fig. V-8 Fault location process dependent on the values of s_1 and s_2

5.3.5 Numerical Evaluation of Short Circuit Angle Effect

All discussions so far have been concentrated on the analysis of the locating scheme applied to a line at which the power system has the fault point to the infeed short circuit angle equal at both ends. In other words, the scheme has been applied to a strong system. With the practical application in mind, it is necessary to examine the scheme when it is applied to a weak system. In such cases, load characteristics might affect the working of the principle. Three types of load are studied. Assume that the operational impedance be Z(s) beyond the remote end of the line.

(1) $Z(s) = R_2 + sL_2$: inductive load

(2) $Z(s) = R_2$: pure-resistive load

(3) $Z(s) = R_2 + \frac{1}{sC_2}$: capacitive load

Fig. V-9 illustrates the settling distance for the double phase short circuit fault. As is expected, the accuracy is highly dependent on the load type. The error is maximum for the capacitive load.

The reason for this is explained as follows. Assume that the operational impedance behind the locator be sL_1. Then, the current distribution factor k(s, x) is given by

$$k(s, x) = \frac{sL_1}{Z(s)} \qquad \text{(V-29)}$$

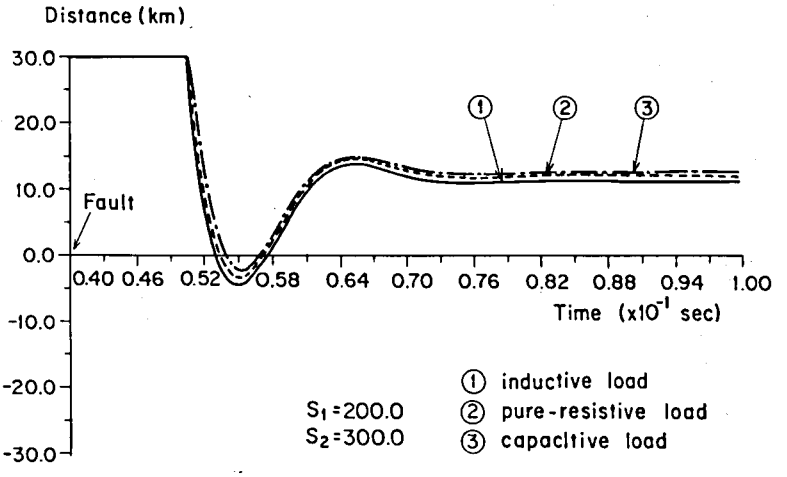

Fig. V-9 Effect of load characteristics on settling distance

For the inductive load, the factor is in the form of

$$k(s, x) = \frac{sL_1}{R_2 + sL_2} = \left(\frac{L_1}{L_2}\right)\left\{1 - \frac{R_2/L_2}{s + (R_2/L_2)}\right\} \tag{V-30}$$

On the other hand, the factor for the capacitive load is

$$k(s, x) = \frac{sL_1}{R_2 + \dfrac{1}{sC_2}} = \left(\frac{L_1}{R_2}\right)\left\{s - \frac{1}{C_2R_2}\left(\frac{1}{s + \dfrac{1}{C_2R_2}}\right)\right\} \tag{V-31}$$

The distribution factor of the inductive load approaches to a constant value L_1/L_2 for a large s, while the factor of the capacitive load becomes a linear function of s. The eqn. (V-11) supposes that k(s, x) be constant for the range of s considered. The capacitive load does not meet the requirement, and accordingly, the locator will be succeptible to failure in estimating the faulted point for the system with the capacitive load. Fig. V-10 gives a clear idea how k(s, x) varies with the complex variable s.

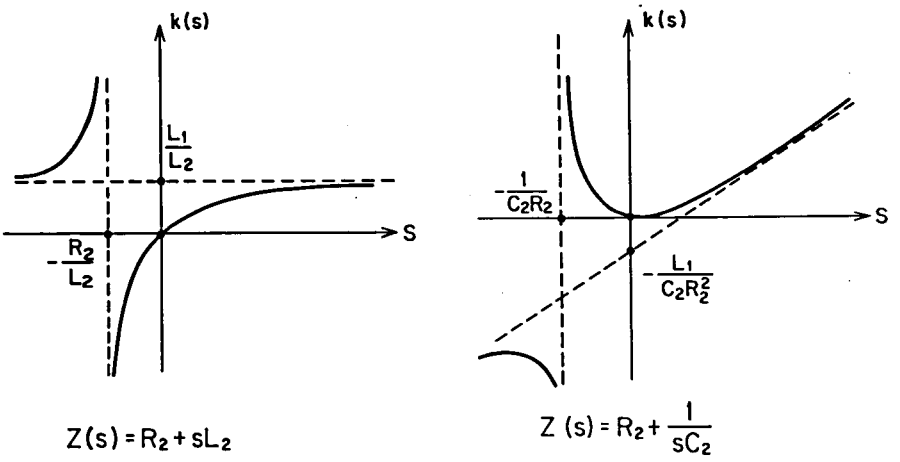

Fig. V-10 Operational current distribution factor k(s,x) as a function of s (= real number)

5.4 OPTIMIZATION OF NUMERICAL LAPLACE TRANSFORM ALGORITHM

The substantial efforts must be made to do a numerical Laplace transform. Two values, 200.0 and 300.0, so far have been substituted to the complex variable s. Now, discussions are made to determine the optimal values. The objects of the transform are voltages and currents. These are considered to consist of three components.

(1) $\exp(-t/T)$: dc offset component
(2) $\exp(-t/T)\sin(\omega t + \theta)$: higher harmonic component
(3) $\sin(\omega_0 t + \theta)$: nominal frequency component

Accordingly, the numerical transform practice used in this paper is examined with its accuracy when applied to these functions.

5.4.1 Numerical Laplace Transform Error of DC Offset Current

Consider a function y(t) given by

$$y(t) = 1.0 \exp(-t/T) \qquad \text{(V-32)}$$

The analytical Laplace transform of y(t), referred to $y^*(s)$, is

$$y^*(s) = \frac{1}{s + \frac{1}{T}} \tag{V-33}$$

On the other hand, the numerical transform of y(t) is calculated with the following formula:

$$y(s) = \sum_{k=0}^{1499} y(k\Delta t)\ \exp(-sk\ \Delta t)\ \Delta t \tag{V-34}$$

where the time step is taken at 40 μsec and the integration period at 60.0 msec. Also is calculated an accuracy index ϵ.

$$\epsilon \triangleq \left| \frac{y(s) - y^*(s)}{y^*(s)} \right| \times 100 \tag{V-35}$$

Fig. V-11 plots the index ϵ for various parameter settings and time constant T. The following conclusion can be drawn. Higher accuracy is expected with the large time constant for a fixed variable value. Higher accuracy is also expected by choosing the variable value as small as possible.

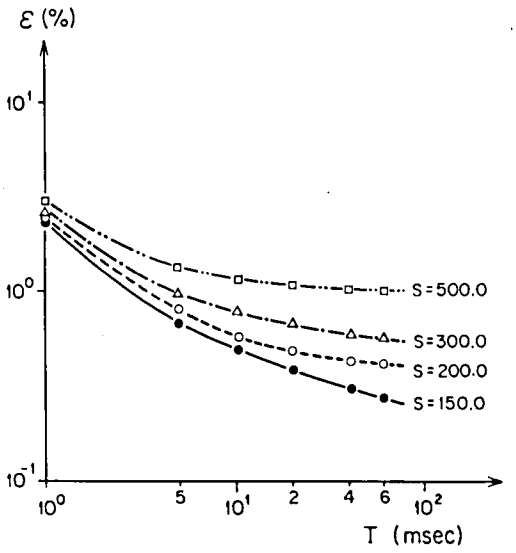

Fig. V-11 Accuracy index of numerical Laplace transform for y(t) = 1.0 exp(-t/T)

5.4.2 Numerical Laplace Transform Error of Higher Harmonic Component

Let y(t) be

$$y(t) = 1.0 \exp(-t/T) \sin(800\pi t + \theta) \tag{V-36}$$

Then, its analytical Laplace transform is given as

$$y^*(s) = \frac{(s + \frac{1}{T}) \sin\theta + (800\pi) \cos\theta}{(s + \frac{1}{T})^2 + (800\pi)^2} \tag{V-37}$$

The index ϵ is calculated for various T and s at θ=0 as is shown in Fig. V-12. General conclusions drawn are follows. For any value s, small time constants give rise to more accurate transform. Setting large values to s results in more accurate transform, too. Finally, the benefits can be expected by setting a large value to s for a large time constant. Accordingly, the large operator value is preferred for the waveform including a slowly damped higher harmonic component.

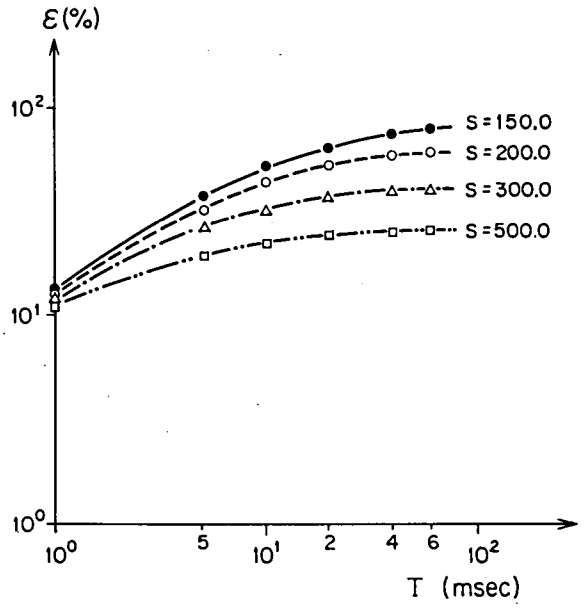

Fig. V-12 Accuracy index of numerical Laplace transform for y(t) = 1.0 exp(-t/T)sin(800πt)

5.4.3 Numerical Laplace Transform Error of Nominal Frequency Component

Consider a nominal frequency component:

$$y(t) = 1.0 \sin(100\pi t + \theta) \tag{V-38}$$

The analytical transform of the eqn. (V-38) is

$$y^*(s) = \frac{s \sin\theta + (100\pi)\cos\theta}{s^2 + (100\pi)^2} \tag{V-39}$$

Fig. V-13 plots the index ϵ for various values of phase angle. Although it seems hard to make a simple comparison, an ordering among operator values such as

$$300.0 <:: 150.0 <:: 200.0 <:: 500.0$$

can be established applying the min-max rule to Fig. V-13. The relation means that the maximum error for s = 300.0 is smaller than that for s = 150.0, and so on.

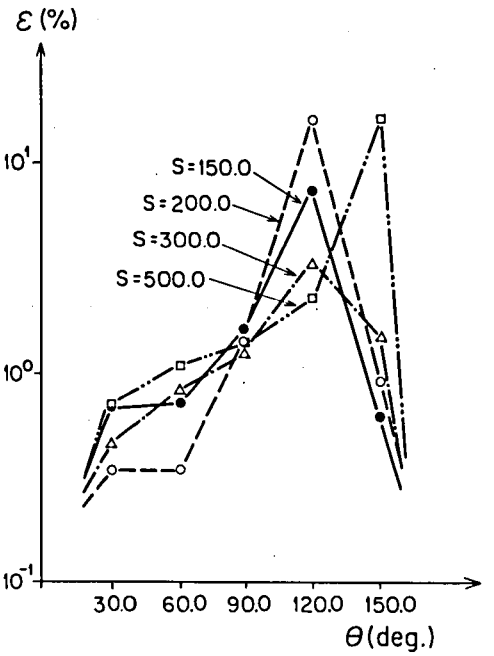

Fig. V-13 Accuracy index of numerical Laplace transform for $y(t) = 1.0 \sin(100\pi t + \theta)$

5.4.4 Determination of Optimal Value for Complex Variable

One way of evaluating the optimality of s is to look at both the accuracy and the speed of numerical transform. The variable value 150.0 through 300.0 may be justified to be used in terms of the accuracy. Taking into account the data length, at least four cycles data at nominal frequency are available. The condition:

$$\exp(-0.08s) \leq 1.0 \times 10^{-6} \qquad \text{(V-40)}$$

which is equivalent to

$$s \geq 173.0$$

seems to guarantee a stable convergence of numerical transform. Therefore, the variable values 200.0 and 300.0 are the most appropriate settings.

5.5 CONCLUSION

As one of the numerical fault location schemes using the fault current distribution factor, the Laplace transform method has been described. Some conclusions have been drawn from the Laplace method.

(1) High accurate location can be expected at the strong AC system, that is the system with large short circuit kVA.

(2) Accuracy will be degraded at the weak AC system, especially at the system supplying to capacitive loads.

(3) Either a large value of the complex variable s or mode-1 quantity, is perferred when the scheme is applied to high r to ℓ ratio networks.

(4) The value of s is set as small as possible for a fault at voltage zero or around.

(5) The optimal values for s are considered to be 200.0 through 300.0

The numerical fault location scheme will be implemented best in the integrated digital protection and control system which is expected to be a main trend of substation system engineering in the eighties.

CHAPTER VI ACCURATE FAULT LOCATION ALGORITHM ON TRANSMISSION LINES BASED ON FOURIER TRANSFORM THEORY[8]

6.1 INTRODUCTION

The theoretical basis and computer simulation of the Laplace transform based fault location were discussed in CHAPTER V. The superposition principle was applied there to the transient state analysis of a faulted network. The location scheme made use of the operational fault current distribution factor k(s, x), which is defined in the s-plane of the Laplace transform. The key idea behind the scheme is written by the following equation:

$$k(s_1, x) = k(s_2, x) \qquad \text{for } s_1 \neq s_2 \tag{VI-1}$$

which means that the distribution factor is independent of the complex variable s. It was shown that the scheme is able to indicate an accurate distance to a fault at a transmission network satisfying the eqn. (VI-1), and also that an EHV/UHV transmission network is such the case.

As the Laplace transform scheme depends on the transient state analysis of a faulted network, it requires an accurate replica of a fault transient voltage and current at the locator input circuit. It also needs an accurate measurement of the voltage or current phase angle at the time of a fault inception. Furthermore, the high frequency data sampling must be made to calculate the operational voltage and current at the point s. Accordingly, a great burden lies in both measurement and computation process.

An attempt is made with the use of Fourier transform to ease the burden associated with the Laplace transform based location scheme. Unlike the Laplace transform, the Fourier method can pick up an operational value, particularly at the nominal frequency, with the less burden at measurement and computation process. The theoretical basis of CHAPTER V, however, must be reformed when one applies the Fourier transform method.

This chapter presents the fundamental theory of the fault location scheme based on the Fourier transform. The superposition principle is applied here to the steady state analysis of a faulted network. The operational fault current distribution factor is used again, but in a different way. The property that the factor becomes a real number at $s = j\omega$:

$$\text{Imaginary part of } k(j\omega, x) = 0 \tag{VI-2}$$

is exploited to define a fault location algorithm. The algorithm is analyzed in more detail particularly on its relation to the Laplace transform scheme.

Digital computer simulations are extensively performed to verify the location theory on a model power system. Efforts are made to study the effects of such factors as a transmission line loss, load characteristics and waveform distortion that might affect the working principle. Then, the orthogonal transform process is optimized to speed up the computation. Short window Fourier transform and Walsh transform are examined. It is shown that the Fourier transform scheme is easy to implement, because the measurement and computation burden is greatly reduced.

6.2 DEFINITION OF FAULT LOCATION ALGORITHM BASED ON FOURIER TRANSFORM THEORY

6.2.1 Fault Location Theory for Single Phase Transmission Line

Consider a midway fault at the point F which is x away from S on a transmission line SR in Fig. VI-1 (a). The law of superposition in the linear network theory separates a faulted network into a pre-fault and pure-fault ones, which are given in Fig. VI-1 (b) and (c) respectively. Let $\dot{V}_F$ be the voltage vector at F, and let $\dot{I}_F$ be the current vector at the fault resistance R_F in the faulted network. Then,

$$\begin{aligned} \dot{V}_F &= R_F \cdot \dot{I}_F \\ &= -R_F(\dot{I}''_{FS} + \dot{I}''_{FR}) \end{aligned} \tag{VI-3}$$

where $\dot{I}''_{FS}$ is the line current at F flowing to S and $\dot{I}''_{FR}$ is that to R, both of which are defined in the pure-fault network. Define an operational fault current distribution factor $\dot{K}(x)$ by

$$\begin{aligned} \dot{K}(x) &= k(j\omega, x) \\ &\triangleq \frac{\dot{I}''_{FR}}{\dot{I}''_{FS}} \end{aligned} \tag{VI-4}$$

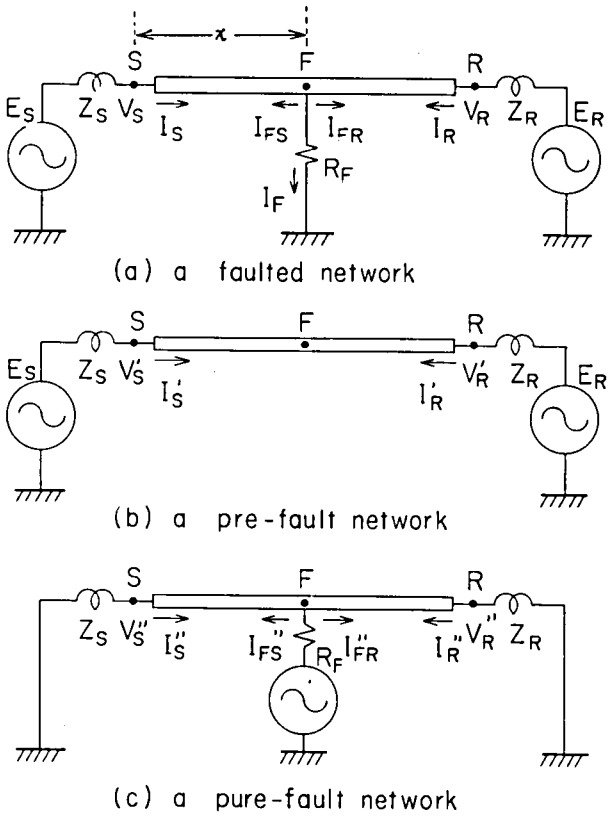

Fig. VI-1 A faulted network and its equivalent decomposition

It is noted that the ratio $\dot{K}(x)$ is a function of the distance x to the fault. Substitution of the eqn. (VI-4) into the eqn. (VI-3) yields

$$\dot{V}_F = -R_F \dot{I}''_{FS}(1 + \dot{K}(x)) \qquad \text{(VI-5)}$$

On the other hand, $\dot{V}_F$ and $\dot{I}''_{FS}$ are estimated by the locally measurable vectors,

$$\dot{V}_F = \dot{A}(x)\dot{V}_S - \dot{B}(x)\dot{I}_S \qquad \text{(VI-6)}$$

$$\dot{I}''_{FS} = \dot{C}(x)\dot{V}''_S - \dot{D}(x)\dot{I}''_S \qquad \text{(VI-7)}$$

where $\dot{A}(x)$, $\dot{B}(x)$, $\dot{C}(x)$ and $\dot{D}(x)$ are the four terminal constants of the line SF, and defined as follows for a distributed-constant circuit.

$$\dot{A}(x) = \dot{D}(x) = \cosh(\dot{q}x) \tag{VI-8}$$

$$\dot{B}(x) = \dot{z}\sinh(\dot{q}x) \tag{VI-9}$$

$$\dot{C}(x) = \sinh(\dot{q}x)/\dot{z} \tag{VI-10}$$

where $\dot{q}$ is the propagation constant, and $\dot{z}$ is the characteristic impedance.

The faulted vectors $\dot{V}_S$ and $\dot{I}_S$ are directly measured at the local end S, while the pure-fault vectors $\dot{V}_S''$ and $\dot{I}_S''$ are computed as the difference between the pre-fault and faulted ones:

$$\dot{V}_S'' \triangleq \dot{V}_S - \dot{V}_S' \tag{VI-11}$$

$$\dot{I}_S'' \triangleq \dot{I}_S - \dot{I}_S' \tag{VI-12}$$

Therefore, the eqn. (VI-5) is written by the locally available vectors.

$$\dot{A}(x)\dot{V}_S - \dot{B}(x)\dot{I}_S = -R_F\{1 + \dot{K}(x)\}\{\dot{C}(x)\dot{V}_S'' - \dot{D}(x)\dot{I}_S''\} \tag{VI-13}$$

which leads to

$$R_F\{1 + \dot{K}(x)\} = -\frac{\dot{A}(x)\dot{V}_S - \dot{B}(x)\dot{I}_S}{\dot{C}(x)\dot{V}_S'' - \dot{D}(x)\dot{I}_S''} \tag{VI-14}$$

As the fault impedance is purely resistive, R_F is a real variable. The ratio $\dot{K}(x)$ also becomes real one on the condition that the transmission line is loss-less, and the source impedances at two ends are purely inductive. See the APPENDIX V for the proof. These facts imply that the left hand side of the eqn. (VI-14) be a real value. Therefore, the right hand side of the eqn. (IV-14) must also be a real value. The basic equation is obtained as follows.

$$\mathrm{Im}\left[\frac{\dot{A}(x)\dot{V}_S - \dot{B}(x)\dot{I}_S}{\dot{C}(x)\dot{V}_S'' - \dot{D}(x)\dot{I}_S''}\right] = 0 \tag{VI-15}$$

where Im[·] denotes the imaginary part of a complex variable. The solution x of the eqn. (VI-15) is the distance from the local end to the faulted point. As the eqn. (VI-13) is a non-linear equation, the iterative solution technique is needed. The Newton-Raphson method is applied throughout this chapter.

The basic equation contains an unknown variable x, locally available vectors, and line parameters. Thus, the fault location can be made without any remote end data. No communication channels are required. Furthermore, the eqn. (VI-15) does not include the fault resistance R_F. This means that the algorithm is able to locate a fault without being affected by the fault resistance. Accordingly, the Fourier transform based scheme preserves the properties of the Laplace transform method of CHAPTER V.

6.2.2 Fault Location Theory for Three Phase Transmission Line

The basic equation is extended to a three phase line in a straightforward way. Let $(\cdot)^{(k)}$ denote a modal quantity. For a single-phase fault,

$$\mathrm{Im}\left[\frac{\dot{V}_F^{(0)} + \dot{V}_F^{(1)} + \dot{V}_F^{(2)}}{\dot{C}^{(j)}(x)\dot{V}_S^{(j)"} - \dot{D}^{(j)}(x)\dot{I}_S^{(j)"}}\right] = 0 \qquad (VI\text{-}16)$$

$$j \in \{0,1,2\}$$

and for a double-phase fault,

$$\mathrm{Im}\left[\frac{\dot{V}_F^{(1)} + \dot{V}_F^{(2)}}{\dot{C}^{(j)}(x)\dot{V}_S^{(j)"} - \dot{D}^{(j)}(x)\dot{I}_S^{(j)"}}\right] = 0 \qquad (VI\text{-}17)$$

$$j \in \{1,2\}$$

The modal voltages at F are estimated by the eqn. (VI-18).

$$\dot{V}_F^{(k)} = \dot{A}^{(k)}(x)\dot{V}_S^{(k)} - \dot{B}^{(k)}(x)\dot{I}_S^{(k)} \qquad (VI\text{-}18)$$

$$k = 0,1,2$$

The fault locator characteristics for a single-phase case are of course applicable to a 3-phase case. In the succeeding sections, the eqn. (VI-16) and (VI-17) are applied to the fault location on the 3-phase lines.

6.2.3 Relation to Laplace Transform Based Fault Location

As is shown in CHAPTER V, the following is the basic equation of the Laplace transform method:

$$\frac{v_F'(s) + v_F''(s)}{i_{FS}''(s)} = -\{1 + k(s, x)\}R_F \qquad \text{(VI-19)}$$

The point is that the operational factor k(s, x) was evaluated at two points on the real axis of s-plane. Generally speaking, there are three ways to evaluate k(s, x) in the s-plane. Fig. VI-2 illustrates these.

(Case 1): $s = \alpha + j\ 0.0$

In this case the eqn. (VI-19) was not enough to solve x when k(s, x) is evaluated at a single point α_1. However, it was shown that k(s, x) takes the same value at two different points α_1 and α_2. One can make use of the property to establish an equation, eliminating k(s, x) and R_F. The unknown variable x is solved without knowing the values of k(s, x) and R_F.

(Case 2): $s = 0.0 + j\beta$

The operational fault current distribution factor takes a real value at $s = j\beta$, while the left hand side of the eqn. (VI-19) takes a complex value. One can solve the distance x by using the imaginary part relation. In other words, single evaluation of k(s, x) is sufficient for the location purpose.

(Case 3): $s = \alpha + j\beta$

As is shown in APPENDIX V, one can not draw a general conclusion on the possibility to solve the problem without knowing the values of k(s, x) and R_F. However, if the operational impedance angle of one side of the network is equal to the other side (at the faulted point), the factor k(s, x) takes a real value, and hence the case 3 turns out to be equivalent to the case 2.

This chapter is intended to study the case 2 and 3, completing the theoretical development of the fault location scheme based on the fault current distribution factor k(s, x).

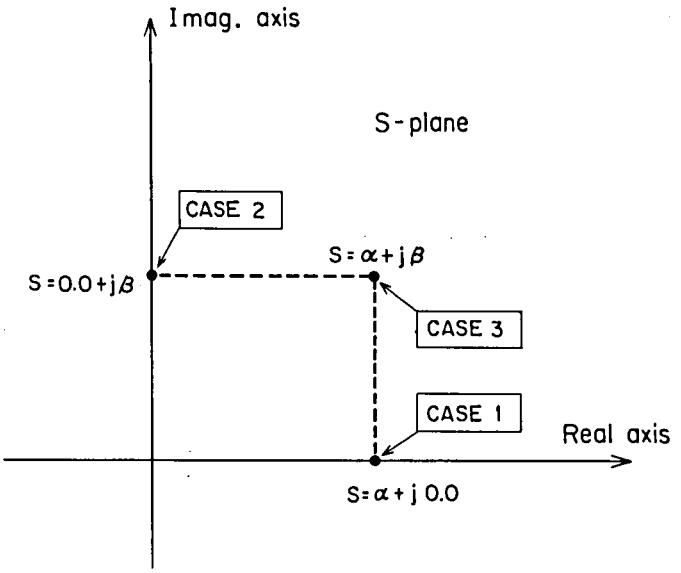

Fig. VI-2 Comparison between Laplace transform method and Fourier transform one

6.3 VERIFICATION OF FOURIER TRANSFORM BASED FAULT LOCATION ALGORITHM

6.3.1 Digital Simulation of Fourier Transform Based Fault Location Algorithm

The computer simulation is outlined in Fig. VI-3. First, the primary data of transient waveforms is smoothed out by a digital filtering program. Second, a transformation program extracts the voltage and current vectors. Last, the Newton-Raphson program is executed to solve the eqn. (VI-16) and the eqn. (VI-17).

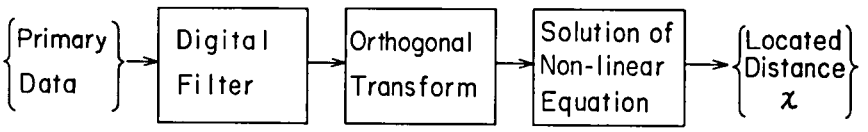

Fig. VI-3 Functional block diagram of computation for fault location

A model power system and its line constants for computer simulations are shown in Fig. VI-4 and Table VI-1, respectively. Fault transients are computed on the model system by the electromagnetic transient program [4], with the time step of 0.04 msec. These original transient waveforms are recorded in a disk file for later processing.

Data sampling for the Fourier transform is assumed to be every 1.0 msec, namely 1,000 Hz. Therefore, the digital filter is programmed to simulate a 500 Hz Butterworth filter of seventh order. There is no special intention of using the Butterworth filter. It was used simply because of its popularity. Fig. VI-5 shows its frequency response. The one-cycle Fourier transform (= OFT) of a function f(t) is defined by the eqn. (VI-20), and it is applied to a steady state vector extraction.

$$F(j\omega_0) = \int_{t-T}^{t} f(u)e^{-j\omega_0 u}\, du \qquad \text{(VI-20)}$$

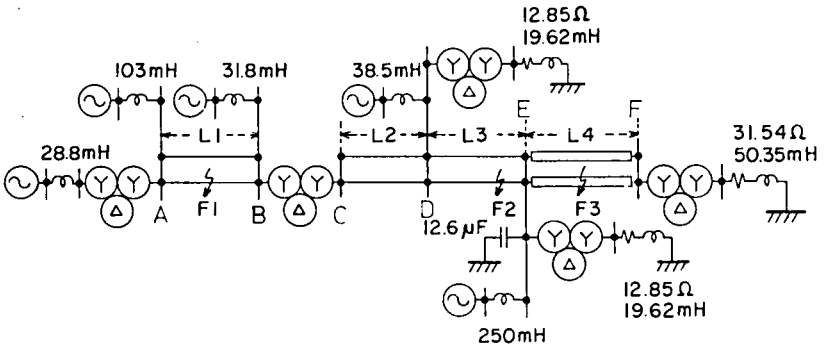

Fig. VI-4 A model transmission system

Constant / line	$r^{(0)}\ \Omega/Km$	$\ell^{(0)}$ mH/Km	$c^{(0)}\ \mu F/Km$	$\alpha^{(0)}\ rad/Km \times 10^{-3}$	$z^{(0)}\ \Omega$
	$r^{(1)}\ \Omega/Km$	$\ell^{(1)}$ mH/Km	$c^{(1)}\ \mu F/Km$	$\alpha^{(1)}\ rad/Km \times 10^{-3}$	$z^{(1)}\ \Omega$
L 1	0.11480	2.2886	0.00523	1.0869	662
	0.02083	0.8984	0.01291	1.0699	264
L 2	0.11570	2.2989	0.00526	1.0925	661
	0.01974	0.7968	0.01456	1.0701	234
L 3	0.11570	2.2989	0.00526	1.0925	661
	0.01974	0.7968	0.01456	1.0701	234
L 4	0.55400	0.9942	0.35567	5.9076	53
	0.02549	0.4020	0.35567	3.7565	34

Table VI-1 Line constants of the model transmission system

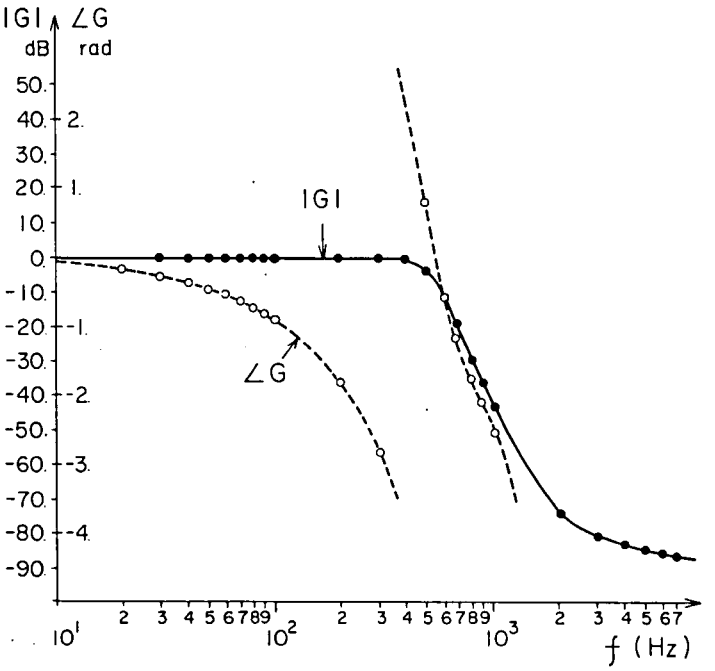

Fig. VI-5 Frequency response of a 500 Hz Butterworth filter of seventh order

where $T = 2\pi/\omega_0$ and ω_0 is the system angular frequency.

Fig. VI-6 shows a result of the fault location at the local end E for a single-phase fault at F3 with the zero fault resistance. The relay settings are as follows.

$$\lambda^{(0)} = \omega_0 \sqrt{\ell^{(0)} c^{(0)}} = 5.908 \times 10^{-3} \text{ rad/km}$$
$$\lambda^{(1)} = \omega_0 \sqrt{\ell^{(1)} c^{(1)}} = 3.756 \times 10^{-3} \text{ rad/km}$$
$$Z^{(0)} = \sqrt{\ell^{(0)}/c^{(0)}} = 53.0 \text{ ohm}$$
$$Z^{(1)} = \sqrt{\ell^{(1)}/c^{(1)}} = 34.0 \text{ ohm}$$

Two statistics $\bar{x}$ and σ are computed to evaluate the locating performance: $\bar{x}$ is the mean value of the located distance x during a period T_1 and σ is the standard deviation of x during the same period. As is shown in Fig. VI-6, T_1 is defined as a half-cycle period beginning one cycle after the fault. The distance $\bar{x}$ of Fig. VI-6 is 11.02 km and σ is 0.28 km, while the true value x* is 11.00 km. Therefore, the location is very accurate and stable. The word "stability" is used to measure the fluctuation of x. The smaller the standard deviation, the more stable is the location. The solution of the eqn. (VI-16) converges in most cases after two iterations. Fig. VI-7 shows an iteration process.

To cover the various situations in an actual power system, digital simulations are carried out extensively. Among them, the effects of a fault resistance, a transmission line loss, a load characteristic, and a waveform distortion are discussed below on the accuracy of fault location. The locator is disposed at the end E, and the fault point is chosen at F3 throughout the simulations.

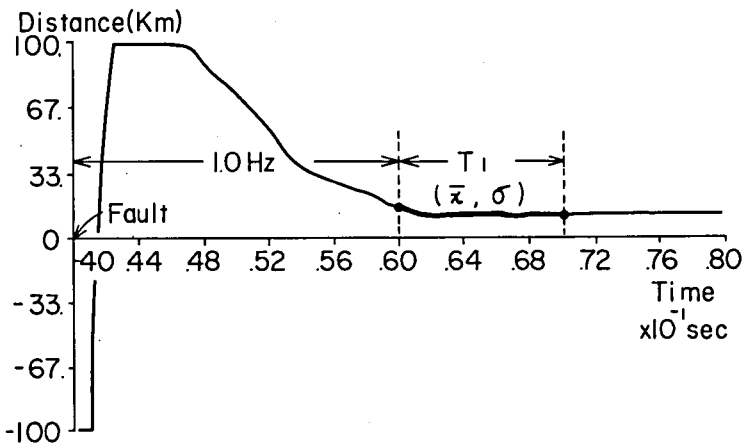

Fig. VI-6 Fault location process until settling at 11.02 km

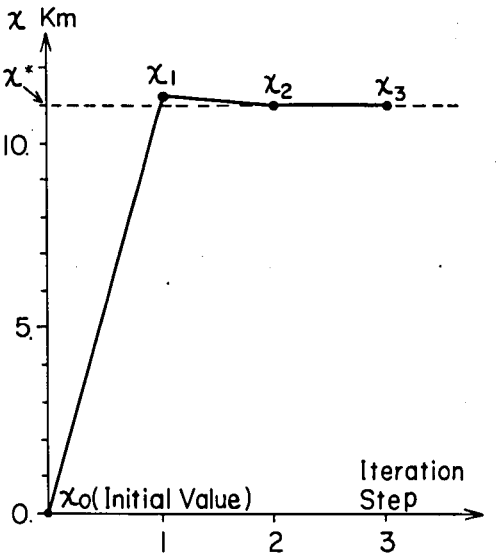

Fig. VI-7 Typical iterative solution process by Newton-Raphson method

6.3.2 Numerical Evaluation of Fault Resistance Effect

The solid line of Fig. VI-8 is the located distance for the same type fault as in Fig. VI-6, but with the fault resistance of 10.0 ohm. For comparison, the result of Fig. VI-6 is superimposed by the dashed line.

Both locations converge to the same distance, which is very close to the true one. The basic equations guarantee an accurate location not affected by the fault resistance, and the property has been confirmed through the digital simulation. Comparing the two schemes, one can conclude that the Fourier method gives almost ten times as accurate as the Laplace method.

6.3.3 Numerical Evaluation of Transmission Line Loss Effect

The Fourier transform method assumes that $\dot{K}(x)$ of the eqn. (VI-4) takes a real value. The assumption seems unsatisfied when a transmission line loss effect is taken into account. Fig. VI-9 compares the result of a loss-less line case with that of a lossy line. For the lossy line case, $\bar{x}$ is 10.85 km and σ is 0.32 km. This is a single-phase fault case that is worst to the Fourier transform method, because the ratio R/X of mode 0 is largest of all modes. Even though Fig. VI-9 shows the worst case, the location error is very small. The same degree of or higher accuracy can be expected for the multiple-phase short circuit, because the mode 0 does not participate in these. It is concluded that the transmission line loss will not degrade the fault location accuracy.

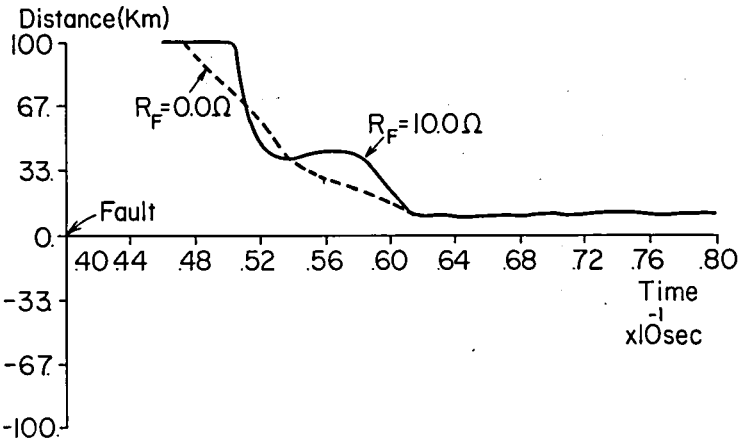

Fig. VI-8 Fault resistance effect on location process

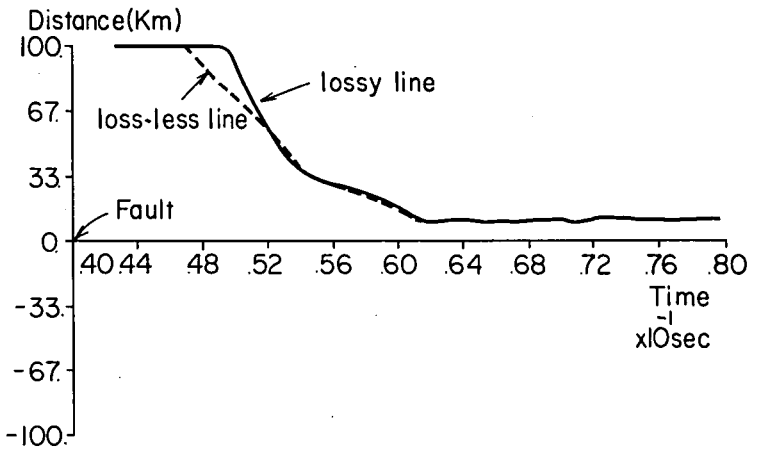

Fig. VI-9 Transmission line loss effect on location process

6.3.4 Numerical Evaluation of Load Characteristics

The source impedance must be purely inductive to guarantee an accurate fault location. An inductive load ($= R_L + jX_L$) at the remote end is studied. The located distance converges to the value slightly different from the true one. Fig. VI-10 illustrates it. For the double-phase fault of Fig. VI-10, $\bar{x}$ is 12.92 km and σ is 0.35 km. Thus, the type of source impedance at the local and remote end must be carefully studied whether they satisfy the condition of $\dot{K}(x)$ or not, prior to applying the algorithm to the fault location.

6.3.5 Numerical Evaluation of Filter Characteristics

The waveform distortion is created by non fundamental frequency components in the voltage and current, which are caused by the transient phenomena due to a fault. The prefilters of different cut off frequencies f_c are used to study the effect. Fig. VI-11 shows the correlation of $\bar{x}$ and σ for the cutoff frequency. As is expected $\bar{x}$ is uncorrelated with f_c but σ increases along with f_c. The filtered data is sampled every 1.0 msec for the Fourier transformation. According to Fig. VI-11, the instability of x appears beyond 500 Hz, which is the half of the sampling frequency. This is caused by the frequency folding error in digital signal processing. The stability will be guaranteed by choosing an appropriate pre-filter.

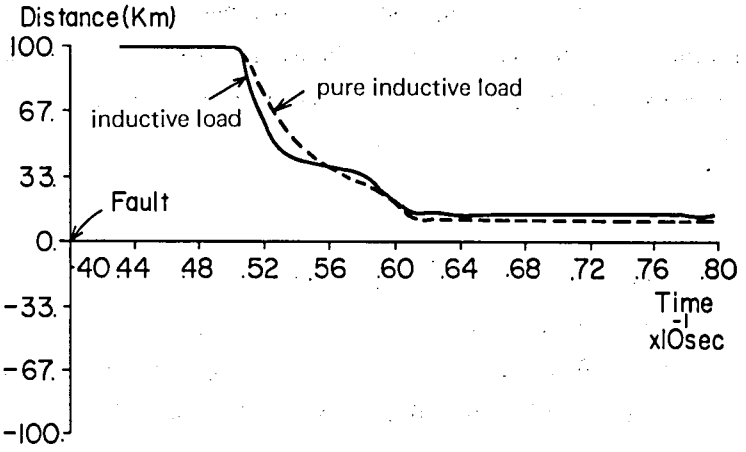

Fig. VI-10 Load characteristic effect on location process

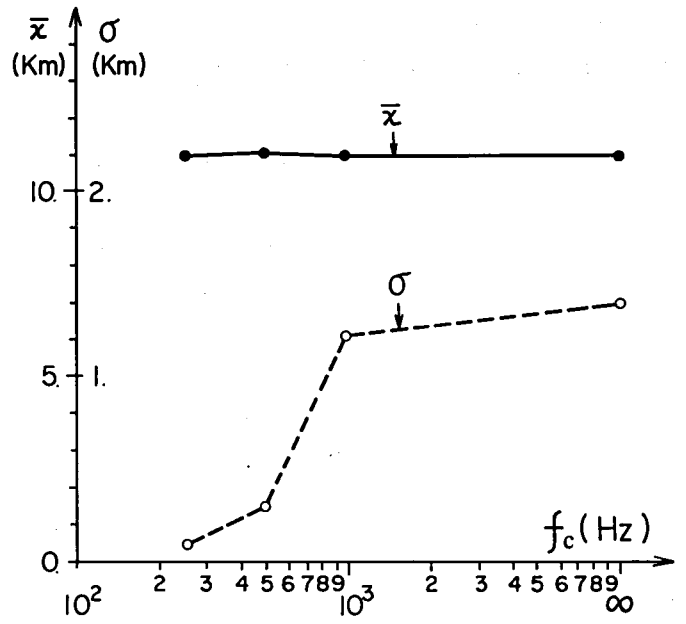

Fig. VI-11 Fault location accuracy and stability versus filter characteristics

6.4 OPTIMIZATION OF NUMERICAL FOURIER TRANSFORM

The developed algorithm basically consists of two numerical computations. One is the Fourier transform of voltage and current waveforms, and the other is the solution of non-linear algebraic equations. Of the two computations, fast and approximate algorithms of the Fourier transform are studied through the digital computer simulations.

6.4.1 Half Cycle Fourier Transform

One cycle Fourier transform (= OFT) defined by the eqn. (VI-19) has been used in the digital computer simulations of the section 6.3. $F(j\omega_0)$ of the eqn. (VI-19) has been evaluated at the angular frequency of $\omega_0 = 2\pi f_0$, where f_0 is the system frequency. A half-cycle Fourier transform (= HFT) is defined here by the eqn. (VI-21).

$$\hat{F}(j\omega_0) = \int_{t-\frac{T}{2}}^{t} f(u)e^{-j\omega_0 u}\, du \qquad \text{(VI-21)}$$

$$T = 2\pi/\omega_0 \qquad \text{(VI-22)}$$

The HFT algorithm is substituted into the Fourier transform block of Fig. VI-3. In Fig. VI-12, the result of the HFT algorithm is compared with that of the OFT one. While the distance to which both algorithms converge are almost equal with each other, the HFT algorithm converges two times faster than the OFT does. As any other differences are not noticed, the HFT algorithm is effective to speed up the fault location.

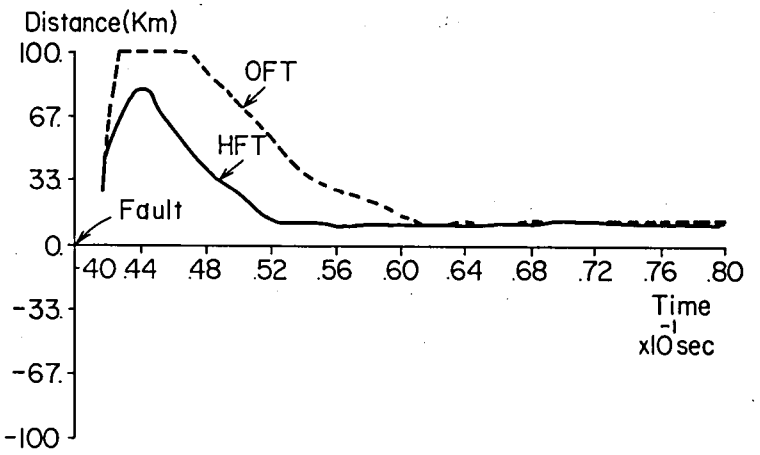

Fig. VI-12 Half-cycle Fourier transform method compared with one-cycle transform

6.4.2 Truncated Fourier Transform

John and Martin proposed a fundamental digital algorithm [5] for the Fourier transform, which is temporarily referred to the truncated Fourier transform (= TFT). The TFT is defined as follows.

For a voltage v(t),

$$\bar{V}(j\omega_e) = \int_{t-\frac{T}{2}}^{t} v(u)e^{-j\omega_e u}\, du \qquad \text{(VI-23)}$$

and for a current i(t),

$$\bar{I}(j\omega_e) = \int_{t-\frac{T}{2}}^{t} i(u)e^{-j\omega_e u}\,du - \tau[i(t-\frac{T}{2})e^{-j\omega_e(t-\frac{T}{2})} - i(t)e^{-j\omega_e t}]/(1 + j\omega_e T_c) \qquad \text{(VI-24)}$$

where ω_e (= $2\pi f_e$) is an arbitrary angular frequency, and T_c (= L/R) is the time constant of a transmission line. As is shown in the eqn. (VI-23), the integral interval is chosen at a half cycle.

It should be noted that the angular frequency ω_e is selected at an arbitrary value. In this study, ω_e is set to 80π (namely f_e = 40.0 Hz). The TFT algorithm is used for the Fourier transform of Fig. VI-3. Fig. VI-13 illustrates a simulation result. The solution by the TFT converges within a half cycle to the final value, which is also the solution by the OFT. As the TFT algorithm provides an accurate and stable solution, it contributes to the acceleration of the fault location speed.

6.4.3 Walsh Transform

To speed up the orthogonal transformation, the Walsh function is frequently used. In the relaying literature, it was applied to the distance protection [6]. An arbitrary function f(t) is expanded as follows:

$$f(t) = \sum_{k=0}^{\infty} w_k \; wal(k,t) \qquad \text{(VI-25)}$$

For fault location, the voltage and current are expanded by wal(1,t) and wal(2,t). The two functions are shown in Fig. VI-14. As no multiplications are needed and only additions are used, the computation time for the orthogonal transformation is greatly reduced. The solution by the Walsh method is shown in Fig. VI-15. It is almost the same distance as the one by the OFT algorithm. The standard deviation σ is 0.64 km and slightly large, since the first two coefficients w_1 and w_2 of the eqn. (VI-25) are used, and the other coefficients are neglected.

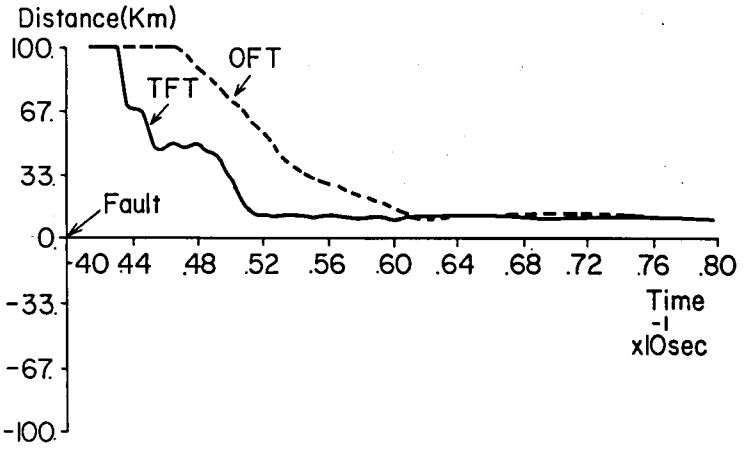

Fig. VI-13 Truncated Fourier transform method compared with one-cycle transform

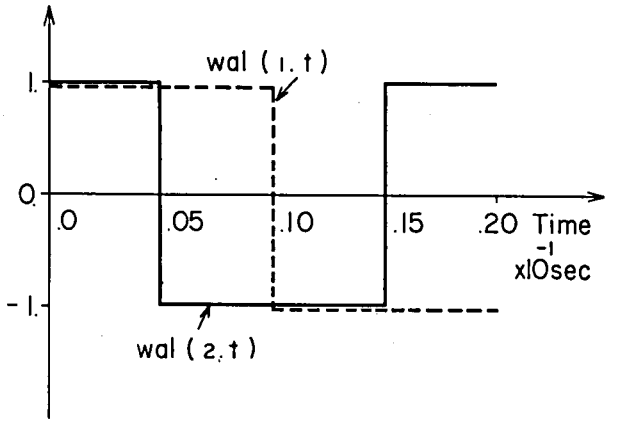

Fig. VI-14 Walsh functions wal(1,t) and wal(2,t)

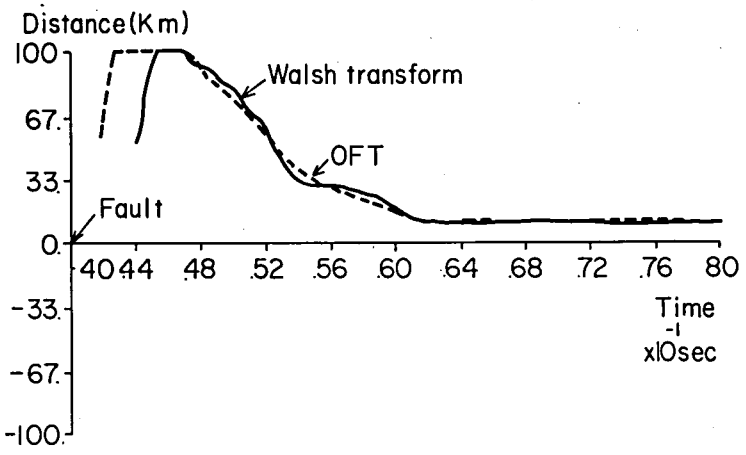

Fig. VI-15 Walsh transform method compared with one-cycle Fourier transform

6.5 CONCLUSION

An algorithm based on the Fourier analysis has been developed for accurate fault location in an EHV/UHV transmission line. The algorithm has made it possible to locate a fault accurately with locally available data set, and without being affected by a fault resistance. Digital computer simulations have confirmed these properties. With practical applications in mind, fast algorithms such as a half-cycle Fourier, a truncated Fourier, and a Walsh transform have been studied, providing promising results.

The scheme requires a strong power for numerical calculations, and it therefore will be suitable for digital processor use, that is computer relaying use.

CHAPTER VII DECISION MAKING ANALYSIS IN COMPUTER RELAYING [6]

7.1 INTRODUCTION

From the decision theoretic point of view, it appears that the algorithms so far have provided the criterion value to discriminate the fault condition. The final decision, trip or nontrip, is usually made through a very simple method. This is done as follows, for instance. The criterion value is compared with the threshold value which is pre-determined. If the former goes above the latter in some successive comparisons, the relay issues a trip signal. This process is very heuristic and seems to be unjustified until now from the mathematical standpoint. The prime purpose of this chapter is to give a mathematical background to the discriminating process. So far any statistical approach has been excluded in the relay engineering. It, however, must be recognized that certain probabilistic nature really exists in the boundary conditions of fault. The fault impedance, fault angle, and fault point are some of them, affecting the criterion value respectively. With this nature in mind, the concept of random variable is introduced to the criterion value, and the discriminating process is formulated through the statistical decision theory.

Another problem, which is important but attacked little [2], is the determination of sampling rates for the digital relay. It has been solved mostly within the frames of speed of the processor and/or the capacity of the communication channel. The formulation of this chapter through the statistical decision theory gives the concept of average number of samples required to reach a final decision, fault or unfault. It is possible to estimate the least sampling rate for digital relay necessary to discriminate the fault condition, given parameters of statistics of the criterion value and the fault detecting speed.

The decision directed approach has been very rare in the relaying field. In analog relays, it seems difficult to incorporate the elaborate decision mechanism due to its weakness in power for logical and numerical calculations. On the other hand, the digital relays have strong capability for information processing. Thus, more attentions should be paid to the ability of making decisions in digital systems, which is one of the important strengths over analog ones. This chapter presents one of the approaches toward this direction [6].

7.2 CONCEPT OF RANDOMNESS IN COMPUTER RELAYING

7.2.1 Formulation of Fault Measure with Random Variable

As one of the mathematical formulations for discriminating process, a statistical decision theoretic approach is applied in this capter. For example, consider the current differential relay with the discriminant value d_1:

$$d_1 = |\dot{I}_1 + \dot{I}_2| \qquad \text{(VII-1)}$$

where $\dot{I}_1$ and $\dot{I}_2$ are current vectors at local and remote terminals. Note that the restraining practice is omitted for the sake of simplicity. Assume that d_1 is a random variable. Two probability density functions (p.d.f.) can be defined:

$p(d_1/\text{unfault})$ = p.d.f. of d_1 under unfault condition
$p(d_1/\text{fault})$ = p.d.f. of d_1 under fault condition

If the two density functions are disjoint with each other, as in Fig. VII-1 (a), a threshold value δ_1 can be determined so as to separate the two events perfectly. In this case, the heuristic strategy widely employed so far is justified as the discriminating process. Practical situation, however, is not a simple one. The two p.d.f.'s overlap generally as in Fig. VII-1 (b). The shape of the p.d.f. depends upon the fault resistance, back impedance, fault point, power flow, and so on. The boundary conditions of these have probabilistic natures, more or less, thus enabling the formulation of the discriminating process with the statistical decision theory.

In Fig. VII-1 (b), there are four regions D_{00}, D_{10}, D_{01} and D_{11}. Their meanings:

D_{00} = probability of deciding unfault as unfault
D_{10} = probability of deciding fault as unfault
D_{01} = probability of deciding unfault as fault
D_{11} = probability of deciding fault as fault

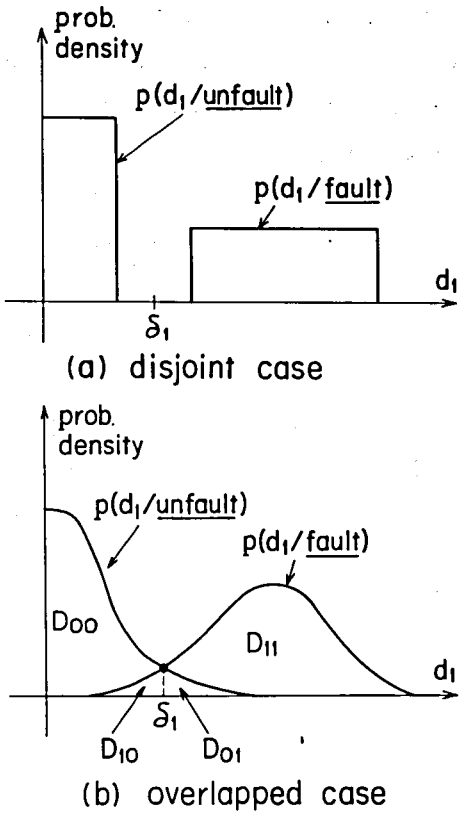

Fig. VII-1 Probability density function of d_1 under fault and unfault condition

On the one hand, the discriminant value d_1 comes to the region D_{10} for an internal fault with a high arcing resistance, therefore causing the relay not to operate. On the other hand, d_1 of the relay with very small value of δ possibly comes to the region D_{01} even for an external fault, making the relay misoperate.

The random variable formulation of fault criterion is made in another type of protection. An impedance R + jX measured by a distance relay has some extent of the random nature, because it is affected by the amount of a pre-fault power flow and an arcing resistance. The power transformer protective relay takes into account the random nature implicitly in its working principle by employing the harmonic restraining. The following is a close look at the power transformer protection from the probabilistic point of view.

It is critical, and difficult at the same time, to separate a fault and inrush current. In both cases, the transformer relay measures a large magnitude of the differential current that is sufficient to make a trip decision. The most popular technique has been the use of the second harmonic restraining. The technique depends on the experienced knowledge such that the second harmonic shows a large magnitude in the inrush current, while showing a small one in the internal fault current. The fault criterion is written as

$$\begin{aligned} d_{tr} &\triangleq 1 - K|\dot{I}_{d_2}|/|\dot{I}_{d_1}| \\ &= 1 - K \cdot r \end{aligned} \qquad \text{(VII-2)}$$

The second harmonic $\dot{I}_{d2}$ to the fundamental component $\dot{I}_{d1}$ ratio r varies with several factors. The line time constant L/R is dominant to determine the ratio r in the fault current. Fig. VII-2 gives the ratio versus time constant relation. On the other hand, the residual flux is a dominant factor to the ratio in the inrush current. Fig. VII-3 illustrates the dependency of r to the residual flux. These two factors can be treated as random events. Accordingly, the probability density function of d_{tr} is drawn like Fig. VII-4. One must make a decision under such an uncertain environment on the fault criterion.

7.2.2 Estimation of Probability Density Function for Fault Criterion

Consider another type of differential relay to estimate the p.d.f. with the discriminant value d_2.

$$d_2 = i_1(t) + i_2(t-\tau) - \frac{1}{z}\{v_1(t) - v_2(t-\tau)\} \qquad \text{(VII-3)}$$

where τ is the surge propagation time between two ends and z is the surge impedance of the line. The eqn. (VII-3) is known as the d'Alembert relay [3]. Fault transients are calculated by the EMTP [4] with the following parameters.

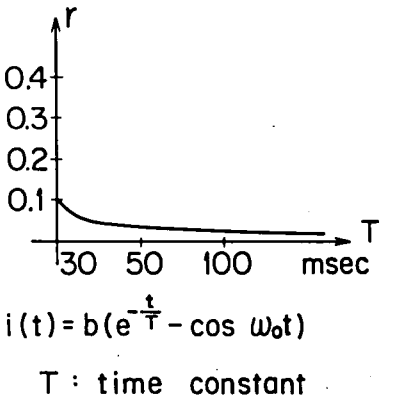

Fig. VII-2 The second harmonic to the fundamental component ratio r versus line constant L/R relation

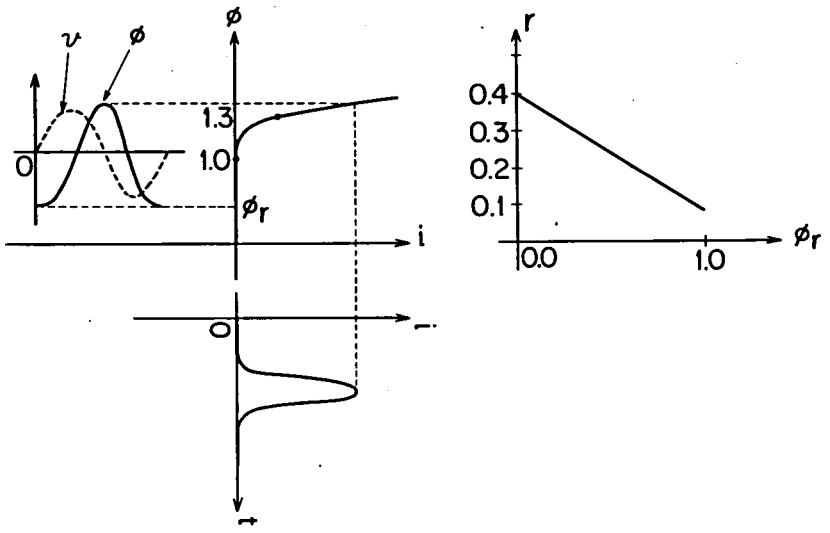

$$v = a \sin(\omega_0 t + \theta) \triangleq \frac{d\phi}{dt}$$

$$\phi = -\frac{a}{\omega_0} \cos(\omega_0 t + \theta) + \phi_r$$

ϕ_r : residual flux

Fig. VII-3 The second harmonic to the fundamental component ratio r versus residual flux ϕ_r relation

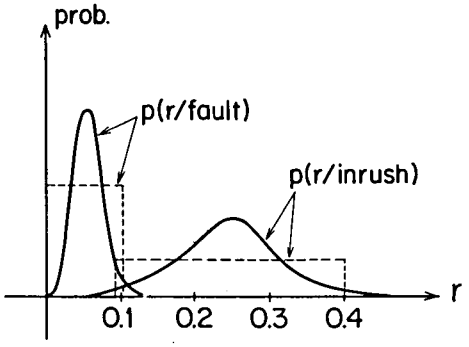

As two density functions overlap, the setting value K must be determined carefully.

$$d_{tr} = 1 - K \cdot r \gtrless 0$$

Fig. VII-4 Probability density function of d_{tr} under fault and inrush condition

(i) pre-fault power flow = {heavy, light}
(ii) back power = {big, small}
(iii) fault angle = {0°, 90°}
(iv) fault resistance = {large, small}
(v) fault point = {close-in, remote}
(vi) fault type = {phase-a-to-ground fault}

Based on the data of $2^5 = 32$ cases, two histograms (or frequency polygons) are drawn in Fig. VII-5. One is drawn from the data of the faulted phase, and the other is from the unfaulted phase. It is unfair to estimate both $p(d_2/\text{unfault})$ and $p(d_2/\text{fault})$ through these very limited number of samples. The normal distributions, however, seem to be reasonable assumptions for both of them. The parameters of normal distribution are not known, but zero for the mean value and the r.m.s. value of the fault current for the standard deviation are the reasonable ones. It is the author's belief that the setting for parameters is a matter of designing, just like a pick up value for the conventional relay.

7.3 PROBABILISTIC APPROACH TO DECISION MAKING IN COMPUTER RELAYING

7.3.1 Sequential Probability Ratio Testing

Assume that the conditional probability density functions of the random variable {x} are known.

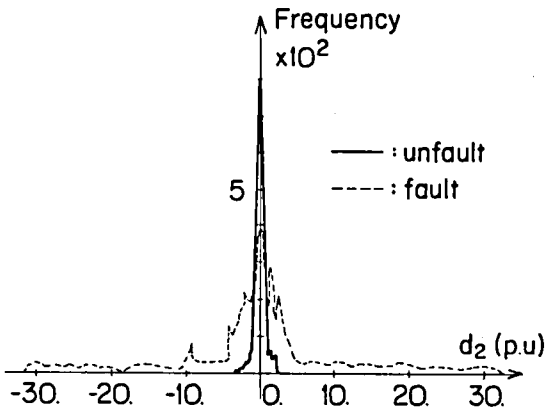

Fig. VII-5 Estimated frequency polygons of the criterion d_2 under fault and unfault condition

$p(x/H_0)$ = p.d.f. of x under hypothesis H_0 (VII-4)

$p(x/H_1)$ = p.d.f. of x under hypothesis H_1 (VII-5)

Then a likelihood ratio θ_k for a sequence of $\{x\}$, X_k, defined by the eqn. (VII-6)

$$\theta_k = \frac{p(X_k/H_1)}{p(X_k/H_0)} \qquad X_k = x_1 x_2 \cdots\cdots x_k \tag{VII-6}$$

is used to test the two hypotheses $\{H_0, H_1\}$ in the following way.

If $\theta_k \leq B$, then the hypothesis H_0 is accepted,
If $B < \theta_k < A$, then the testing is continued, and
If $A \leq \theta_k$, then the hypothesis H_1 is accepted.

Two constants A and B are defined by

$$A = (1 - \epsilon_1)/\epsilon_0 \tag{VII-7}$$

$$B = \epsilon_1/(1 - \epsilon_0) \tag{VII-8}$$

where ϵ_0 is the probability of identifying H_0 as H_1, and ϵ_1 is that of identifying H_1 as H_0. The testing process is illustrated in Fig. VII-6. This is called the sequential probability ratio test [5], one of the statistical decision methods. When x is independent and identically distributed, θ_k is given by the eqn. (VII-9).

$$\theta_k = \frac{p(x_1/H_1)\cdot p(x_2/H_1)\cdot\cdots\cdot p(x_k/H_1)}{p(x_1/H_0)\cdot p(x_2/H_0)\cdot\cdots\cdot p(x_k/H_0)} \tag{VII-9}$$

Taking the logarithm of this equation, one obtains the recursive formula:

$$\log\theta_k = \log\theta_{k-1} + \log\frac{p(x_k/H_1)}{p(x_k/H_0)}$$

$$\triangleq \log\theta_{k-1} + \log\Delta\theta_k \tag{VII-10}$$

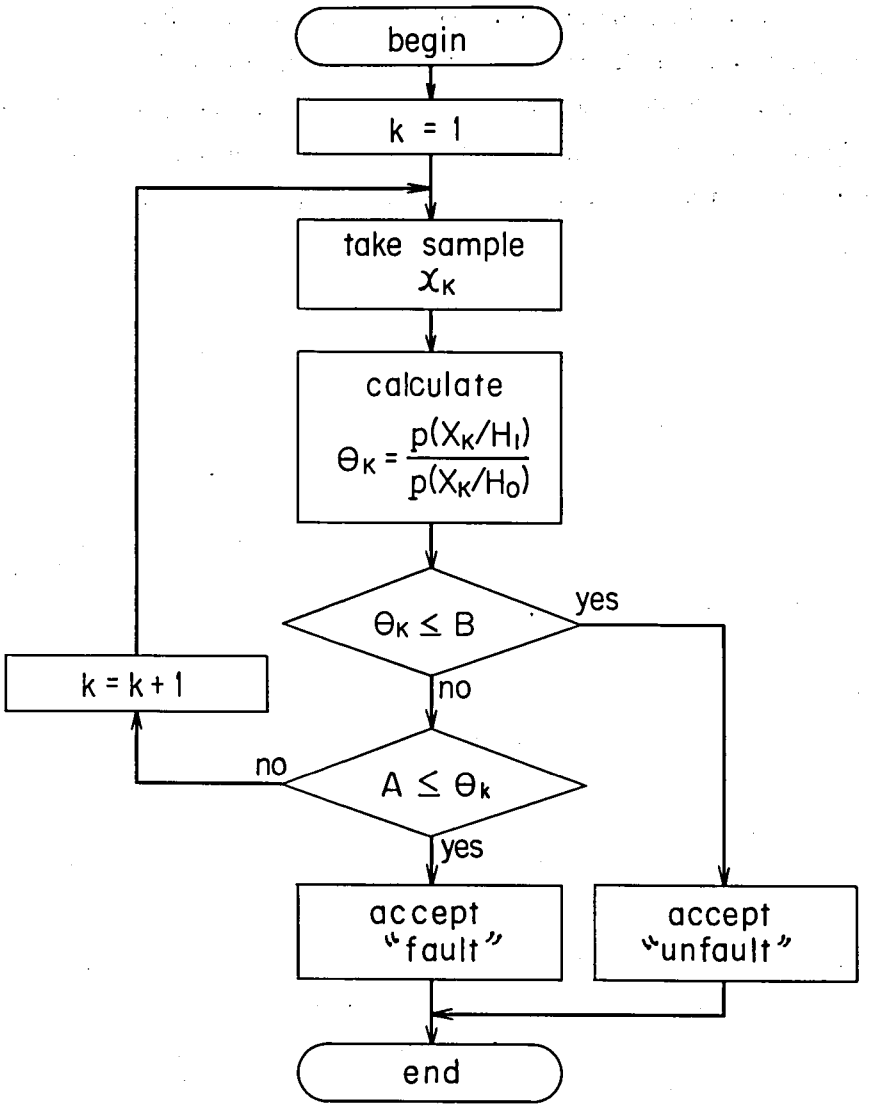

Fig. VII-6 A flow chart of sequential probability ratio testing

This is very effective in real time calculation of the probability ratio. In terms of the relay engineering, H_0, H_1 and x read unfault, fault, and the discriminant value respectively. The error probabilities ϵ_0 and ϵ_1 are equivalent to the region D_{01} and D_{10} in Fig. VII-1 (b).

7.3.2 Probabilistic Decision Making in Travelling Wave Differential Relay

Consider that the d'Alembert relay of the eqn. (VII-3) is applied to the evaluating process, or equivalently the measuring algorithm, and the sequential probability ratio test to the discriminating process. Assume that the sequence of the criterion value d_2 is the independent and identically distributed random variable with the p.d.f. of normal distribution.

$$p(d_2/H_i) = \frac{1}{\sqrt{2\pi}\,\sigma_i} \exp(-d_2^2/2\sigma_i^2) \qquad i=0,1 \qquad \text{(VII-11)}$$

H_0: unfault

H_1: fault

σ_i^2: variance of d_2 for H_i

The testing is applied to the four cases with the parameters of

(a) $\sigma_0 = 0.15, \quad \sigma_1 = 15.0, \quad \epsilon_0 = \epsilon_1 = 0.01$

(b) $\sigma_0 = 0.15, \quad \sigma_1 = 15.0, \quad \epsilon_0 = \epsilon_1 = 0.001$

(c) $\sigma_0 = 0.15, \quad \sigma_1 = 1.5\ , \quad \epsilon_0 = \epsilon_1 = 0.01$

(d) $\sigma_0 = 0.15, \quad \sigma_1 = 1.5\ , \quad \epsilon_0 = \epsilon_1 = 0.001$

The solid line in Fig. VII-7 is the criterion value d_2 for a faulted phase, and the dashed line in Fig. VII-7 is that for an unfaulted phase. The testing procedure for the case (a) is carried out as follows. The initial value of θ_0 is set to 1.0, therefore $\log\theta_0 = 0.0$. First consider the faulted phase. The details of numerical results are summarized in Table VII-1. The relay evaluates the eqn. (VII-2), getting 0.01 for d_2 at time step 1. Then it calculates the likelihood ratio $\log\Delta\theta_1$ at this time step, which becomes -4.603. Since this value goes below the threshold value $\log B = -4.595$, the relay accepts the hypothesis of unfault and initializes the testing procedure for restart. In the same way, the relay accepts unfault for the next four observations. At time step 6, the criterion d_2 rises to 2.55 (due to actual fault), and the likelihood ratio also jumps to 139.9. This ratio is far higher than the other threshold value $\log A = 4.595$. Thus, the relay accepts the hypothesis of fault, which means issuing the trip signal to circuit breaker. The fault hypothesis is accepted at every time step thereafter, with the exception of step 15. At time step 15, the calculated d_2 is -0.17, which is too small to reach the fault region. Next value of d_2, however, brings the procedure to termination with accepting fault hypothesis.

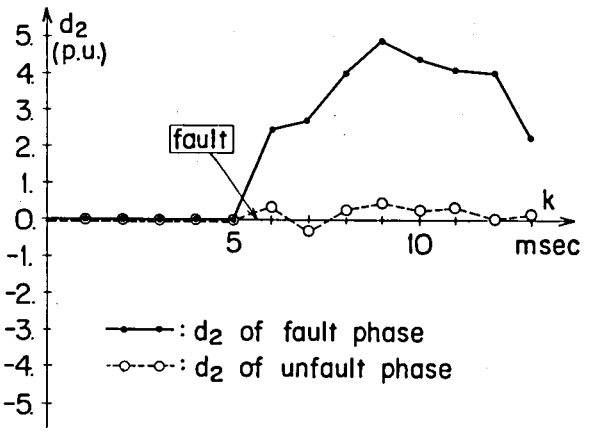

Fig. VII-7 Fault criterion d_2 at fault and unfault phase

Time step	d_2	Log $\Delta\theta_k$	Log θ_k	FinaL decision
1	0.01	-4.603	-4.603	U
2	0.01	-4.603	-4.603	U
3	0.01	-4.603	-4.603	U
4	0.01	-4.603	-4.603	U
5	0.01	-4.603	-4.603	U
6	2.55	139.9	139.9	F
7	2.88	179.0	179.0	F
8	4.16	379.3	379.3	F
9	4.88	524.8	524.8	F
10	4.22	390.4	390.4	F
11	3.98	346.5	346.5	F
12	3.91	335.1	335.1	F
13	2.32	115.0	115.0	F
14	0.76	8.095	8.095	F
15	-0.17	-3.998	-3.998	?
16	-1.84	70.17	66.19	F
17	-3.34	238.7	238.7	F
18	-4.19	384.6	384.6	F
19	-4.90	529.4	529.4	F
20	-5.29	616.4	616.4	F

Log A = 4.595, Log B = -4.595

U : unfault

F : fault

? : suspended

Table VII-1 Decision making process at fault phase by hypothesis testing method

Next consider the unfaulted phase. Refer to Table VII-2 for the details of numerical results. The hypothesis of unfault is accepted until time step 5. The fault brings the value of d_2 to 0.38 at time step 6, for which the likelihood ratio becomes -1.770 and thus the final decision is suspended to the next step. At time step 7, the likelihood ratio $\log\Delta\theta_2$ of -2.852 is added to the previous one, resulting with the total ratio of -4.622 which is smaller than logB. Therefore, the relay accepts the hypothesis of unfault at time step 7. The testing procedure is initialized and restarted. Thereafter, it takes a few time steps for the relay to reach the unfault decision.

The process of the testing mentioned above is illustrated in Fig. VII-8. Other testings for the case (b) to (d) are shown in Fig. VII-9 to Fig. VII-11. Throughout these cases, the hypothesis of fault is accepted just after the actual fault takes place, and there is no significant difference among the testing procedures. On the other hand, a significant difference can be observed in the unfaulted phase. The time to reach the final decision varies significantly with both ϵ_i and σ_i. Table VII-3 shows this fact. It is easy to note that the smaller ϵ_i, the longer the time step required for final decision is. This is due to the conservativeness in decision which tries to keep the error rate within the specified value. It is also noted that the closer σ_0 and σ_1 with each other, the longer the time step is. The closeness of σ_0 and σ_1 means that the part which is overlapped in the two distributions is large, therefore causing the time step to be longer until coming to the final decision.

Now let us try to interprete the heuristic discriminating procedure, in which the relay issues the trip signal after some number of successive discriminations satisfy the relation of $d_2 > \delta_2$. Select the pick up value so as to satisfy the eqn. (VII-12):

$$\frac{p(\delta_2/H_1)}{p(\delta_2/H_0)} = A^{\frac{1}{n}} \qquad \text{(VII-12)}$$

If at least n successive discriminations end in fault ($d_2 \geq \delta_2$), then the final decision as fault can be justified by the termination of the sequential probability ratio test with the same discrimination. It can be said that the heuristic method is based on the counter concept, compared with the accumulator concept of the probabilistic method. The counter counts up everytime the simple test, $d_2 > \delta_2$, succeeds and it is reset everytime the test fails. On the other hand, the accumulator sums up the likelihood ratio until it overflows (fault) or underflows (unfault), and it is cleared everytime either one takes place.

Time step	d_2	Log $\Delta\theta_k$	Log θ_k	Final decision
1	-0.01	-4.603	-4.603	U
2	-0.01	-4.603	-4.603	U
3	-0.01	-4.603	-4.603	U
4	-0.01	-4.603	-4.603	U
5	-0.01	-4.603	-4.603	U
6	0.38	-1.770	-1.770	?
7	-0.28	-2.852	-4.622	U
8	0.29	-2.815	-2.815	?
9	0.50	0.943	-1.872	?
10	0.27	-2.966	-4.838	U
11	0.32	-2.358	-2.358	?
12	0.01	-4.603	-6.960	U
13	0.01	-4.363	-4.363	?
14	0.23	-3.447	-7.810	U
15	-0.10	-4.396	-4.396	?
16	-0.11	-4.319	-8.715	U
17	-0.14	-4.200	-4.200	?
18	-0.07	-4.507	-8.707	U
19	-0.03	-4.595	-4.595	U
20	-0.17	-3.942	-3.942	?

Log A = 4.595, Log B = -4.595

U : unfault

F : fault

? : suspended

Table VII-2 Decision making process at unfault phase by hypothesis testing method

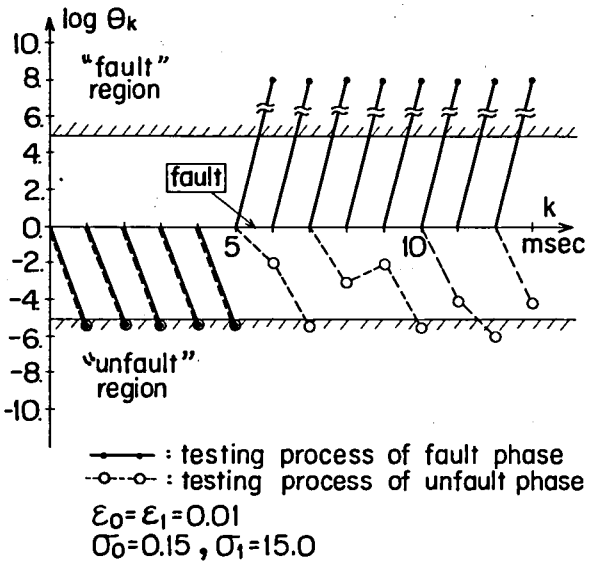

Fig. VII-8 Result of the hypothesis testing for $\epsilon_0 = \epsilon_1 = 0.01$, $\sigma_0 = 0.15$ and $\sigma_1 = 15.0$

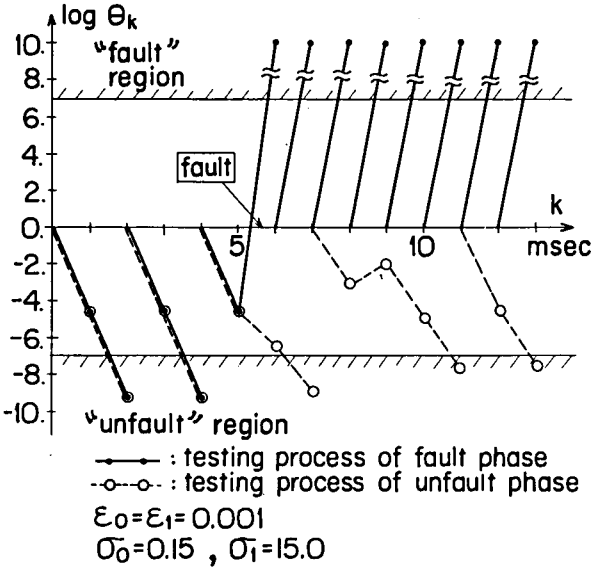

Fig. VII-9 Result of the hypothesis testing for $\epsilon_0 = \epsilon_1 = 0.001$, $\sigma_0 = 0.15$ and $\sigma_1 = 15.0$

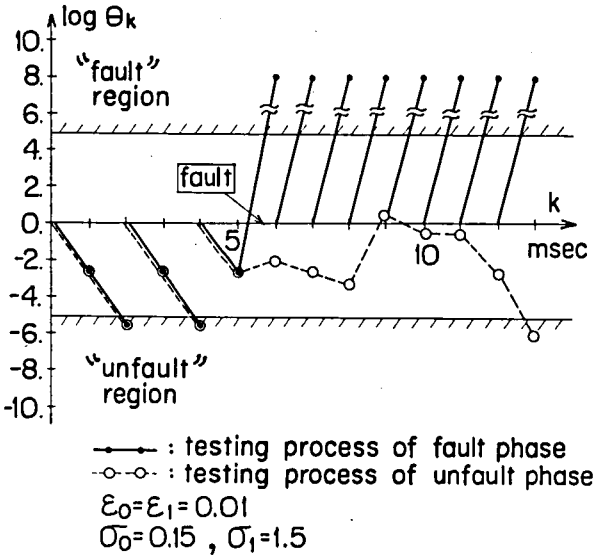

Fig. VII-10 Result of the hypothesis testing for $\epsilon_0 = \epsilon_1 = 0.01$, $\sigma_0 = 0.15$ and $\sigma_1 = 1.5$

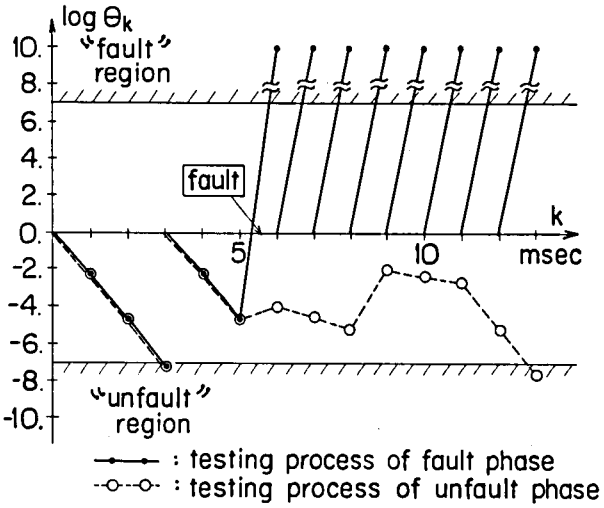

Fig. VII-11 Result of the hypothesis testing for $\epsilon_0 = \epsilon_1 = 0.001$, $\sigma_0 = 0.15$ and $\sigma_1 = 1.5$

ε \ σ_1	15.0	1.5
0.01	2	8
0.001	3	10

Table VII-3 Actual number of samples until accepting the hypothesis unfault

7.4 APPLICATION OF PROBABILISTIC CONCEPT TO DETERMINATION OF SAMPLING RATES

7.4.1 Average Number of Samples to Final Decision

In the probabilistic method, the incremental value of likelihood ratio is obtained at the k-th step of its testing. It is written as the difference between the log-conditional probability densities of x_k.

$$\begin{aligned} \log\Delta\theta_k &= \log\theta_k - \log\theta_{k-1} \\ &= \log p(x_k/H_1) - \log p(x_k/H_0) \end{aligned} \tag{VII-13}$$

Assume the normal distributions, then the eqn. (VII-13) becomes

$$\log\Delta\theta_k = \log\frac{\sigma_0}{\sigma_1} + \frac{1}{2}\left\{\left(\frac{x_k}{\sigma_0}\right)^2 - \left(\frac{x_k}{\sigma_1}\right)^2\right\} \tag{VII-14}$$

Thus it is possible to calculate the expected value of $\log\Delta\theta_k$ when x_k is known to come from the hypothesis H_i. Taking the expectations of the eqn. (VII-14),

$$E\{\log\Delta\theta_k/H_0\} = \log\frac{\sigma_0}{\sigma_1} + \frac{1}{2}\left\{1 - \left(\frac{\sigma_0}{\sigma_1}\right)^2\right\} \tag{VII-15}$$

$$E\{\log\Delta\theta_k/H_1\} = \log\frac{\sigma_0}{\sigma_1} + \frac{1}{2}\left\{\left(\frac{\sigma_1}{\sigma_0}\right)^2 - 1\right\} \tag{VII-16}$$

are obtained. Each equation implies that $E\{\log\Delta\theta_k/H_i\}$ is the average value of one sample effective to discrimination for the hypothesis H_i. Since the value for termination is either logA or logB, the average number of samples to termination is easily calculated as follows.

$$E\{n/H_0\} = \log\left(\frac{\epsilon_1}{1-\epsilon_0}\right)/\left[\log\frac{\sigma_0}{\sigma_1} + \frac{1}{2}\left\{1-\left(\frac{\sigma_0}{\sigma_1}\right)^2\right\}\right] \quad \text{(VII-17)}$$

$$E\{n/H_1\} = \log\left(\frac{1-\epsilon_1}{\epsilon_0}\right)/\left[\log\frac{\sigma_0}{\sigma_1} + \frac{1}{2}\left\{\left(\frac{\sigma_1}{\sigma_0}\right)^2-1\right\}\right] \quad \text{(VII-18)}$$

7.4.2 Determination of Optimal Sampling Rate

The sampling rates for digital relaying have been discussed in terms of the specific algorithm for distance protection, or the communication capacity for the carrier protection. The concept of the average number of samples can be used to determine the sampling rates. Table VII-4 shows the simple calculations of $E\{n/H_0\}$ for γ = 2.0, 5.0, 10.0 and ϵ = 0.1, 0.01, 0.001, 0.0001. Here γ is the ratio of σ_1 to σ_0 and $\epsilon = \epsilon_0 = \epsilon_1$. Table VII-5 gives the result of the same calculation of $E\{n/H_1\}$. Let $\hat{n}$ be the average number of samples. When the relay must discriminate the fault no later than the half cycle (180°) with ϵ = 0.001 and γ = 10.0, $\hat{n}$ for unfault is 4 (>3.8) and $\hat{n}$ for fault is 1 (>0.14). Since 180°/4 = 45°, the sampling rate of every 45° is at least necessary to detect either unfault or fault. This is the determination process of the sampling rates for digital relay through the probabilistic approach.

ϵ \ γ	2.0	5.0	10.0
0.1	6.9	1.9	1.2
0.01	14.4	4.1	2.5
0.001	21.7	6.1	3.8
0.0001	28.9	8.2	5.1

Table VII-4 Average number of samples to reach "unfault" region

ϵ \ γ	2.0	5.0	10.0
0.1	2.7	0.2	0.04
0.01	5.7	0.4	0.09
0.001	8.6	0.7	0.14
0.0001	11.4	0.9	0.19

Table VII-5 Average number of samples to reach "fault" region

It is straightforward to notice that for fixed ϵ the larger γ, the smaller $\hat{n}$ is, and that for fixed γ the smaller ϵ, the larger $\hat{n}$ is. The large γ implies the well-separation of the two p.d.f.'s. On the other hand, the small ϵ implies the conservativeness in discriminating process. It is an interesting result that $\hat{n}$ for unfault is always larger than that for fault. This fact means the longer time for the relay to take to identify an unfaulted condition than a faulted one. It coincides well with the common knowledge of the engineers that the unfault condition is hard to be identified.

7.5 CONCLUSION

This chapter has analyzed the digital relaying process, separating into sensing, evaluating, and discriminating ones. The evaluating process is understood as the algorithm how to calculate the criterion value, which is used to discriminate a fault at the last process. With the probabilistic natures of the fault condition in mind, it is shown that the discriminating process can be formulated with the statistical decision theory. The statistical approach has been so far very rare in the relay engineering, but it can give a mathematical background for the final decision process, which has been treated as a heuristic problem. This formulation is also shown to be very effective in determination of sampling rates for the digital relay.

The digital relay has drastically changed the operating principle from the torque so far to the information. One of the purposes of this chapter has been to stress an important strength of the digital systems over analog ones, which is the strong ability of making decisions. Very few have been concerned with it until now, therefore more attentions should be paid to this ability.

CHAPTER VIII DESIGN OF A PROTOTYPE COMPUTER RELAY AND EXPERIMENTAL STUDIES AT ARTIFICIAL TRANSMISSION LINE

8.1 INTRODUCTION

A minicomputer based prototype relay was designed and connected to an artificial transmission line to test the actual performance of the high speed protection algorithms that have been dealt in this thesis. From viewpoint of the cost-effectiveness, microprocessors are best as a commercial computer relay. It was felt, however, that a minicomputer relay might be better than the microprocessor for the research purpose. The prototype relay had to simulate a wide spectrum of protection algorithm that extends from travelling wave differential protection to fault location. A computer system was needed to analyze the signal processing made at the prototype relay. Accordingly, it was decided that the prototype relay be based on a minicomputer.

Three algorithms were tested: travelling wave differential protection, directional protection, and Fourier transform based fault location. Although the Laplace transform based fault location was dealt in CHAPTER V, it was felt that the Fourier method would be more promising to an immediate application, and therefore it was tested in the prototype relay.

8.2 OUTLINE OF EXPERIMENTAL FACILITIES

Experiments were performed in a mini-scale power system to test the practical ability of the proposed schemes for high voltage transmission line protection. Fig. VIII-1 shows the facilities for experiments. A three-phase single circuit line is connected at each end to a 10 kVA power transformer, whose rated voltage is 220/220 V. One transformer is connected to a micromachine rated 4 kVA, and the other one is connected to a 220 V bus line. The transmission line consists of four serially connected line units. The whole system simulates 10 GW power transmission over 100 km length by a 500 kV line.

At each end of the artificial transmission line, phase-to-ground voltages are measured by potential transformers, whose secondary windings are connected to the input circuits of analog to digital converters (= ADC). Line currents are picked up through coaxial resistances which are serially disposed in the transmission line, and whose voltages are brought into DC isolation amplifiers. The outputs of DC amplifiers are then connected to the input circuits of the ADC. The signals are filtered and sampled at the input circuits every thirty degree of electrical angle. Data sampling at each end of the line is made at the same time, while sampling at one end can be synchronized to the other end or delayed by a short time period that is pre-settable. The delayed sampling is vital to simulate the travelling wave differential protection. Eleven bits plus one sign bit of data are transferred from the ADC to the minicomputer MELCOM 70/25. The CPU has 500 nsec cycle time and 32 kilowords of IC memory, and 10 M bytes of magnetic disk memory to save the pre- and post-fault waveforms.

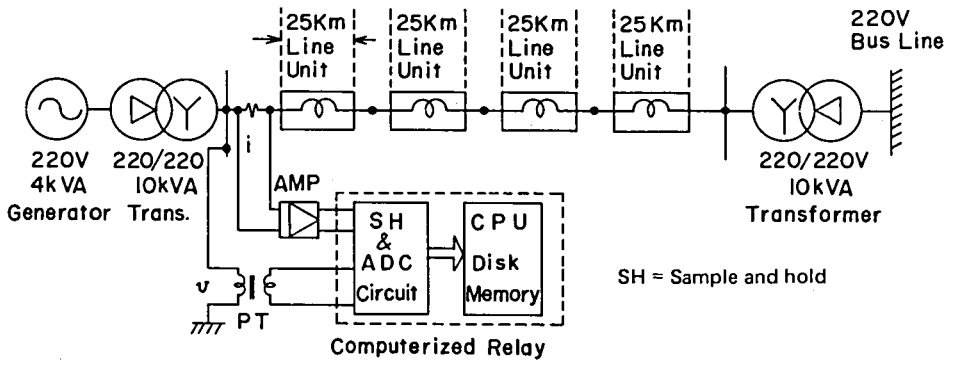

Fig. VIII-1 Experimental facilities for a prototype computer relay

8.3 EXPERIMENTAL STUDY OF TRAVELLING WAVE DIFFERENTIAL PROTECTION

The following are line constants of one unit transmission line:

$\ell^{(0)}$ = 0.756 mH/km
$\ell^{(1)}$ = 0.300 mH/km
$c^{(0)}$ = 0.012 μF/km
$c^{(1)}$ = 0.02328 μF/km
d = 25.0 km (line length)

The setting values of the d'Alembert relay are computed as

$$\tau = \sqrt{\ell^{(1)} \cdot c^{(1)}} \cdot d$$
$$= 264 \ \mu\text{sec} \qquad \text{(VIII-1)}$$

$$z = \sqrt{\ell^{(1)} / c^{(1)}}$$
$$= 114 \ \text{ohm} \qquad \text{(VIII-2)}$$

The threshold value δ was set at 1,024 which corresponds to 1.2 A at the artificial transmission line. As the per unit bases for voltage and capacity were 220 V and 4,000 VA respectively, the threshold means 0.11 p.u. current. This value implies 1,270 A at real power system, because 1.0 p.u. current amounts to 11,547 A.

Fig. VIII-2 shows a curve of the fault criterion $\xi(t)$ at the faulted phase. The fault was detected within one quarter cycle at the nominal frequency, although the communication time was not taken int account. The total computation time requires 0.6 msec, which amounts to 40% of the sampling interval. The oscillogram measured at this experiment is shown in Fig. VIII-3.

8.4 EXPERIMENTAL STUDY OF DIRECTIONAL PROTECTION

Voltage and current at one end of the line were used to study the performance of directional protection. Fig. VIII-4 shows a result of the directional detection at a faulted phase for a double-phase short circuit fault, and the fault transients are recorded in Fig. VIII-5. The MacLaurin's method of the first order is applied to the solution of the eqn.

(IV-17). The fault criterion function $\eta(t)$ increases monotonously, and it will soon reach the threshold level at which a fault is identified in the forward direction. Because of the existence of a loss in the laboratory system, the weighting function looks like an impulse response of $1/(R+sL)$, $R \ll L$. This effect makes the increasing rate of $\eta(t)$ slow down as the time passes, but will not affect the high speed relay operation.

8.5 EXPERIMENTAL STUDY OF FOURIER TRANSFORM BASED FAULT LOCATION

Two computer programs are stored in the CPU. One is to detect a faulted condition in the transmission line, and the d'Alembert relay is applied to this end. The other is to analyze the pre- and post-fault waveforms and to solve the basic equation (VI-16) or (VI-17). The first program initiates the second one, after detecting a fault and recording a data in a disk file for later processing.

The related parameters are set to the following values, and the experiments are performed.

$$\lambda^{(0)} = \omega_0 \sqrt{\ell^{(0)} \cdot c^{(0)}}$$
$$= 1.135 \times 10^{-3} \text{ rad/km} \qquad \text{(VIII-3)}$$

$$\lambda^{(1)} = \omega_0 \sqrt{\ell^{(1)} \cdot c^{(1)}}$$
$$= 0.996 \times 10^{-3} \text{ rad/km} \qquad \text{(VIII-4)}$$

$$z^{(0)} = \sqrt{\ell^{(0)}/c^{(0)}}$$
$$= 251 \text{ ohm} \qquad \text{(VIII-5)}$$

$$z^{(1)} = \sqrt{\ell^{(1)}/c^{(1)}}$$
$$= 114 \text{ ohm} \qquad \text{(VIII-6)}$$

Fig. VIII-6 shows a location process, where a fault is initiated at t = 0.0 sec. The located distance settled at 48.7 km, while a fault was actually 50.0 km away from the relaying point. The oscillogram recorded in this case is shown in Fig. VIII-7. Other faults were located within the same degree of accuracy as the case presented here.

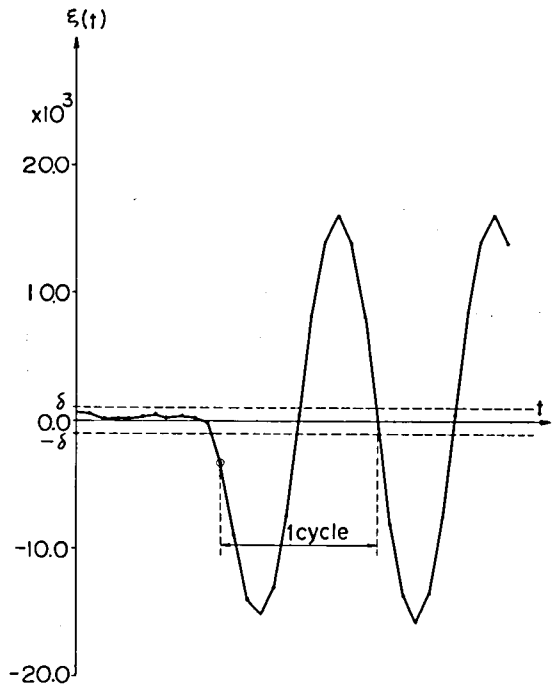

Fig. VIII-2 A curve of fault criterion $\xi(t)$ at a faulted phase

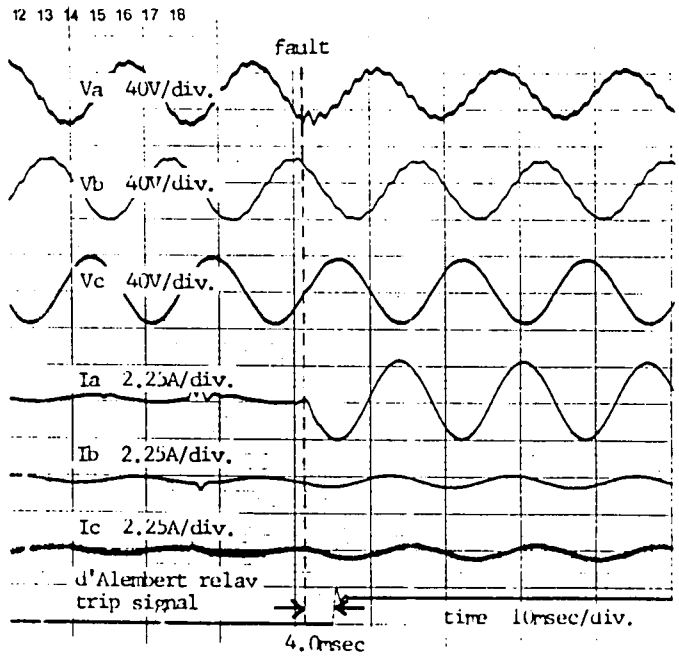

Fig. VIII-3 Oscillogram recorded at an experiment for d'Alembert relay

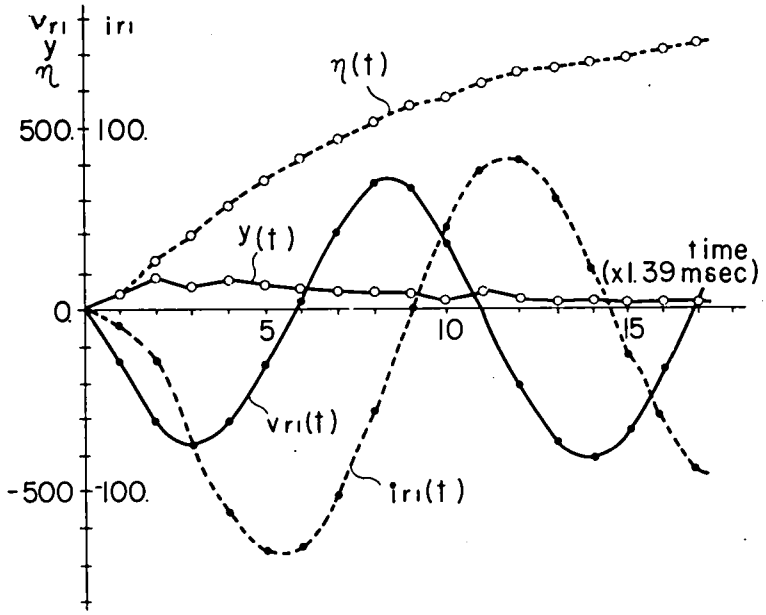

Fig. VIII-4 Result of y(t) and η(t) based on experimental data

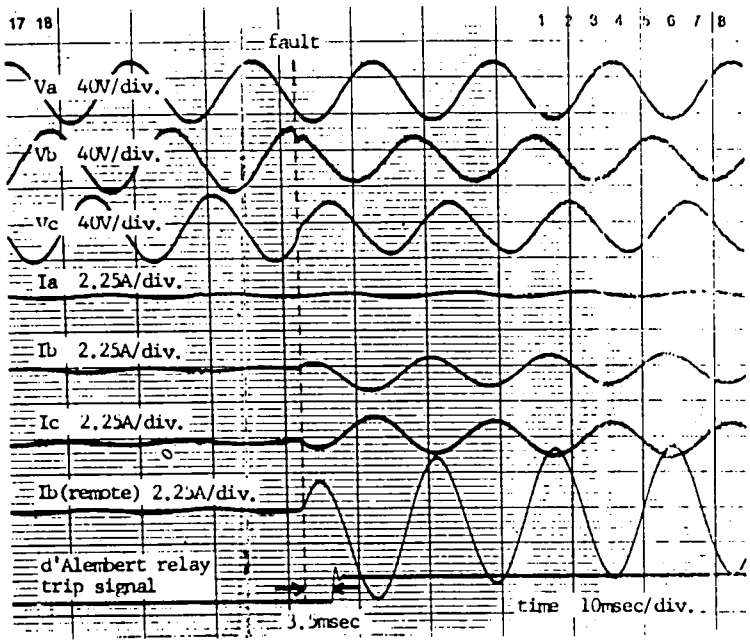

Fig. VIII-5 Oscillogram recorded at an experiment for directional relay

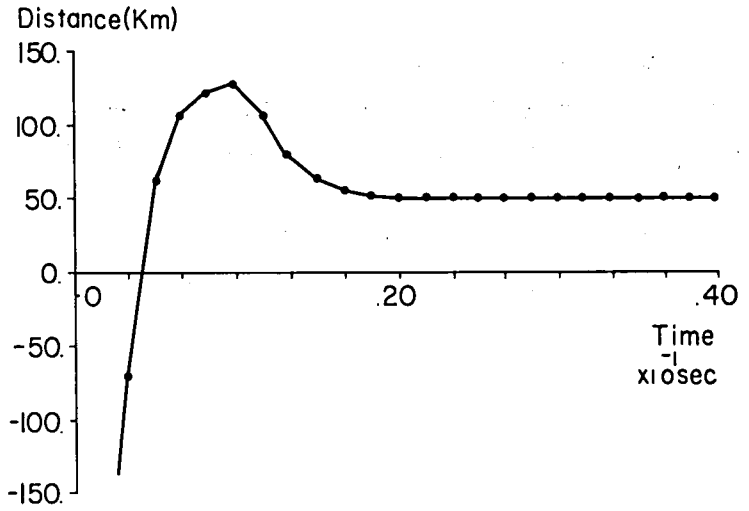

Fig. VIII-6 Estimated distance by a prototype computerized locator

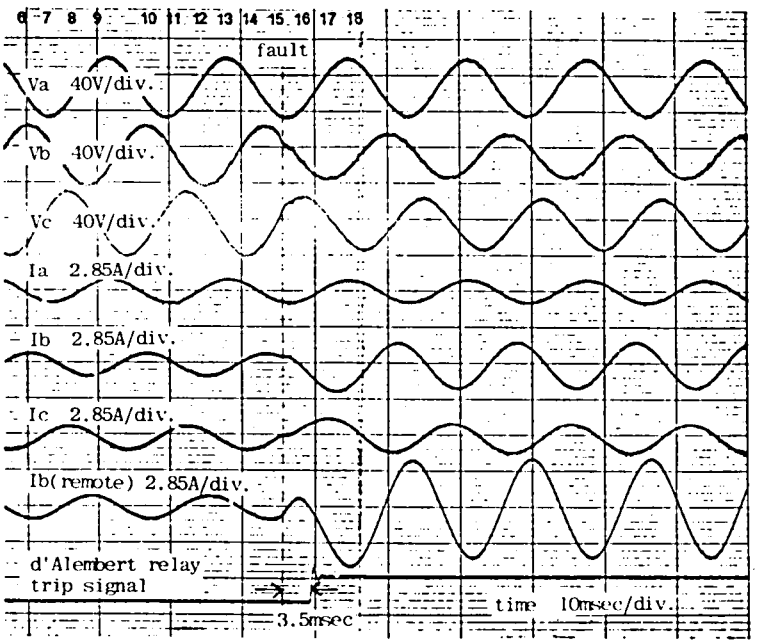

Fig. VIII-7 Oscillogram recorded at an experiment for fault location

8.6 CONCLUSION

Although the primary objective of this thesis is to design the high speed digital protection algorithm, a need for experimental studies is felt to evaluate the performance at a small scale power system. A minicomputer based prototype relay was designed and connected to the artificial transmission line. Three algorithms have been tested: travelling wave differential protection, directional protection, and Fourier transform based fault location. The ability to detect a fault within one quarter cycle at the nominal frequency has been verified in the first two algorithms, while the ability to locate a fault with measuring error of less than three percent has been confirmed in the last algorithm.

CHAPTER IX CONCLUSIONS AND AREAS OF A FUTURE RESEARCH

9.1 CONCLUSIONS

Impacts of system characteristics of recent UHV/EHV transmission networks are first analyzed to identify the requirements of protection system. They crystalize as the need of high speed operating time under severe fault transients, which implies the increasing potential of systems analysis in the power system protection. On the other hand, the new electronic technologies could have a strong impact on the power system protection as a technological basis. With these impacts in the background, the thesis presents a systems approach to the high speed digital protection for transmission lines.

In CHAPTER I, the problem solving methodology undertaken in this thesis is described. The systems methodology is applied to define, verify and optimize a digital protection alogirthm. Also described is a brief overview of computer relaying to make clear the status of this thesis in the state of art of the new relaying practice.

In CHAPTER II, the protection algorithm based on the concept of travelling wave is defined regard to the carrier protection for the first time. Efforts are made mainly to establish a theoretical basis for fault detection, fault selection, and fault location. The main contribution here is that the travelling wave differential protection meets the fundamental requirement calling for high speed operating time under severe fault transients. The new scheme is shown to be a generalized concept of differential current in a transmission line.

Following the theoretical development, CHAPTER III has made assessment studies of the new scheme. A need of simplifying the original scheme was felt in its practical application because of the computational complexity, and single phase algorithm was decided to be used as a reasonable compromise between speed and accuracy. Sensitivity study in regard to system characteristics has shown that the new scheme shows high sensitivity to the surge propagation time τ while its sensitivity to the surge impedance z and the line loss R is very low. It has been also shown that the frequency dependent nature of line constants turns out to be preferable to the working principle.

CHAPTER IV describes a high speed directional protection algorithm whose working principle depends upon the network transient response. There has been a new trend in transmission line protection that measures a fault criterion using the transient components in voltage and current. This thesis has made clear the ability of the fault criterion to identify the fault direction through a rigid mathematical analysis. As somewhat artistic taste was felt in other literatures, this chapter has contributed to establish a scientific basis of the new fault criterion. It has been also shown that the scheme would be fittingly implemented as a computer relay.

The following two chapters are devoted to the development of an accurate fault location algorithm that can estimate the distance with locally measured data. CHAPTER V presents a Laplace transform based scheme. As the working principle depends upon the transient state analysis of a faulted network, the scheme is inherently able to estimate the distance under fault transients. The accurate location has been verified in digital simulation studies, and the optimal computation has been made clear in regard to the numerical Laplace transform. In CHAPTER VI, an effort has been made to ease the burden of the Laplace scheme at measurement and computation. A Fourier transform based scheme is shown to be more promising to the immediate application. The present technologies have advanced so much as to embody the Fourier scheme. In both approaches, a fault current distribution factor plays an essential role in developing the algorithms. The contribution of this thesis here is an addition of the new concept to fault location practices.

CHAPTER VII has identified a new computation in computer relaying. It was well known that a signal conditioning and fault measuring are fundamental computations for computer relaying. Most efforts were made to develop algorithms for these computations. This thesis has pointed out a decision making as the third, but as important as the first two computations. This chapter has emphasized an uncertainty in decision making, and presented a probabilistic method as a reasonable approach. It has been also shown that the computer relay has a potential to control a decision making. As a result of the control, a requirement of the sampling rate has been determined.

In CHAPTER VIII, a need of experimental study is identified. The design of a prototype computer relay is described with the relaying performance at a mini-scale power system. Experimental studies have confirmed those conclusions derived by the digital simulation technique.

9.2 AREAS OF A FUTURE RESEARCH

Two areas of a future research are felt at this time (1981):

(1) Extension to total system protection

(2) Integration of protection and control system

The first area arises from a system need. Power system protection so far has been developed as a local and direct control equipment. The principal mission of protection is to remove a faulted element as fast as possible. There seems to be an assumption that the power system would go into another stable equilibrium after removing the fault. However, there is a growing possibility in a recent transmission network that the assumption is not true because the system can not localize the fault disturbance. Here is an opportunity of a research on total system protection. The second area arises from a technological need. As is discussed in INTRODUCTION, one reason for the slow penetration of computer systems lies in a disadvantage of their cost-effectiveness over existing systems. One way of improving cost-effectiveness is to integrate protection and control system. There is a growing trend of an integrated system design in substation digital control. As the system design is critical to maximize the cost-effectiveness of computer systems, there is a great need of research in the integration methodology.

132項欠

REFERENCES TO INTRODUCTION

1. "UHV: Onward and Upward", IEEE Spectrum, pp. 57-65, February, 1977.

2. Y. Sekine and M. Yasui, "UHV AC/DC Project in Japan", CIGRE REPORT, SC14/31, October, Johannesburg, 1975.

3. E. Rumpf, "The Operational Performance of HVDC Systems throughout the World during 1975 – 1978", A Symposium on Incorporating HVDC Power Transmission into System Planning, pp. 1-23, March, 1980.

4. "The Effects of EHV Relaying of Fault and Switching Generated Transients", Working Group 04 of Study Committee No. 34 Report, Paper No. CIGRE 34-10, 1978.

5. "Computers in Transmission/Distribution", Electrical World, pp. 67-80, April 15, 1980.

6. "Digital Technique for Control and Protection of Transmission Class Substation", Paper presented at the EPRI Workshop of the Control and Protection of Transmission Class Substations, No. WS79-184, November, 1979.

7. J.S. Deliyannides, M. Kezunovic and T.H. Schwalenstocker, "An Integrated Microprocessor Based Substation Protection and Control System", IEE Conference on Power System Monitoring and Control, June, 1980.

8. K. Tanaka, K. Kanou, Y. Harumoto, T. Mori, K. Suzuki and T. Gouda, "Application of Microprocessors to the Control and Protection System at Substation", IEEE PES Summer Meeting, Paper No. F79 629-7, July, 1979.

9. "Computer Relaying", IEEE Tutorial Course Text, 79 EH0148-7-PWR, 1979.

10. D.I. Rummer and M. Kezunovic, "A Survey and Classification of the Digital Computer Relaying Literature", IEEE PES Summer Meeting, Paper No. A79 417-7, July, 1979.

REFERENCES TO CHAPTER I

1. T. Sakaguchi, "A Statistical Decision Theoretic Approach to Digital Relaying", IEEE PES Winter Meeting, Paper No. F80 196-6, February, 1980.

2. "Computer Relaying", IEEE Tutorial Course Text, 79 EH0148-7-PWR, 1979.

3. G.S. Hope and O.P. Malik, "Sampling Rates for Computer Transmission Line Protection", IEEE PES Summer Meeting, Paper No. A75 544-7, July, 1975.

4. L.R. Rabiner and B. Gold, "Theory and Application of Digital Signal Processing", Prentice-Hall Inc., Englewood Cliffs, New Jersey, 1975.

5. B.J. Mann and I.F. Morrison, "Digital Calculation of Impedance for Transmission Line Protection", IEEE Trans. PA & S, Vol. 90, No. 1, pp. 270-279, January/February, 1971.

6. M. Ramamoorty, "Application of Digital Computers to Power System Protection", Journal of Inst. Eng. (India), Vol. 52, No. 10, pp. 235-238, June, 1972.

7. A.G. Phadke, T. Hlibka and M. Ibrahim, "A Digital Computer System for EHV Substations: Analysis and Field Tests", IEEE Trans. on PA & S, Vol. PAS-95, No. 1, pp. 291-301, January/February, 1976.

8. A.T. John and M.A. Martin, "Fundamental Digital Approach to the Distance Protection of E.H.V. Transmission Lines", Proc. of the IEE, Vol. 125, No. 5, pp. 377-384, May, 1978.

9. A.D. McInnes and I.F. Morrison, "Real Time Calculation of Resistance and Reactance for Transmission Line Protection by Digital Computers", EE Trans., Inst. of Engineers, Australia, Vol. EE7, No. 1, pp. 16-23, No. 1, 1970.

10. A.M. Ranjbar and B.J. Cory, "An Improved Method for the Digital Protection of High Voltage Transmission Lines", IEEE Trans. on PA & S, Vol. PAS-95, No. 2, pp. 544-550, March/April, 1975.

11. J. Kohlas, "Estimation of Fault Locations on Power Lines", Proc. of the 3rd IFAC Symposium, the Hague/Delft, the Netherland, pp. 393-402, June, 1973.

12. M.T. Yee and J. Esztergalyos, "Ultra High Speed Relay for EHV/UHV Transmission Lines – Installation, Staged Fault Tests and Operational Experience", IEEE Trans. on PA & S, Vol. PAS 97, No. 5, pp. 1814-1825, September/October, 1978.

13. M. Chamia and S. Liberman, "Ultra High Speed Relay for EHV/UHV Transmission Lines – Development, Design and Application", IEEE Trans. on PA & S, Vol. PAS-97, No. 6, pp. 2104-2116, November/December, 1978.

14. H.W. Dommel and J.M. Michels, "High Speed Relaying Using Traveling Wave Transient Analysis", IEEE PES Winter Meeting, Paper No. A78 214-9, January, 1978.

15. M. Vitins, "A correlation Method for Transmission Line Protections", IEEE PES Summer Meeting, Paper No. F77 733-9, July, 1977.

16. M. Vitins, "A fundamental Concept for High Speed Relaying", IEEE PES Winter Meeting, Paper No. F80 232-9, February, 1980.

17. G.D. Rockefeller, "Fault Protection with a Digital Computer", IEEE Trans. on PA & S, Vol. PAS-88, No. 4, pp. 438-464, April, 1969.

18. K. Suzuki, K. Maeda, H. Yamaguchi and A. Nakano, "Result of Field Experiments of Digital Relays Utilizing Mini-Computer and Micro-Processor", IFAC Symposium, pp. 312-316, February, 1977.

19. G.B. Gilchrist, G.D. Rockefeller and E.A. Udren, "High-Speed Distance Relaying Using a Digital Computer, Part I – System Description", IEEE Trans. on PA & S, Vol. PAS-91, No. 3, pp. 1235-1243, May/June, 1972.

20. G.D. Rockefeller and E.A. Udren, "High-Speed Distance Relaying Using a Digital Computer, Part II", IEEE Trans. on PA & S, Vol. PAS-91, No. 3, pp. 1244-1258, May/ June, 1972.

21. W.D. Breingan, M.M. Chen and T.F. Gallan, "Laboratory Investigation of a Digital System for the Protection of Transmission Lines", IEEE PES Winter Meeting, Paper No. F77 052-4, January, 1977.

22. T.F. Gallan, M.M. Chen and W.D. Breingan, "A Digital System for Directional-Comparison Relaying", IEEE PES Summer Meeting, Paper No. F78 699-4, July, 1978.

23. M.M. Chen and W.D. Breingan, "Field Experience with a Digital System with Transmission Line Protection", IEEE PES Winter Meeting, Paper No. F79 252-8, February, 1979.

24. K. Tanaka, K. Kanou, Y. Harumoto, T. Mori, K. Suzuki and T. Gouda, "Application of Microprocessors to the Control and Protection System at Substation", IEEE PES Summer Meeting, Paper No. F79 629-7, July, 1979.

25. T. Takagi, Y. Yamakoshi, M. Yamaura, R. Kondow, T. Matsushima and M. Masui, "Digital Differential Relaying System for Transmission Line Primary Protection Using Travelling Wave Theory – Its Theory and Field Experience", IEEE PES Winter Meeting, Paper No. A79 096-9, February, 1979.

26. Y. Miki, Y. Sano and J. Makino, "Study of High-Speed Distance Relay Using Microcomputer", IEEE Trans. on PA & S, Vol. PAS-96, No. 2, pp. 602-613, March/ April, 1977.

27. J.S. Deliyannides, M. Kezunovic and T.H. Schwalenstocker, "An Integrated Microprocessor Based Substation Protection and Control System", IEE Conference on Power System Monitoring and Control, June, 1980.

28. H.M. Dommel and W.S. Meyer, "Computation of Electromagnetic Transients", Proc. of the IEEE, Vol. 62, No. 7, pp. 983-993, July, 1974.

29. J.P. Bickford, N. Mullineux and J.R. Reed, "Computation of Power System Transients", IEE Monograph Series 18, Peter Peregrinus Ltd., 1976.

30. L.M. Wedepohl, "Application of Matrix Methods to the Solution of Travelling-Wave Phenomena in Polyphase Systems", Proc. of the IEE, Vol. 110, No. 12, pp. 2200-2212, December, 1963.

31. S.J. Day, N. Mullineux and J.R. Reed, "Developments in Obtaining Transient Response Using Fourier Transforms – Part I: Gibbs Phenomena and Fourier Integrals", Int. Journal of Electrical Engineering Education, Vol. 3, pp. 501-506, 1965.

32. S.J. Day, N. Mullineux and J.R. Reed, "Developments in Obtaining Transient Response Using Fourier Transforms – Part II: Use of the Modified Fourier Transform", Int. Journal of Electrical Engineering Education, Vol. 4, pp. 31-40, 1966.

33. W. Frey and P. Althammer, "The Calculation of Electromagnetic Transients on Lines by Means of a Digital Computer", The Brown Boveri Review, Vol. 48, No. 5/6, pp. 344-355, May/June, 1961.

34. L.M. Wedepohl and S.E.T. Mohamed, "Multiconductor Transmission Lines: Theory of Natural Modes and Fourier Integral Applied to Transient Analysis", Proc. IEE, Vol. 116, No. 9, pp. 1553-1563, September, 1969.

35. A. Semlyen and A. Roth, "Calculation of Exponential Propagation Step Responses – Accurately for Three Base Frequencies", IEEE Trans. on PA & S, Vol. PAS-96, No. 2, pp. 667-672, March/April, 1977.

36. A. Ametani, "A Highly Efficient Method for Calculating Transmission Line Transients", IEEE PES Winter Meeting, Paper No. F76 159-4, February, 1976.

37. A. Ametani, "The Application of the Fast Fourier Transform to Electrical Transient Phenomena", Int. J. Electrical Engineering Education, Vol. 10, No. 4, pp. 277-287, 1972.

38. H.W. Dommel, "Digital Computer Solution of Electromagnetic Transients in Single- and Multiphase Networks", IEEE Trans. on PA & S, Vol. PAS-88, No. 4, pp. 388-396, April, 1969.

39. J.K. Snelson, "Propagation of Travelling Waves on Transmission Lines – Frequency Dependent Parameters", IEEE Trans. on PA & S, Vol. PAS-91, No. 1, pp. 85-91, January/February, 1972.

40. W.S. Meyer and H.W. Dommel, "Numerical Modelling of Frequency-Dependent Transmission-Line Parameters in an Electromagnetic Transients Program", IEEE Trans. on PA & S, Vol. PAS-92, No. 5, pp. 1401-1409, September/October, 1974.

41. EMTP User's Manual, Bonneville Power Administration, Branch of System Engineering, Portland, Oregon, November, 1977.

REFERENCES TO CHAPTER II

1. K. Suzuki, M. Hatada and T. Yoshida, "The Study of Fault Transients and the Development of the Wave Distortion – Proof Distance Relay", IEEE PES Winter Meeting, Paper No. A79 097-7, February, 1979.

2. C. Concordia and P.G. Brown, "Effects of Trends in Large Steam Turbine Driven Generator Parameters on Power System Stability", IEEE PES Winter Meeting, Paper No. 71 TP 74-PWR, February, 1971.

3. G.D. Rockefeller, "Fault Protection with a Digital Computer", IEEE Trans. on PA & S, Vol. PAS-88, No. 4, pp. 438-464, April, 1969.

4. B.J. Mann and I.F. Morrison, "Digital Calculation of Impedance for Transmission Line Protection", IEEE Trans. on PA & S, Vol. PAS-90, No. 1, pp. 270-279, January/February, 1971.

5. B.J. Mann and I.F. Morrison, "Relaying a Three Phase Transmission Line with a Digital Computer", IEEE Trans. on PA & S, Vol. PAS-90, No. 2, pp. 742-750, March/April, 1971.

6. R. Poncelet, "The Use of Digital Computers for Network Protection", CIGRE International Conference, Paper No. 32-08, August, 1972.

7. A.M. Ranjbar and B.J. Cory, "An Improved Method for the Digital Protection of High Voltage Transmission Line", IEEE PES Summer Meeting, Paper No. T74 380-2, July, 1974.

8. W. Frey and P. Althammer, "The Calculation of Electromagnetic Transients on Lines by Means of a Digital Computer", The Brown Boveri Review, Vol. 48, No. 5/6, pp. 344-355, May/June, 1961.

9. L.M. Wedepohl, "Application of Matrix Methods to the Solution of Travelling-Wave Phenomena in Polyphase Systems", Proc. of the IEE, Vol. 110, No. 12, pp. 2200-2212, December, 1963.

10. H.W. Dommel, "Digital Computer Solution of Electromagnetic Transients in Single- and Multiphase Networks", IEEE Trans. on PA & S , Vol. PAS-88, No. 4, pp. 388-396, April, 1969.

11. H.W. Dommel and W.S. Meyer, "Computation of Electromagnetic Transients", Proc. of the IEEE, Vol. 62, pp. 983-993, July, 1974.

12. J. Kohlas, "Estimation of Fault Locations on Power Lines", Proc. of 3rd IFAC Symposium, the Hague/Delft, the Netherland, pp. 393-402, June, 1973.

13. T. Takagi, J. Baba, K. Uemura and T. Sakaguchi, "Fault Protection Based on Travelling Wave Theory: Part I Theory", IEEE PES Summer Meeting, Paper No. A77 750-3, July, 1977.

14. Y. Akimoto, T. Yamamoto, H. Hosokawa, T. Sakaguchi, T. Yoshida and S. Nishida, "Wave Propagation Theory Applied to Transmission Line Protection: Part I", Trans. of IEE of Japan, Vol. 98-B, No. 1, January, pp. 79-86, 1978. (in Japanese)

REFERENCES TO CHAPTER III

1. T. Takagi, K. Uemura and T. Sakaguchi, "Protective Relaying System", U.S. Patent, No. 4183072, January 8, 1980.

2. T. Takagi, J. Baba, K. Uemura and T. Sakaguchi, "Fault Protection Based on Travelling Wave Theory: Part I Theory", IEEE PES Summer Meeting, Paper No. A77 750-3, July, 1977.

3. "Electrical Transmission and Distribution Reference Book", Westinghouse Electric Corp., 1950.

4. H.W. Dommel and W.S. Meyer, "Computation of Electromagnetic Transients", Proc. of the IEEE, Vol. 62, No. 7, pp. 983-993, July, 1974.

5. H.W. Dommel, "Digital Computer Solution of Electromagnetic Transients in Single- and Multiphase Networks", IEEE Trans. on PA & S, Vol. PAS-88, No. 4, pp. 388-396, April, 1969.

6. J.K. Snelson, "Propagation of Travelling Waves on Transmission Lines – Frequency Dependent Parameters", IEEE Trans. on PA & S, Vol. PAS-91, No. 1, pp. 85-91, January/ February, 1972.

7. W.S. Meyer and H.W. Dommel, "Numerical Modelling of Frequency-Dependent Transmission-Line Parameters in an Electromagnetic Transients Program", IEEE Trans. on PA & S, Vol. PAS-92, No. 5, pp. 1401-1409, September/October, 1974.

8. A. Budner, "Introduction of Frequency-Dependent Line Parameters into an Electromagnetic Transient Program", IEEE Trans. on PA & S, Vol. PAS-89, No. 1, pp. 88-97, January, 1970.

9. EMTP User's Manual, Bonneville Power Administration, Branch of System Engineering, Portland, Oregon, November, 1977.

10. T. Takagi, J. Baba, K. Uemura and T. Sakaguchi, "Fault Protection Based on Travelling Wave Theory: Part II Sensitivity Analysis and Laboratory Test", IEEE PES Winter Meeting, Paper No. A78 220-6, February, 1978.

11. Y. Akimoto, T. Yamamoto, H. Hosokawa, T. Sagaguchi, T. Yoshida and S. Nishida, "Wave Propagation Theory Applied to Transmission Line Protection: Part II", Trans. of IEE of Japan, Vol. 98-B, No. 8, August, pp. 711-718. 1978. (in Japanese)

REFERENCES TO CHAPTER IV

1. T. Sakaguchi, "A Statistical Decision Theoretic Approach to Digital Relaying", IEEE PES Winter Meeding, Paper No. F80 196-6, February 1980.

2. A.G. Phadke, T. Hlibka, and U. Ibrahim, "A Digital Computer System for EHV Substations: Analysis and Field Tests", IEEE Trans. on PA & S, Vol. PAS-95, No. 1, January/February 1976, pp. 291-301.

3. A.M. Ranjbar, and B.J. Cory, "An Improved Method for the Digital Protection of High Voltage Transmission Lines", IEEE Trans. on PA & S, Vol. PAS-95, No. 2, March/April 1975, pp. 544-550.

4. K. Uemura, and T. Sakaguchi, "A New Directional Protection Based on Laplace Transformation with Special Reference to Computer Relaying", Second International Conference on "Developments in Power-System Protection", June 1980.

5. M. Chamia, and S. Liberman, "Ultra High Speed Relay for EHV/UHV Transmission Lines – Development, Design and Application", IEEE Trans. on PA & S, Vol. PAS-97, No. 6, November/December 1978, pp. 2104-2116.

6. A.T. Johns, and M.A. Martin, "Fundamental Digital Approach to the Distance Protection of E.H.V. Transmission Lines", Proc. of the IEE, Vol. 125, No. 5, May 1978, pp. 377-384.

7. EMTP User's Manual, Bonneville Power Administration, Branch of System Engineering, Portland, Oregon, November 1977.

8. K. Hidaka, "Applied Integral Equation", Kawade Shobo, 1943. (in Japanese).

9. Y. Yamakoshi, K. Uemura and T. Sakaguchi, "A New Directional Protection for Digital Processor Use", IFAC Symposium on Automatic Control in Power Generation, Distribution and Protection, September 15-19, Pretoria, Republic of South Africa, 1980.

REFERENCES TO CHAPTER V

1. A.D. McInnes and I.F. Morrison, "Real-Time Calculation of Resistance and Reactance for Transmission Line Protection by Digital Computer", EE Trans., Inst. of Engineers, Australia, EE-7, No. 1, pp. 1623, 1971.

2. A.M. Ranjbar and B.J. Cory, "An Improved Method for the Digital Protection of High Voltage Transmission Line", IEEE Trans., PAS-94, No. 2, pp. 554-560, 1975.

3. G. Ziegler, "Fault Location in H.V. Power Systems", IFAC Symposium on Automatic Control in Power Generation, Distribution and Protection, pp. 121-129, 15-19 September, 1980.

4. S.E. Westlin and J.A. Bubenko, "Newton-Raphson Technique Applied to the Fault Location Problem", IEEE PES Summer Meeting, Paper No. A76 334-3, 1976.

5. EMTP User's Manual, Bonneville Power Administration, Branch of System Engineering, Portland, Oregon, November, 1977.

6. T. Takagi, Y. Yamakoshi, J. Baba, K. Uemura and T. Sakaguchi, "A New Algorithm of an Accurate Fault Location for EHV/UHV Transmission Lines: Part II-Laplace Transform Method", IEEE PES Summer Meeting, Paper No. 81 SM 411-8, July, 1981.

REFERENCES TO CHAPTER VI

1. A.D. McInnes and I.F. Morrison, "Real-Time Calculation of Resistance and Reactance for Transmission Line Protection by Digital Computer", EE Trans., Inst. of Engineers, Australia, EE-7 No. 1, pp. 1623, 1971.

2. A.M. Ranjbar and B.J. Cory, "An Improved Method for the Digital Protection of High Voltage Transmission Line", IEEE Trans. PAS-94, No. 2, pp. 554-560, 1975.

3. S.E. Westlin and J.A. Bubenko, "Newton-Raphson Technique Applied to the Fault Location Problem", IEEE PES Summer Meeting, A76 334-3, 1976.

4. EMTP User's Manual, Bonneville Power Administration, Branch of System Engineering, Portland, Oregon, November, 1977.

5. A.T. John and M.A. Martin, "Fundamental Digital Approach to the Distance Protection of EHV Transmission Lines", Proc. IEE Vol. 125, No. 5, pp. 377-384, 1978.

6. J.W. Horton, "The Use of Walsh Functions for High-Speed Relaying", IEEE PES Summer Meeting, A75 582-7, 1975.

7. T. Takagi, J. Baba, K. Uemura and T. Sakaguchi, "Fault Protection Based on Travelling Wave Theory: Part I – Theory", IEEE PES Summer Meeting, A77 750-3, 1977.

8. T. Takagi, Y. Yamakoshi, J. Baba, K. Uemura and T. Sakaguchi, "A New Algorithm of an Accurate Fault Location for EHV/UHV Transmission Lines: Part I – Fourier Transformation Method", IEEE PES Summer Meeting, Paper No. 80 SM 648-6, July, 1980.

REFERENCES TO CHAPTER VII

1. J.G. Gilbert, E.A. Udren, and M. Sackin, "Evaluation of Algorithms for Computer Relaying". IEEE PES Summer Meeting, A77 520-0, July, 1977.

2. G.S. Hope, and O.P. Malik, "Sampling Rates for Computer Transmission Line Protection". IEEE PES Summer Meeting, A75 544-7, July, 1975.

3. T. Takagi, J. Baba, K. Uemura, and T. Sakaguchi, "Fault Protection Based on Travelling Wave Theory – Part I Theory". IEEE PES Summer Meeting, A77 750-3, July, 1977.

4. EMTP User's Manual, Bonneville Power Administration, Branch of System Engineering, Portland, Oregon, November, 1977.

5. A. Wald, "Sequential Analysis". Wiley, New York, 1947.

6. T. Sakaguchi, "A Statistical Decision Theoretic Approach to Digital Relaying", IEEE PES Winter Meeting, Paper No. F80 196-6, February, 1980.

148項欠

APPENDEX I BERGERON'S EQUATION

The wave equation in a single-phase line of Fig. II-1 is written as

$$-\frac{\partial v}{\partial x} = \ell \frac{\partial i}{\partial t} \tag{AI-1}$$

$$-\frac{\partial i}{\partial x} = c \frac{\partial v}{\partial t} \tag{AI-2}$$

The solution of the above equation is given by d'Alembert as

$$v(x, t) = z\{F(t-\frac{x}{v}) + f(t+\frac{x}{v})\} \tag{AI-3}$$

$$i(x, t) = F(t-\frac{x}{v}) - f(t+\frac{x}{v}) \tag{AI-4}$$

where

$$v = \frac{1}{\sqrt{\ell c}} \text{(surge travelling velocity)} \tag{AI-5}$$

$$z = \sqrt{\frac{\ell}{c}} \text{(surge impedance)} \tag{AI-6}$$

$F(\cdot)$ and $f(\cdot)$ are arbitrary functions defined by the boundary conditions. $f(\cdot)$ can be eliminated from eqn. (AI-3) and (AI-4).

$$i(x, t) + \frac{1}{z} v(x, t) = 2\ F\ (t-\frac{x}{v}) \tag{AI-7}$$

This equation is written at both terminal S and R.

$$i_S(t) + \frac{1}{z} v_S(t) = 2\ F\ (t) \tag{AI-8}$$

$$-i_R(t) + \frac{1}{z} v_R(t) = 2\ F\ (t-\frac{d}{v}) \tag{AI-9}$$

Substituting t–(d/v) in t in eqn. (AI-8) gives the Bergeron's equation,

$$i_S(t-\tau) + \frac{1}{z} v_S(t-\tau) = -i_R(t) + \frac{1}{z} v_R(t) \tag{AI-10}$$

where

$$\tau = d/v \text{ (surge travelling time)} \tag{AI-11}$$

The elimination of F(·) from eqn. (AI-3) and (AI-4) leads to another Bergeron's equation,

$$-i_S(t) + \frac{1}{z} v_S(t) = i_R(t-\tau) + \frac{1}{z} v_R(t-\tau) \tag{AI-12}$$

The wave equation in a three-phase line of Fig. II-2 is written as

$$-\frac{\partial [v]}{\partial x} = [L] \frac{\partial [i]}{\partial t} \tag{AI-13}$$

$$-\frac{\partial [i]}{\partial x} = [C] \frac{\partial [v]}{\partial t} \tag{AI-14}$$

The modal transforms defined by

$$[v] = [S]\,[v^{(mode)}] \tag{AI-15}$$

$$[i] = [Q]\,[i^{(mode)}] \tag{AI-16}$$

give the new equations

$$-\frac{\partial[v^{(mode)}]}{\partial x} = [S]^{-1}[L][Q]\frac{\partial[i^{(mode)}]}{\partial t} \tag{AI-17}$$

$$-\frac{\partial[i^{(mode)}]}{\partial x} = [Q]^{-1}[C][S]\frac{\partial[v^{(mode)}]}{\partial t} \tag{AI-18}$$

which lead to

$$\frac{\partial^2[v^{(mode)}]}{\partial x^2} = [S]^{-1}[L][C][S]\frac{\partial^2[i^{(mode)}]}{\partial t^2} \tag{AI-19}$$

$$\frac{\partial^2[i^{(mode)}]}{\partial x^2} = [Q]^{-1}[C][L][Q]\frac{\partial^2[i^{(mode)}]}{\partial t^2} \tag{AI-20}$$

The eqn. (AI-17) and (AI-18) are decoupled by solving the eigen value problem. The decoupled equations are given as

$$-\frac{\partial[v^{(mode)}]}{\partial x} = [L^{(mode)}]\frac{\partial[i^{(mode)}]}{\partial t} \tag{AI-21}$$

$$-\frac{\partial[i^{(mode)}]}{\partial x} = [C^{(mode)}]\frac{\partial[v^{(mode)}]}{\partial t} \tag{AI-22}$$

where

$$[L^{(mode)}] = \begin{bmatrix} \ell(0) & & \\ & \ddots & \\ & & \ell(n-1) \end{bmatrix}$$

$$[C^{(mode)}] = \begin{bmatrix} c^{(0)} & & \\ & \ddots & \\ & & c^{(n-1)} \end{bmatrix}$$

n = dimension of [v(t)]

The derivation procedure in a single phase line is applicable to each modal equation (AI-21) and (AI-22). Thus one obtains the Bergeron's equation in a three phase line as

$$i_S^{(k)}(t-\tau^{(k)}) + \frac{1}{z^{(k)}} v_S^{(k)}(t-\tau^{(k)}) = -i_R^{(k)}(t) + \frac{1}{z^{(k)}} v_R^{(k)}(t) \qquad \text{(AI-23)}$$

$$-i_S^{(k)}(t) + \frac{1}{z^{(k)}} v_S^{(k)}(t) = i_R^{(k)}(t-\tau^{(k)}) + \frac{1}{z^{(k)}} v_R^{(k)}(t-\tau^{(k)}) \qquad \text{(AI-24)}$$

$$k = 0, 1, \cdots, (n-1)$$

where

$$\tau^{(k)} = \sqrt{\ell^{(k)} \cdot c^{(k)}}\, d \qquad \text{(AI-25)}$$

$$z^{(k)} = \sqrt{\frac{\ell^{(k)}}{c^{(k)}}} \qquad \text{(AI-26)}$$

APPENDEX II PROPERTY OF TRAVELLING WAVE DIFFERENCE

In Fig. II-1 the following equations are satisfied.

$$-i_S(t) + \frac{1}{z}v_S(t) = i_{FS}(t-\tau_1) + \frac{1}{z}v_F(t-\tau_1) \tag{AII-1}$$

$$i_R(t-\tau_1-\tau_2) + \frac{1}{z}v_R(t-\tau_1-\tau_2) = -i_{FR}(t-\tau_1) + \frac{1}{z}v_F(t-\tau_1) \tag{AII-2}$$

Thus,

$$i_S(t) - \frac{1}{z}v_S(t) + i_R(t-\tau) + \frac{1}{z}v_R(t-\tau) = -i_{FS}(t-\tau_1) - i_{FR}(t-\tau_1) \tag{AII-3}$$

which means

$$\xi(t) = i_F(t-\tau_1) \tag{AII-4}$$

The eqn. (II-5) is derived in the same way.

APPENDIX III NUMERICAL SOLUTION OF INTEGRAL EQUATION

In order to obtain a numerical solution of the integral equation:

$$i(t) = \int_0^t v(t - u)y(u)du \tag{AIII-1}$$

provided that i(t) and v(t) are known, first consider a numerical calculation of the integral

$$I = \int_{-\frac{H}{2}}^{\frac{H}{2}} f(x)dx \tag{AIII-2}$$

A formula to approximate the eqn. (AIII-2) is given as

$$A = (R_1^n f_1 + R_2^n f_2 + \cdots + R_n^n f_n)\cdot H \tag{AIII-3}$$

where f_i is the value of f(x) at $x = x_i$, and R_i^n is the weight corresponding to the value f_i. The weighting values are determined such that the formula of the eqn. (AIII-3) will be the best approximation of the eqn. (AIII-2). Let a Maclaurin series expansion of f(x) be

$$f(x) = a_0 + a_1 x + a_2 x^2 + \cdots + a_n x^n + \cdots \tag{AIII-4}$$

where $a_0 = f(0)$, and $a_n = f^{(n)}(0)/n!$. Substituting the eqn. (AIII-2) yields

$$I = a_0 H + \frac{a_2 H^3}{3.2^2} + \frac{a_4 H^5}{5.2^4} + \cdots \tag{AIII-5}$$

whereas by the equation

$$\begin{aligned} f_i &\triangleq f(x_i) \\ &= a_0 + a_1 x_i + a_2 x_i^2 + \cdots + a_n x_i^n + \cdots \end{aligned} \tag{AIII-6}$$

A is evaluated as follows:

$$A = a_0 H \sum_{i=1}^{n} R_i^n + a_1 H \sum_{i=1}^{n} R_i^n x_i + a_2 H \sum_{i=1}^{n} R_i^n x_i^2 + \cdots \qquad \text{(AIII-7)}$$

Subtracting the eqn. (AIII-7) from the eqn. (AIII-5), one obtains

$$\begin{aligned} I - A = & -a_0 [\sum_{i=1}^{n} R_i^n - 1] H - a_1 [\sum_{i=1}^{n} R_i^n x_i - 0] H \\ & - a_2 [\sum_{i=1}^{n} R_i^n x_i^2 - \frac{H^2}{3 \cdot 2^2}] H - \cdots \\ & - a_{2j} [\sum_{i=1}^{n} R_i^n x_i^{2j} - \frac{H^{2j}}{(2j+1) \cdot 2j}] H \\ & - a_{2j+1} [\sum_{i=1}^{n} R_i^n x_i^{2j+1} - 0] H - \cdots \end{aligned} \qquad \text{(AIII-8)}$$

In order to satisfy the equation I = A, each coefficient of a_i must be zero. Assume that the first n coefficients be zero, then 2n variables of $R_1^n, R_2^n, \cdots, R_n^n$ and $x_1, x_2, \cdots, x_n$ satisfy the n independent relations. Therefore, additional constraint conditions must be placed between the variables. The MacLaurin's method does it by giving $x_1, x_2, \cdots, x_n$ in an a priori way. The interval [–H/2, H/2] is equally partitioned into n subintervals, and x_i is chosen at the center of the i-th subinterval. Then $\{R_i^n | i=1,2, \cdots, n\}$ is determined as follows:

for n=1, $x_1 = 0$, $R_1^1 = 1$; 1st order formula

for n=2, $x_1 = -\frac{1}{4}H$, $R_1^2 = \frac{1}{2}$

$x_2 = \frac{1}{4}H$, $R_2^2 = \frac{1}{2}$; 2nd order formula

$$\text{for } n=3,\ x_1 = -\frac{1}{3}H,\ R_1^{\,3} = \frac{3}{8}$$

$$x_2 = 0\ ,\ R_2^{\,3} = \frac{2}{8}$$

$$x_3 = \frac{1}{3}H,\ R_3^{\,3} = \frac{3}{8}\ ;\ \text{3rd order formula}$$

$$\text{for } n=4,\ x_1 = -\frac{3}{8}H,\ R_1^{\,4} = \frac{13}{48}$$

$$x_2 = -\frac{1}{8}H,\ R_2^{\,4} = \frac{11}{48}$$

$$x_3 = \frac{1}{8}H,\ R_3^{\,4} = \frac{11}{48}$$

$$x_4 = \frac{3}{8}H,\ R_4^{\,4} = \frac{13}{48}\ ;\ \text{4th order formula}$$

$$\vdots$$

The eqn. (AIII-19) to the eqn. (AIII-21) is obtained by applying the 1st order formula iteratively to the intervals $[0, T]$, $[T, 2T]$, $\cdots$ $[(k-1)T, kT]$, $\cdots$. The MacLaurin's method of the first order is derived in this way.

APPENDIX IV SIGNAL SELECTION FOR LAPLACE TRANSFORM

The discussion is first made on the relay voltage and current selection by the eqn. (IV-8) and (IV-9). Assume that the transfer function Y(s) corresponding to y(t) be 1/(R+sL), that is a R-L lumped constant line model. To apply the Laplace transformation, the primary circuit voltage v(t) is written as the sum of $v_1(t)$ and $v_2(t)$. See Fig. AIV-1.

$$v(t) \triangleq v_1(t) + v_2(t) \tag{AIV-1}$$

where

$$v_1(t) \triangleq \begin{cases} v(t) & t < 0 \\ 0 & t \geq 0 \end{cases} \tag{AIV-2}$$

$$v_2(t) \triangleq \begin{cases} 0 & t < 0 \\ v(t) & t \geq 0 \end{cases} \tag{AIV-3}$$

Then, the primary circuit current i(t) is also expressed by

$$i(t) \triangleq i_1(t) + i_2(t) \tag{AIV-4}$$

where

$$i_1(t) = Y(s)v_1(t) \tag{AIV-5}$$

$$i_2(t) = Y(s)v_2(t) \tag{AIV-6}$$

Let v(t) be $\cos\omega t$. For the case that i(t) does not include the transient component, i(t) is written by

$$i(t) = \frac{1}{\sqrt{R^2 + (\omega L)^2}} \cos(\omega t - \psi) \tag{AIV-7}$$

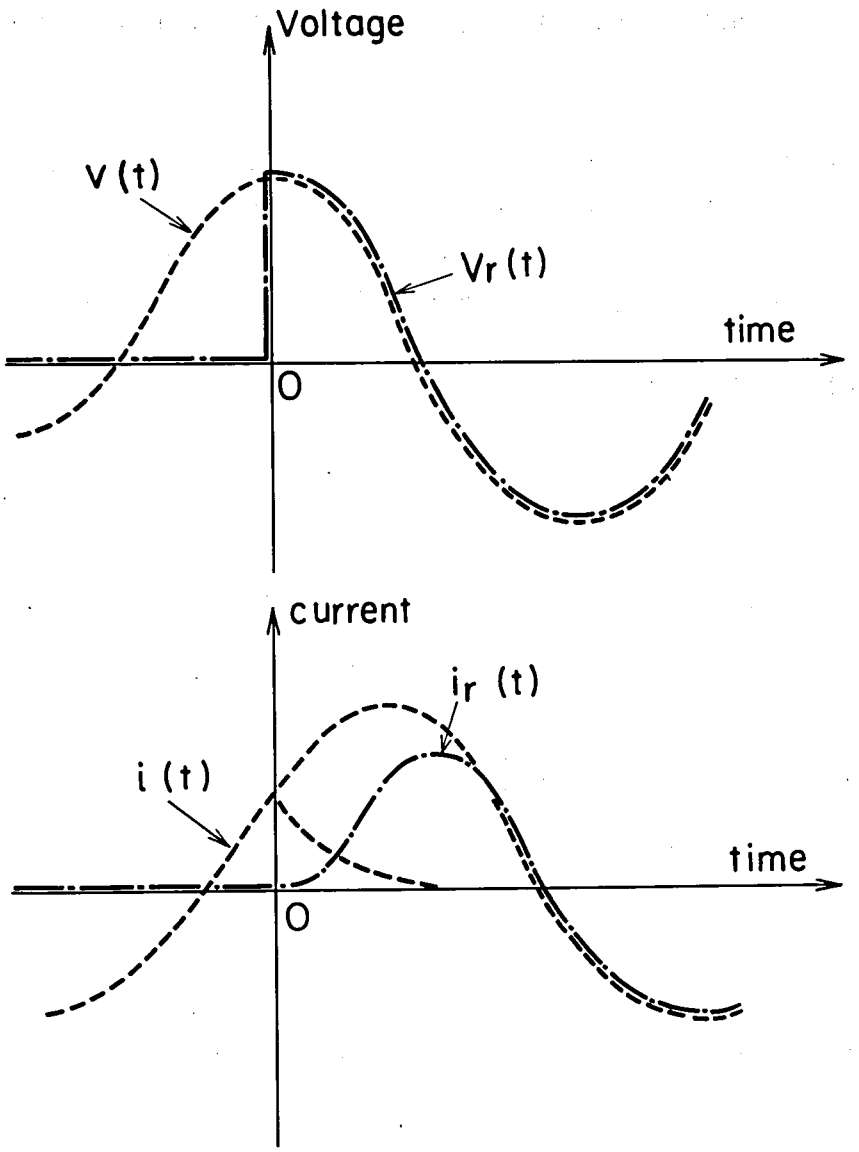

Fig. AIV-1 Relay voltage and current selection scheme

where $\tan\psi = \omega L/R$. On the other hand, the current $i_2(t)$ due to the voltage $v_2(t)$ is

$$i_2(t) = -\frac{R}{R^2 + (\omega L)^2} e^{-\frac{R}{L}t} + \frac{1}{\sqrt{R^2 + (\omega L)^2}} \cos(\omega t - \psi)$$

$$= -\frac{R}{R^2 + (\omega L)^2} e^{-\frac{R}{L}t} + i(t) \qquad \text{(AIV-8)}$$

As $i(0) = -R/[R^2 + (\omega L)^2]$, $i_2(t)$ is written by

$$i_2(t) = i(t) - i(0)e^{-\frac{R}{L}t} = i_{r0}(t) \qquad \text{(AIV-9)}$$

In this case, the relay voltage and current selection is consistent with the eqn. (IV-9). Next consider the case that i(t) includes the dc transient component, that is

$$i(t) = \frac{1}{\sqrt{R^2 + (\omega L)^2}} \cos(\omega t - \psi) + ae^{-\frac{t}{b}} \qquad \text{(AIV-10)}$$

As $i(0) = -R/[R^2 + (\omega L)^2]$, it is clear that

$$i_2(t) \neq i(t) - i(0)e^{-\frac{R}{L}t} \qquad \text{(AIV-11)}$$

Therefore, the relay voltage and current selection is inconsistent with the eqn. (IV-9).

One method to circumvent the above difficulty, is to use a differential filter to remove the dc offset component of the eqn. (AIV–10). The differential filter having the Z-transform of

$$F(z^{-1}) = A(1 - z^{-k}) \qquad \text{(AIV-12)}$$

where

$$z^{-1} = e^{-sT}, \qquad T = 40\ \mu\text{sec} \qquad \text{(AIV-13)}$$

is added after the Butterworth low pass filter in the signal conditioning subprogram. Fig. AIV-2 shows the frequency response of the filter $F(z^{-1})$ and the simulation result $y^{(bc)}(t)$ for a fault initiating the maximum dc offset current. The differential filter has proved effective in alleviating the dc offset current effect.

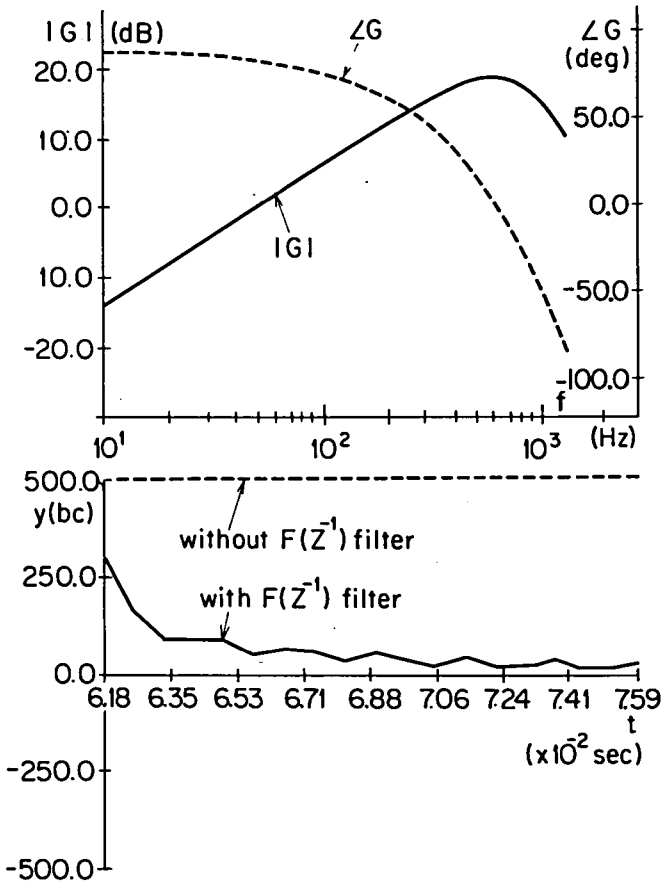

Fig. AIV-2 Frequency response of the filter and its effect on improvement of the directional detection

APPENDIX V PROOF OF PROPERTY OF $\dot{K}(x)$

Consider a loss-less transmission line. Let ℓ be the inductance per unit length and let c be the capacitance per unit length. Fig. AV-1 shows a transmission line connected to a source impedance $j\omega L_S$, and also shows a fault at F x away from the local end S. The total impedance Z_{FS} viewing one side of the network from the faulted point becomes

$$\dot{Z}_{FS} = \dot{z} \tanh(\dot{\lambda}x + \dot{\theta}_S) \tag{AV-1}$$

where

$$\dot{z} = \sqrt{\ell/c} \tag{AV-2}$$

$$\dot{\lambda} = j\omega\sqrt{\ell c} \tag{AV-3}$$

$$\dot{\theta}_S = \alpha_S + j\beta_S = \tanh^{-1}\left(\frac{j\omega L_S}{\dot{z}}\right) \tag{AV-4}$$

Substituting the eqn. (AV-2) to (AV-4) into the eqn. (AV-1) obtains

$$\dot{Z}_{FS} = j\dot{z} \tan(\omega\sqrt{\ell c}x + \beta_S) \tag{AV-5}$$

In a similar way, the total impedance $\dot{Z}_{FR}$ looking at the other side of the network becomes

$$\dot{Z}_{FR} = j\dot{z} \tan(\omega\sqrt{\ell c}(d-x) + \beta_R) \tag{AV-6}$$

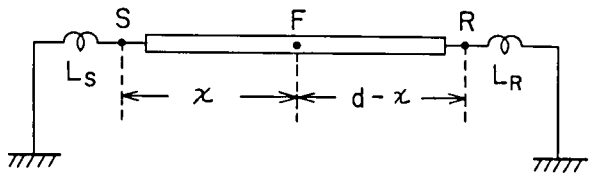

Fig. AV-1 Model system with inductive source impedance

The ratio $\dot{K}(x)$ is defined by the eqn. (AV-7).

$$\dot{K}(x) \triangleq \frac{\dot{I}''_{FR}}{\dot{I}''_{FS}} = \frac{\dot{Z}_{FS}}{\dot{Z}_{FR}} \tag{AV-7}$$

Therefore, $\dot{K}(x)$ is represented by

$$\dot{K}(x) = \frac{\tan(\omega\sqrt{\ell c}x + \beta_S)}{\tan(\omega\sqrt{\ell c}(d-x) + \beta_R)} \tag{AV-8}$$

which means that $\dot{K}(x)$ be a real variable. Q.E.D.

APPENDIX VI MATHEMATICAL BACKGROUND OF STATISTICS

Some of the mathematical background for statistics are provided to define terms and to make the present thesis selfcontained.

A6.1 Distribution and Density Function

A random number x, which is used throughout CHAPTER VII, is characterized by probability distribution function P(x).

Definition The distribution function P(x) is defined by

$$P(x_1) = Pr\{x \leq x_1\} \tag{AVI-1}$$

where $Pr\{x \leq x_1\}$ is the probability that the value of x is smaller than or equal to x_1. In the context of relaying, $P(\delta)$ means the probability that the discriminant d comes below a threshold value of δ.

Definition The probability density function $p(x_1)$ is defined by

$$p(x_1) = \lim_{\Delta x_1 \to 0} \frac{Pr\{x_1 \leq x \leq x_1 + \Delta x_1\}}{\Delta x_1} \tag{AVI-2}$$

Therefore, $p(d_1)\,\Delta d_1$ is the probability that the discriminant d lies between $d = d_1$ and $d = d_1 + \Delta d_1$.

Definition The conditional distribution function of x, given the hypothesis H, is defined by

$$P(x_1/H) = Pr\{x \leq x_1/H\} \tag{AVI-3}$$

where $Pr\{A/B\}$ is the conditional probability of event A, given the event B has occurred.

A6.2 Sequential Hypothesis Testing

Hypothesis testing is a process of making decisions which event has taken place, given the sample which is generally a vector. In some problems, all of the information is provided at one instant, and the decision is made immediately. In other problems, however, the observations are sequential, and the information becomes richer and richer. The latter seems to model more of the practical problems. In the digital relays, the voltage and current are observed to determine whether a transmission line is in unfaulted or faulted condition. A sequence of observed waveforms should be analyzed to aid this determination. The distance relay updates the impedance each time new samples are given, and make decision for protection. A basic approach to this problem is the averaging of the sequence of the measured impedance. However, it is not clear when to terminate the observations, namely when to issue the final decision. The sequential hypothesis test is a mathematical tool for this type of problem.

The Wald Sequential Test The Wald sequential test is run as follows. Let $x_1, x_2, \cdots$ be the random number observed sequentially, and assume that they are independent and identically distributed with the expected value η_i and variance σ_i. The log-likelihood ratio is calculated for x_i

$$z_i = \log \frac{p(x_i/H_1)}{p(x_i/H_0)} \tag{AVI-4}$$

where H_0 and H_1 are two hypotheses to be decided. Since z_i is also a random number, the total likelihood ratio of k samples is

$$\begin{aligned} u_k &= \log \frac{p(x_1 x_2 \cdots x_k/H_1)}{p(x_1 x_2 \cdots x_k/H_0)} \\ &= \sum_{i=1}^{k} \log \frac{p(x_i/H_1)}{p(x_i/H_0)} \\ &= \sum_{i=1}^{k} z_i \end{aligned} \tag{AVI-5}$$

The expected values and variances of u_k for H_0 and H_1 are

$$\eta_{ik} = E\{u_k/H_i\} = k_i \eta_i \tag{AVI-6}$$

$$\sigma_{ik}^2 = E\{(u_k - \eta_i)^2/H_i\} = k\sigma_i^2 \tag{AVI-7}$$

Thus, as k increases, η_{ik} increases for $\eta_i > 0$ and η_{ik} decreases for $\eta_i < 0$. σ_{ik} also increases for $\sigma_i > 0$, and σ_{ik} decreases for $\sigma_i < 0$, but the rate of increase and decrease is slower than that for η_{ik}. Therefore, the decision rule such that

$$\begin{aligned}
&\text{if } u_k \leq a \quad \rightarrow x_1 x_2 \cdots x_k \text{ belongs to } H_0 \\
&\text{if } a < u_k < b \rightarrow \text{continue to test} \\
&\text{if } b \leq u_k \quad \rightarrow x_1 x_2 \cdots x_k \text{ belongs to } H_1
\end{aligned} \tag{AVI-8}$$

will terminate in making decisions with probability 1. Two values of threshold are given [5] by

$$a = \log A = \log(1 - \epsilon_1)/\epsilon_0 \tag{AVI-9}$$

$$b = \log B = \log\epsilon_1/(1 - \epsilon_0) \tag{AVI-10}$$

AUTHOR'S PAPERS

1. T. Takagi, J. Baba, K. Uemura and T. Sakaguchi, "Fault Protection Based on Travelling Wave Theory: Part I-Theory", IEEE PES Summer Meeting, Paper No. A77 750-3, 1977.

2. T. Takagi, J. Baba, K. Uemura and T. Sakaguchi, "Fault Protection Based on Travelling Wave Theory: Part II-Sensitivity Analysis and Laboratory Test", IEEE PES Winter Meeting, Paper No. A78 220-6, 1978.

3. Y. Akimoto, T. Yamamoto, H. Hosokawa, T. Sakaguchi, T. Yoshida and S. Nishida, "Wave Propagation Theory Applied to Transsission Line Protection : Part I", Trans. of IEE of Japan, Vol. 98-B, No. 1, January, pp. 79-86, 1978. (in Japanese)

4. Y. Akimoto, T. Yamamoto, H. Hosokawa, T. Sakaguchi, T. Yoshida and S. Nishida, "Wave Propagation Theory Applied to Transmission Line Protection : Part II", Trans. of IEE of Japan, Vo,. 98-B, No. 8, August, pp. 711-718, 1978. (in Japanese)

5. F. Aoki, Y. Akimoto, K. Uemura, and T. Sakaguchi, "Totally Digiralized Control System with Simultaneous Data Sampling and Fault Protection Principle Applied to the System", 6th Power Systems Computation Conference, Darmstadt, 1979.

6. F. Aoki, Y. Akimoto, K. Uemura, and T. Sakaguchi, "Digitalized Control System with Simultaneous Data Sampling and Fault Protection", International Journal of Electrical Power and Energy Systems, Vol. 1 No. 3, pp. 166-174, 1979.

7. T. Sakaguchi, "Statistical Decision Theoretic Approach to Digital Relaying", IEEE PES Winter Power Meeting, Paper No. F80 196-6, Februay, 1980.
   (also appeared in IEEE Trans. on PA & S, Vol. PAS-99, No. 5 September/October, pp. 1918-1926, 1980.)

8. T. Sakaguchi, and K. Uemura, "A New Directional Protection Based on Laplace Transformation with Special Reference to Computer Relaying", Second International Conference on 'Development in Power-System Protection' London: 10-12 June 1980.

9. Y. Yamakoshi, K. Uemura, and T. Sakaguchi, "A New Directional Protection for Digital Processor Use", IFAC Symposium on Automatic Control in Power Generation, Distribution and Protection, Pretoria, Republic of South Africa, 15-19 September 1980.

10. T. Takagi, Y. Yamakoshi, J. Baba, K. Uemura, and T. Sakaguchi, "A New Algorithm of An Accurate Fault Location for EHV/UHV Transmission Lines: Part I-Fourier Transformation Method", IEEE PES Summer Meeting, Paper No. 80 SM 648-6, July, 1980. (also appeared in IEEE Trans. on PA & S, Vol. PAS-100, No. 3 March, pp. 1316-1323, 1981)

11. T. Takagi, Y, Yamakoshi, J. Baba, K. Uemura and T. Sakaguchi, "A New Algorithm of An Accurate Fault Location for EHV/UHV Transmission Lines: Part II-Laplace Transform Method", IEEE PES Summer Meeting, Paper No. 81 SM 411-8, July, 1981.